# Potential use of CAMS modelling results in air quality mapping under ETC/ATNI

May 2020

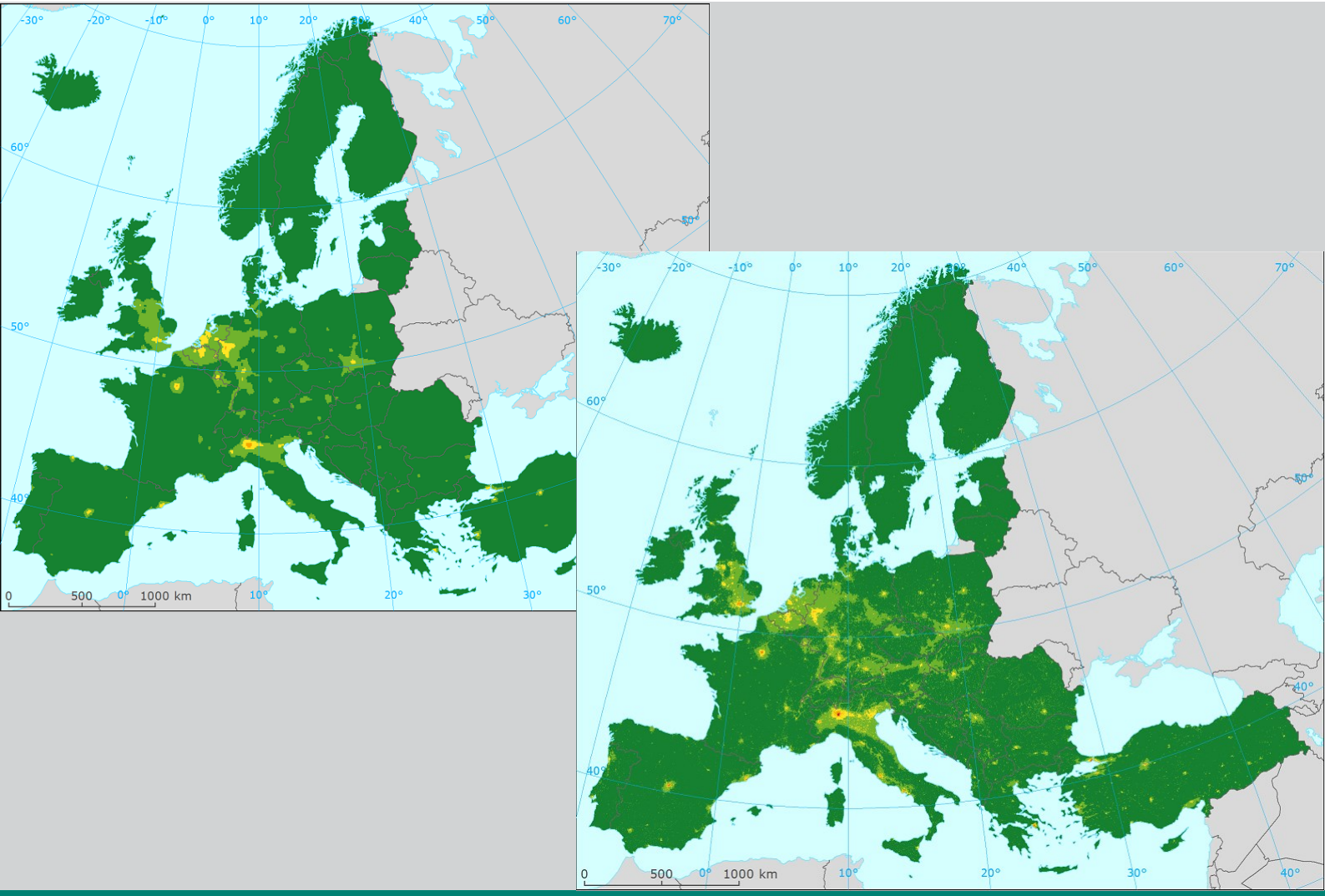


Authors:
Jan Horálek (CHMI), Paul Hamer (NILU), Markéta Schreiberová (CHMI), Augustin Colette (INERIS), Philipp Schneider (NILU), Laure Malherbe (INERIS)

ETC/ATNI consortium partners:
NILU – Norwegian Institute for Air Research, Aether Limited, Czech Hydrometeorological Institute (CHMI), EMISIA SA, Institut National de l'Environnement Industriel et des risques (INERIS), Universitat Autònoma de Barcelona (UAB), Umweltbundesamt GmbH (UBA-V), 4sfera Innova, Transport & Mobility Leuven NV (TML)

European Environment Agency
European Topic Centre on Air pollution, transport, noise and industrial pollution

Cover pictures: CAMS Ensemble Forecast model output (top left) and Interim RIMM map using the CAMS Ensemble Forecast model output (bottom right) for $NO_2$ annual avergare 2017.

**Legal notice**
The contents of this publication do not necessarily reflect the official opinions of the European Commission or other institutions of the European Union. Neither the European Environment Agency, the European Topic Centre on Air pollution, noise, transport and industrial pollution nor any person or company acting on behalf of the Agency or the Topic Centre is responsible for the use that may be made of the information contained in this report.

**Copyright notice**
© European Topic Centre on Air pollution, transport, noise and industrial pollution , 2020

Reproduction is authorized provided the source is acknowledged.
Information about the European Union is available on the Internet. It can be accessed through the Europa server (https://europa.eu/).

*The withdrawal of the United Kingdom from the European Union did not affect the production of the report.*
*Data reported by the United Kingdom are included in all analyses and assessments contained herein, unless otherwise indicated.*

**Authors**
Jan Horálek, Markéta Schreiberová: Czech Hydrometeorological Institute (CHMI, Czechia)
Paul Hamer, Philipp Schneider: Norwegian Institute for Air Research (NILU, Norway)
Augustin Colette, Laure Malherbe: National Institute for Industrial Environment and Risk (INERIS, France)

ETC/ATNI c/o NILU
ISBN 978-82-93752-21-9

European Topic Centre on Air pollution,
transport, noise and industrial pollution
c/o NILU – Norwegian Institute for Air Research
P.O. Box 100, NO-2027 Kjeller, Norway
Tel.: +47 63 89 80 00
Email: etc.atni@nilu.no
Web : https://www.eionet.europa.eu/etcs/etc-atni

# Contents

## Acknowledgements

The EEA task manager was Alberto González Ortíz. The ETC/ATNI reviewers were Laurence Rouïl (INERIS, France) and Leonor Tarassón (NILU, Norway).

The paper also benefited from the expertise of Anthony Ung (INERIS, France) and Jana Marková (CHMI, Czechia).

# 1 Introduction

Air quality European-wide maps based on spatial interpolation and data fusion have been produced under ETC/ATNI (resp. previous consortia ETC/ACM and ETC/ACC) since 2005 (Horálek, 2020 and references therein). The mapping methodology combines monitoring data, chemical transport model results and other supplementary data using a linear regression model followed by kriging of the residuals produced from that model ('residual kriging'). Separate mapping layers (rural, urban background, and urban traffic, where relevant) are created separately and subsequently merged together into the final map. In order to reflect the three steps applied, the methodology is called *Regression – Interpolation – Merging Mapping (RIMM)*. These maps are constructed regularly for the main air pollutants ($PM_{10}$, $PM_{2.5}$, $O_3$, $NO_2$), based on validated air quality measurement data that are reported to EEA by its member countries (for the EU Member States under the AQ Directives) and other voluntary reporting countries. In order to add more information on concentration levels in areas with no measurements, the EMEP atmospheric dispersion model (produced by Met Norway) has been used as a secondary source of information, together with other supplementary data like altitude, land cover and meteorological data.

Apart from the validated measurement data, reported by end of September of year YY for data corresponding to year YY-1 and uploaded to the EEA's AQ e-reporting database, preliminary measurement data provided up-to-date (UTD) on an hourly basis by many EEA's member and cooperating states are available in this database. The validated data are stored in the so-called E1a data set, while the UTD data in the E2a data set of the AQ e-reporting database. In this report, we evaluate the use of the E2a data for potential preparing of preliminary spatial maps. To enable early creation of such preliminary maps, we also evaluate in this report potential use of modelling output from the Copernicus Atmospheric Monitoring Service (CAMS), which is available earlier than the EMEP model output. Specifically, we use the ensemble mean (the median of seven regional atmospheric dispersion models) forecast and analysis products. Two different CAMS modelling results have been used, i.e. CAMS Ensemble Forecast and CAMS Ensemble Interim Reanalysis (which uses the UTD measurement data in the reanalysis), on top of the EMEP model output. $PM_{10}$ and $NO_2$ annual average preliminary maps for 2017 based on E2a (UTD) measurement data, including the evaluation of their quality have been examined.

Additionally, we examine and discuss a potential substitution of the EMEP model by CAMS modelling data in the regular validated maps, taking into account the recommendations of Horálek et al. (2014). The comparison is executed for 2017 for the $PM_{10}$ annual average, the $PM_{2.5}$ annual average, the ozone indicator SOMO35 and the $NO_2$ annual average. Again, the use of three different model products in the mapping is evaluated, i.e. CAMS Ensemble Forecast, CAMS Ensemble Interim Reanalysis and EMEP. We have not examined another CAMS modelling product, i.e. CAMS Ensemble Validated Reanalysis (which uses the validated measurement data in the reanalysis), due to its lately availability for a potential use in the routine RIMM spatial mapping.

For comparison of the spatial mapping results using different chemical transport models, we apply a thorough evaluation strategy to account for the fact that CAMS assimilates AQ measurement data. We specifically take note that CAMS deliberately leaves some stations outside of the assimilation procedure to keep them for validation purposes.

Next to the evaluation of the different modelling results in the spatial mapping, the comparison of the spatial interpolation mapping results (as routinely prepared, i.e. using the EMEP model outputs) with the CAMS Ensemble modelling results have been carried out. The reason for this comparison was to verify the assumption that the spatial interpolation maps, where the main input are AQ concentration data measured at monitoring stations, are better suited for exposure calculations in urban areas.

Chapter 2 describes the methodological aspects. Chapter 3 documents input data and the comparison approach. Chapter 4 presents the evaluation of the spatial mapping results using different chemical transport models both for the preliminary and regular maps. Chapter 5 shows the evaluation of the spatial mapping results with the CAMS Ensemble modelling results. Chapter 6 gives the conclusions and recommendations. Annex provides additional difference maps.

# 2 Mapping Methodology

## 2.1 Spatial Mapping Methodology: Regression – Interpolation – Merging Mapping (RIMM)

The Regression – Interpolation – Merging Mapping method (RIMM) routinely used in the spatial mapping under ETC/ATNI consists of a linear regression model followed by kriging of the residuals from that regression model (residual kriging):

$$\hat{Z}(s_0) = c + a_1 X_1(s_0) + a_2 X_2(s_0) + \ldots + a_n X_n(s_0) + \hat{\eta}(s_0), \qquad (2.1)$$

where $\hat{Z}(s_0)$ is the estimated concentration at a point $s_o$,

$X_1(s_0)$ is the chemical transport modelling data at point $s_o$,

$X_2(s_0),\ldots, X_n(s_0)$ are $n-1$ other supplementary variables at point $s_o$,

$c, a_1, a_2,,\ldots, a_n$ are the $n+1$ parameters of the linear regression model calculated based on the data at the points of measurement,

$\hat{\eta}(s_0)$ is the spatial interpolation of the residuals of the linear regression model at point $s_o$, based on the residuals at the points of measurement.

For different pollutants and area types (rural, urban background, and for $PM_{10}$, $PM_{2.5}$ and $NO_2$ also urban traffic), different supplementary data are used. The spatial interpolation of the regression residuals is carried out using ordinary kriging, according to

$$\hat{\eta}(s_0) = \sum_{i=1}^{N} \lambda_i \eta(s_i) \quad \text{with} \quad \sum_{i=1}^{N} \lambda_i = 1, \qquad (2.2)$$

where $\hat{\eta}(s_0)$ is the interpolated value at a point $s_o$, derived from the residuals of the linear regression model at the points of measurement $s_i$, $i = 1, \ldots, N$,

$N$ is the number of the measurement points used in the interpolation, which is fixed based on the variogram; in any case, $20 \le N \le 50$,

$X_2(s_0),\ldots, X_n(s_0)$ are $n-1$ other supplementary variables at point $s_o$,

$\eta(s_i)$ are the residuals of the linear regression model at $N$ points of measurement $s_i$, $i = 1, \ldots, N$,

$\lambda_1,\ldots, \lambda_N$ are the estimated weights based on the variogram, see Cressie (1993).

For $PM_{10}$ and $PM_{2.5}$, prior to linear regression and interpolation, a logarithmic transformation to measurements and CTM modelled concentrations is executed as that contributes to an improved fit of the regression model. After interpolation, a back-transformation is applied.

In the case of $PM_{2.5}$ map creation, in addition to the $PM_{2.5}$ measurement data, so-called pseudo $PM_{2.5}$ stations are also used, i.e. estimates of $PM_{2.5}$ concentrations at the locations of $PM_{10}$ stations with no $PM_{2.5}$ measurement (Horálek et al., 2020).

Separate map layers are created for rural and urban background areas on a grid at resolution of 1x1 $km^2$ (for $PM_{10}$, $PM_{2.5}$ and $NO_2$) and 10x10 $km^2$ (for ozone), and for urban traffic areas at 1x1 $km^2$ (for $PM_{10}$, $PM_{2.5}$ and $NO_2$). The rural background map layer is based on rural background stations, the urban background map layer on urban and suburban background stations and the potential urban traffic map layer is based on urban and suburban traffic stations. Subsequently, the separate map layers are merged into one combined final map using a weighting procedure based on the population density grid at 1x1 $km^2$ resolution, according to

$$\hat{Z}_F(s_0) = \left(1 - w_U(s_0)\right) \cdot \hat{Z}_R(s_0) + w_U(s_0) \cdot \hat{Z}_{UB}(s_0) \quad \text{resp.}$$
$$\hat{Z}_F(s_0) = \left(1 - w_U(s_0)\right) \cdot \hat{Z}_R(s_0) + w_U(s_0)\left(1 - w_T(s_0)\right) \cdot \hat{Z}_{UB}(s_0) + w_T(s_0) \cdot \hat{Z}_{UT}(s_0) \qquad (2.3)$$

where $\hat{Z}_F(s_0)$ is the resulting estimated concentration in a grid cell $s_o$ for the final map,

$\hat{Z}_R(s_0)$ is the estimated concentration in a grid cell $s_o$ for the rural background map layer,

$\hat{Z}_{UB}(s_0)$ is the estimated concentration in a grid cell $s_o$ for the urban background map layer,

$\hat{Z}_{UT}(s_0)$ is the estimated concentration in a grid cell $s_o$ for the urban traffic map layer,

$w_U(s_0)$ is the weight representing the ratio of the urban character of the grid cell $s_o$.

$w_T(s_0)$ is the weight representing the ratio of areas exposed to traffics in a grid cell $s_o$.

The weight $w_U(s_0)$ is based on the population density, while the weight $w_T(s_0)$ is based on the buffers around the roads (Section 3.1.3). For details, see Horálek et al. (2020 and references therein).

Such a methodology using the merge of the map layers is particularly efficient at producing high spatial variability patterns in fine resolution in the air quality maps since these patterns derive directly from the population density and road data.

## 2.2 CAMS Modelling Data Products

CAMS is one of the six Copernicus services. CAMS provides a diverse range of environmental atmospheric information, which specifically includes the provision of air quality information at a regional scale over Europe. This European regional service is of specific interest for this current work. The European regional production consists of an ensemble of seven (resp. nine since October 2019) air quality models run operationally over the domain outlined in Map 2.1.

*Map 2.1. Example map showing the spatial extent of the CAMS European regional air quality domain. This example shows hourly ozone concentrations (µg m$^{-3}$) from the CAMS Ensemble Forecast during an ozone pollution episode that occurred towards the end of July 2019.*

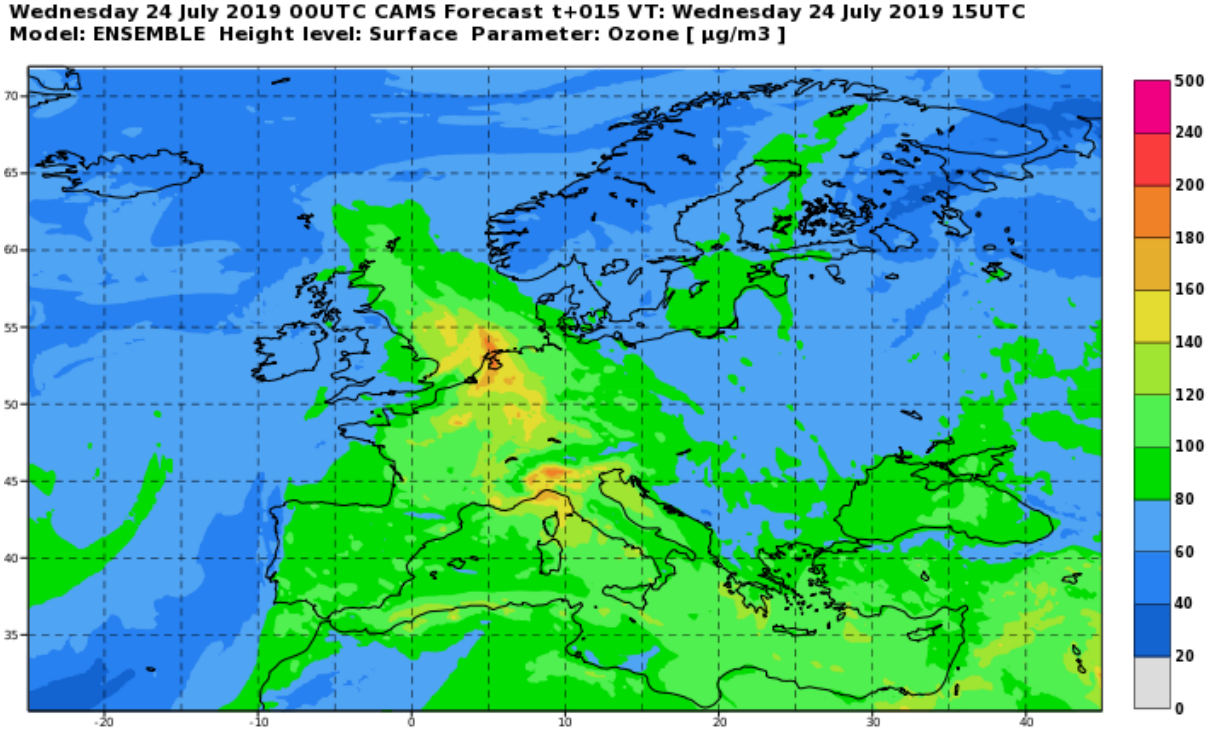


The seven different models considered for this report and the institutes responsible for running each one are summarised in Table 2.1. (It should be noted that In October 2019, two other models have

been added to this set, namely DEHM model run by Aarhus University and GEM-AQ model run by Polish Institute of Environmental Protection – National Research Institute.) All of the models are *chemical transport models*, which means they simulate atmospheric chemistry but rely on an external meteorological model to provide the weather forecast that governs the transport of pollutants in the model. The European Centre for Medium Range Weather Forecasts (ECMWF) provides the meteorological data for each of the regional models in CAMS, which ensures homogeneity of input data. For further details of each model please consult Marécal et al. (2015).

*Table 2.1. A table summarising the chemistry-transport models used in CAMS (before addition of two other models in October 2019) and the institutions responsible for running the models*

| Institute | Model |
|---|---|
| INERIS | CHIMERE |
| Norwegian Meteorological Institute | EMEP/MSC-W |
| Rhenish Institute for Environmental Research at the University of Cologne | EURAD-IM |
| KNMI/TNO | LOTOS-EUROS |
| Swedish Meteorological and Hydrological Institute | MATCH |
| Météo France | MOCAGE |
| Finnish Meteorological Institute | SILAM |

The models provide four distinct air quality products available on different timescales:

- a 72-hour forecast made available at 07:00 UTC the day of the forecast;
- a 24-hour analysis that involves data assimilation of near real time (up-to-date, UTD) surface station air quality observations, which is available at 11:00 UTC the day of the forecast;
- a 24-hour interim reanalysis repeated 20 days later to benefit from short term adjustment in UTD observations and complemented for missing days in the first weeks of the following year to produce an interim reanalysis available 3 month after the end of a calendar year (in March of the year + 1);
- a yearly validated reanalysis that is a data assimilation product using validated surface station data, which is provided as an entire year but only 21 months after the end of a calendar year (In September of the year +2).

Each data product is available on an hourly time resolution and at a spatial resolution of 0.1° x 0.1°, i.e. ca. 10x10 $km^2$. The output from the seven models are combined together and the median for each grid cell and each time step is taken to create an ensemble product. CAMS is currently running a dedicated project (coordinated by INERIS) to improve this ENSEMBLE product using more elaborated statistical techniques (including machine learning) than this simple median. This improved methodology is scheduled to become operational after 2021. Extensive validation and verification demonstrate that the ensemble forecast, analysis, and reanalysis have superior skill compared to any of the individual model ensemble members (if RMSE, bias and correlation are evaluated together)[1].Thus, for this work, we will focus on the use of the ensemble products. Furthermore, due to the time delay in creating the ensemble validated reanalysis, it was not be possible to use this data product to look at air quality in 2017. We therefore use only the forecast and interim reanalysis CAMS Ensemble products in this work.

Each model carries out data assimilation of some kind to create its analysis and reanalysis. The models use a variety of different assimilation algorithms. In addition, while all of the models use near real time surface observations in the assimilation process, a small subset of the models also uses satellite observations of air pollutants in the assimilation process. Further, each modelling team chooses to

[1] https://atmosphere.copernicus.eu/regional-services

assimilate different pollutants in their models. All of this information is summarised and presented in more detail in Table 2.2.

Explaining the technical details of each of the different assimilation methods described in Table 2 is beyond the scope of this report. However, we can give a rough idea of the sophistication of each of these methods and their expected quality relative to one another. We list each method in order of increasing complexity: data fusion by kriging, 3D-variational methods, 3D-First Guess at Appropriate Time, Ensemble Kalman Filter, and 4D-variational methods. Note, however, that a higher level of complexity does not necessarily translate into increased performance/accuracy levels.

*Table 2.2 A summary of the data assimilation systems used within each of the seven CAMS regional models. The table also summarises which observations are assimilated in order to create each model analysis.*

| Model | Assimilation Algorithm | Observations |
|---|---|---|
| CHIMERE | Data fusion (external drift kriging) | Surface ozone and $PM_{10}$ |
| EMEP | 3D-variational method | $NO_2$ satellite columns; Surface $NO_2$ and ozone |
| EURAD | 4D-variational method | $NO_2$ satellite columns; Surface $NO_2$, ozone, $PM_{10}$ and $PM_{2.5}$ |
| LOTOS-EUROS | Ensemble Kalman Filter | Surface ozone |
| MATCH | 3D-variational method | Surface ozone, $NO_2$, CO, $SO_2$, $PM_{10}$, $PM_{2.5}$ |
| MOCAGE | 3D/4D-variational method and 3D-First Guess at Appropriate Time (FGAT) | Surface ozone, $NO_2$ and $PM_{10}$ |
| SILAM | 3D/4D-variational methods | Surface ozone, $NO_2$, $PM_{2.5}$ |

The use of the ensemble forecast results in the annual air quality mapping will mean that no information from surface observations will be contained in the modelling product used in the data fusion. However, the ensemble analysis and interim reanalysis products are created by assimilating surface observations as presented in Table 2.2, and so the modelling products already contain some information from the surface station observations. We will therefore explore and highlight the effect of having additional surface observation upon the mapping procedure in the course of this report.

## 2.3 Use of CAMS Modelling Data in RIMM Spatial Mapping

In this report, the use of CAMS modelling data in the RIMM spatial mapping is examined. In principle, the CAMS modelling data are used as the chemical transport modelling data in Equation 2.1, instead of the routinely used EMEP modelling data.

As discussed in Horálek et al. (2014), the potential use of reanalysis (data assimilated) fields in the spatial mapping would lead to situations where an observation might be used twice: once for the model reanalysis and then again for data fusion mapping. This is not expected to be a problem for the actual quality of the map, but it limits the uncertainty analysis, leading to underestimation of the resulting map's uncertainty. Such an underestimation would take place both in cross-validation (if applied stations used in reanalysis) and in uncertainty maps (created based on geostatistical theory). Thus, it should be kept in mind that a potential use of the CAMS Ensemble reanalysis products in the spatial mapping would make the uncertainty analysis of the spatial maps more difficult (and make the creation of the uncertainty maps impossible), unless the stations used for the data assimilation in the CAMS model were not considered for the production of the spatial maps.

When selecting the CAMS modelling products for examining their use in the RIMM spatial mapping, we have chosen (i) the CAMS Ensemble Interim Reanalysis due to its earlier availability compared to

the validated reanalysis and (ii) the CAMS Ensemble Forecast, being a modelling product not using data assimilation, see above. In both cases, we use the annual set of the hourly data. In the case of the CAMS Ensemble Forecast, for each day we use the first 24 hours of the 72-hour forecast.

# 3 Data Used and Comparison Approach

## 3.1 Data Used

### *3.1.1 Air quality monitoring data*

**Data for preliminary maps: AQ e-reporting E2a data set**

For the preliminary maps (Section 4.1), we have used air quality station monitoring data for the year 2017 coming from the E2a data set of the Air Quality e-Reporting database (EEA, 2018). The data was extracted by the EEA in the first half of the year 2018. The data of the dataflow E2a are being provided up-to-date (UTD) on an hourly basis from most of the EEA's member and cooperating countries. Some member states provide an update of these data on a monthly basis, including supplementing this data set by PM data coming from stations measuring with gravimetric devices (i.e. not automatically). In order to reflect the status of the E2a data set in the first weeks of a year (i.e. in time of potential routine construction of interim maps), we have not used the data of the gravimetric stations, which were added to the E2a data set in a later stage (this means that we have excluded 99 $PM_{10}$ stations, consisting of 16 rural background, 41 urban/suburban background and 42 urban/suburban traffic stations). Like in the routine regular maps (Horálek et al., 2020), only data from stations classified as background (for the three types of area, rural, suburban and urban), and also the stations classified as traffic for the types of area suburban and urban are used. In addition, only the stations with annual data coverage of at least 75 percent are used.

The following pollutants and aggregations are considered:
$PM_{10}$ – annual average [$\mu g \cdot m^{-3}$], year 2017
$NO_2$ – annual average [$\mu g \cdot m^{-3}$], year 2017

Table 3.1 shows the number of the measurement stations selected for the individual pollutants. Next to the stations used in preliminary mapping, the stations used for validation and mutual comparison of different map variants are also presented.

As further described in Section 3.2, stations of the E1a dataset (see below) with no E2a data (i.e. stations not used in the preliminary mapping) are used for validation of the preliminary map. Next to this, cross-validation is additionally applied, based on a subset of the stations used in mapping. The subset consists of the stations used in CAMS in the so-called "validation set". Thus, the total E2a set of the stations used in mapping consists of this subset applied in the cross-validation and of "other" stations not applied in the cross-validation. For detailed description of the validation approaches and for the motivation of the subset selection, see Section 3.2.

*Table 3.1 Number of stations with E2a data selected for each station type as used in mapping of preliminary maps and number of stations with E1a data used for their validation, for $PM_{10}$ (left) and $NO_2$ (right), 2017*

| Station type | $PM_{10}$ | | | | $NO_2$ | | | |
|---|---|---|---|---|---|---|---|---|
| | mapping (E2 data set) | | | validation (E1 data) | mapping (E2 data set) | | | validation (E1 data) |
| | cross-val. | other | total | | cross-val. | other | total | |
| Rural background | 40 | 153 | 193 | 176 | 68 | 217 | 285 | 176 |
| Urban/suburban background | 152 | 519 | 671 | 736 | 241 | 602 | 843 | 510 |
| Urban/suburban traffic | | | 354 | | | | 511 | |

Figure 3.1 shows the spatial distribution of the rural and urban/suburban background $PM_{10}$ stations used in the preliminary map creation (i.e. E2a stations, in blue and green) and validation (E1a stations not included in the E2a data set, in red). Note that using validated observations (E1a) to test the map produced with UTD observations (E2a), also implies that the UTD measurements used in the mapping

might have been modified in the meanwhile; we are therefore not only testing here the mapping algorithm, but the final map itself. Figure 3.2 shows the similar spatial distribution for $NO_2$ stations.

In both figures, within the E2a stations used in preliminary map creation, the stations used (in blue) and not used (in green) in the cross-validation are distinguished. In the figures, traffic stations are not shown due to their relatively minor influence in the final 1x1 $km^2$ merged map.

*Figure 3.1 Spatial distribution of $PM_{10}$ background stations used in mapping and validation of preliminary maps, 2017*

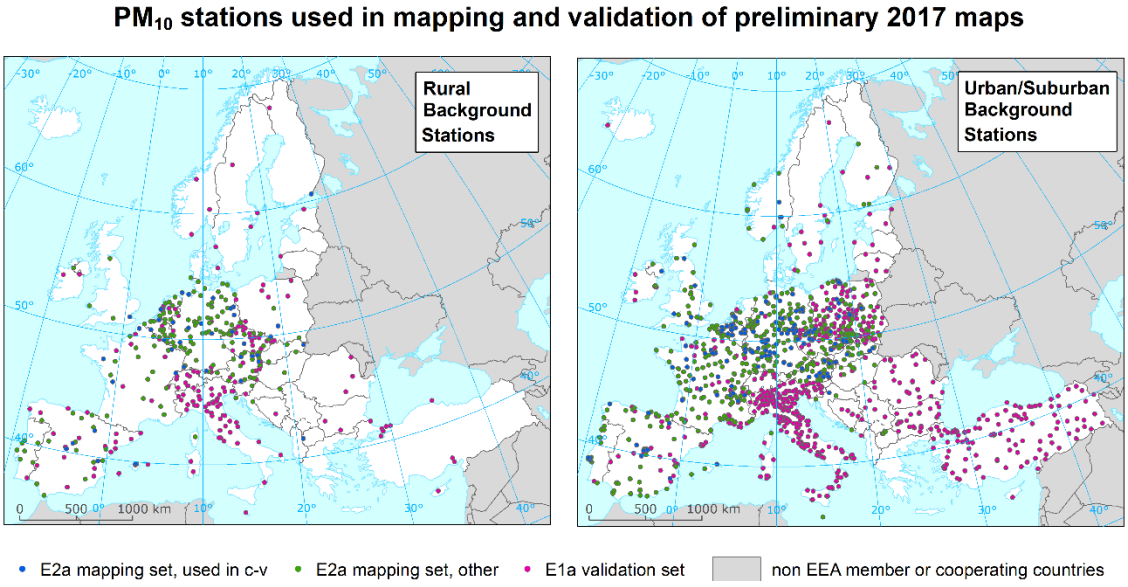


*Figure 3.2 Spatial distribution of $NO_2$ background stations used in mapping and validation of preliminary maps, 2017*

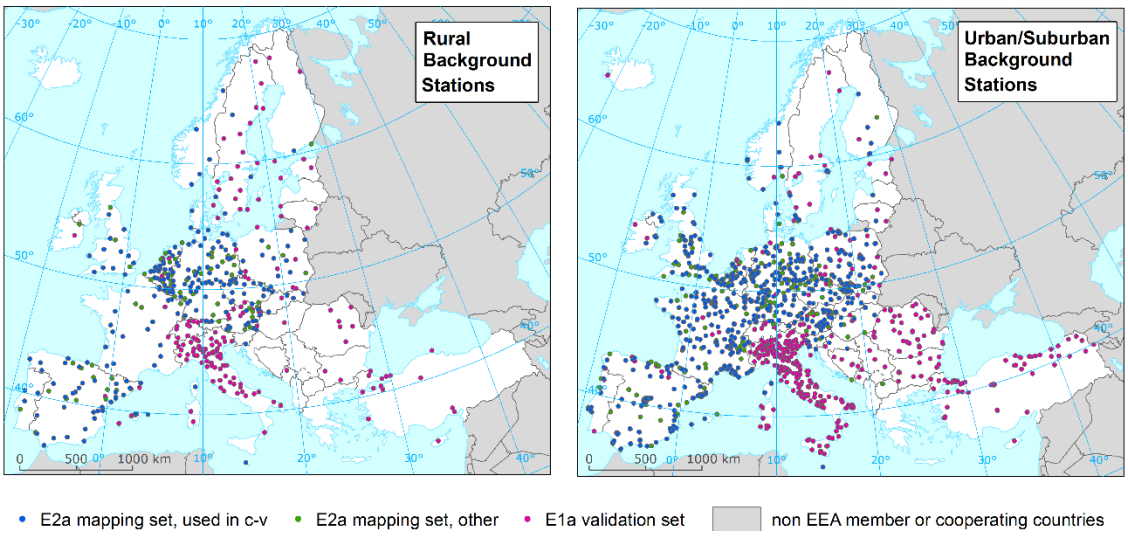

**Data for regular validated maps: AQ e-reporting E1a data set supplemented by EBAS stations**

For the analysis of the regular validated maps (Section 4.2 and Chapter 5), the same set of the air quality station monitoring data for 2017 as applied in the routine 2017 mapping (Horálek et al., 2020) has been used, i.e. the data of the E1a data set of the Air Quality e-Reporting database (EEA, 2019). The data was extracted by the EEA in January–March 2019. The data of the dataflow E1a is reported to EEA by its member and coo perating countries every September and covers the year before the deliver. This E1a data set has been supplemented with several EMEP rural stations from the database EBAS (NILU, 2019) not reported to the Air Quality e-Reporting database. Specifically, 7 additional stations for $PM_{10}$, 4 for $PM_{2.5}$, and 6 for $NO_2$. For $PM_{10}$ and $NO_2$, and also for $PM_{2.5}$, we use the same classification types of stations and areas as we do for the E2a data, i.e. stations classified as background (for the three types of area), and also traffic for the types of area suburban and urban. For ozone, we use only data from stations classified as background (for the three types of area, rural, suburban and urban).

The following pollutants and aggregations are considered:

$PM_{10}$ – annual average [$\mu g \cdot m^{-3}$], year 2017
$PM_{2.5}$ – annual average [$\mu g \cdot m^{-3}$], year 2017
Ozone – SOMO35 [$\mu g \cdot m^{-3} \cdot d$], year 2017
$NO_2$ – annual average [$\mu g \cdot m^{-3}$], year 2017

In the mapping, all these stations were used, apart from the stations of the so-called "validation set" as used in CAMS (see Section 3.2). Only the stations with annual data coverage of at least 75 percent have been used, both for the mapping and for the validation.

Table 3.2 shows the number of the stations used in both mapping and validation. In the mapping, rural background stations are used for the rural layer, urban and suburban stations for the urban background layer and urban and suburban traffic stations for the urban traffic layer (Section 2.1).

For validation of the maps, the CAMS "validation set" is used in this paper, being the set of stations not used in the mapping. Next to this validation, cross-validation is additionally applied, based on a subset of the stations used in mapping. The subset consists of all stations used in mapping, apart from the so-called "assimilation set" as used in CAMS in data assimilation (as described in Table 2.2), and in the case of $PM_{2.5}$ the stations located in Turkey. The reason for not using the Turkish $PM_{2.5}$ stations in the subset is that the area of Turkey is not mapped for $PM_{2.5}$, due to the lack of rural $PM_{2.5}$ stations in Turkey, see Horálek et al. (2020). For detailed description of the validation approaches and for the motivation of the subset selection, see Section 3.2.

*Table 3.2 Number of stations selected for each station type, as used in mapping and validation, for $PM_{10}$ (upper left), $PM_{2.5}$ (upper right), ozone (bottom left) and $NO_2$ (bottom right), 2017*

| Station type | $PM_{10}$ | | | | $PM_{2.5}$ | | | |
|---|---|---|---|---|---|---|---|---|
| | mapping | | | validation | mapping | | | validation |
| | cross-val. | other | total | | cross-val. | other | total | |
| Rural background | 171 | 139 | 310 | 52 | 108 | 74 | 182 | 20 |
| Urban/suburban background | 812 | 394 | 1206 | 179 | 392 | 196 | 588 | 98 |
| Urban/suburban traffic | | | 747 | | | | 330 | |

| Station type | Ozone | | | | $NO_2$ | | | |
|---|---|---|---|---|---|---|---|---|
| | mapping | | | validation | mapping | | | validation |
| | cross-val. | other | total | | cross-val. | other | total | |
| Rural background | 75 | 338 | 413 | 120 | 111 | 243 | 354 | 98 |
| Urban/suburban background | 215 | 618 | 833 | 306 | 323 | 692 | 1015 | 318 |
| Urban/suburban traffic | | | | | | | 977 | |

For the $PM_{2.5}$ mapping, 163 additional rural background, 683 additional urban/suburban background and additional 431 urban/suburban traffic $PM_{10}$ stations (at locations without $PM_{2.5}$ measurement) have been also used for the purpose of calculating the pseudo $PM_{2.5}$ station data.

Figures 3.3–3.6 show the spatial distribution of the rural and urban/suburban background stations used in the mapping (in blue and green) and in the validation (in red), for different pollutants. In all figures, the stations used (in blue) and not used (in green) in the cross-validation are distinguished.

Only true, not pseudo stations are shown. Traffic stations are not shown due to their relatively minor influence in the final 1x1 $km^2$ merged map and their non-occurrence in the validation set.

*Figure 3.3 Spatial distribution of $PM_{10}$ background stations used in mapping and validation, 2017*

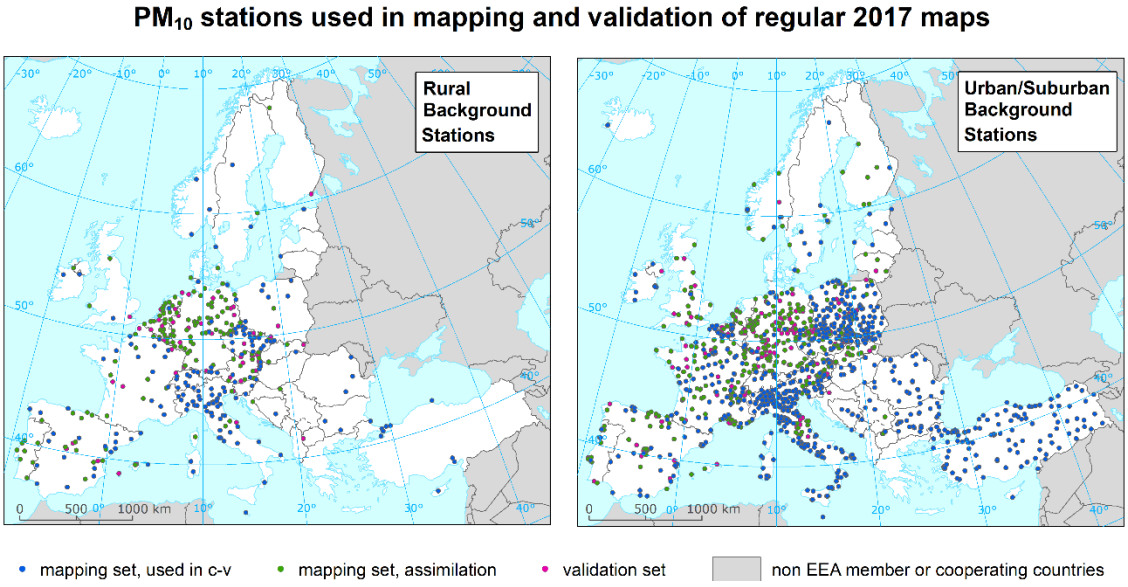


*Figure 3.4 Spatial distribution of $PM_{2.5}$ background stations used in mapping and validation, 2017*

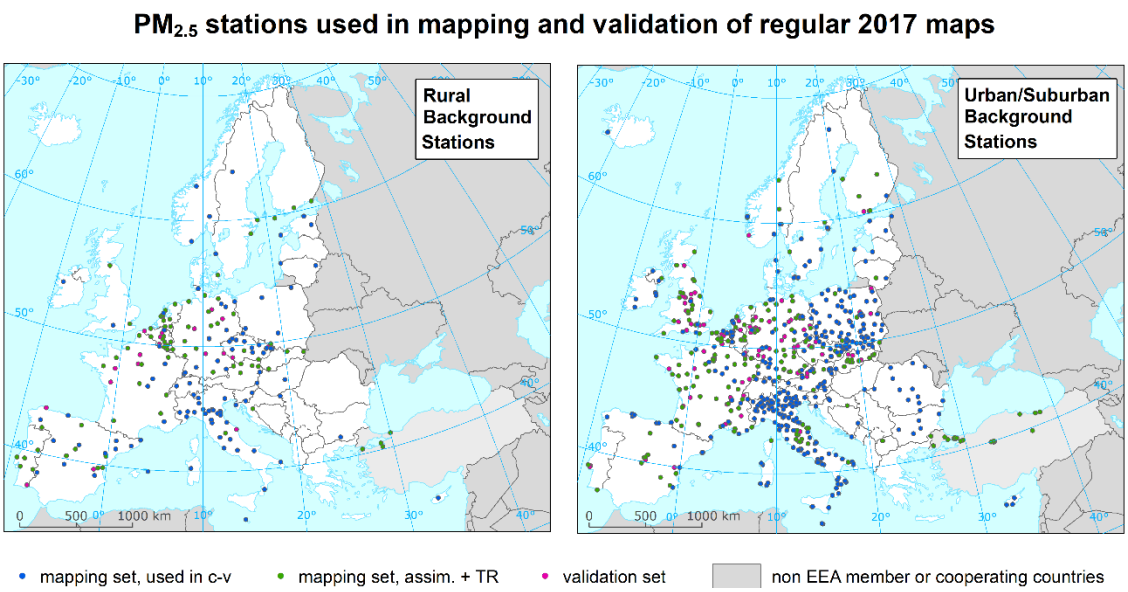

*Figure 3.5 Spatial distribution of ozone background stations used in mapping and validation, 2017*

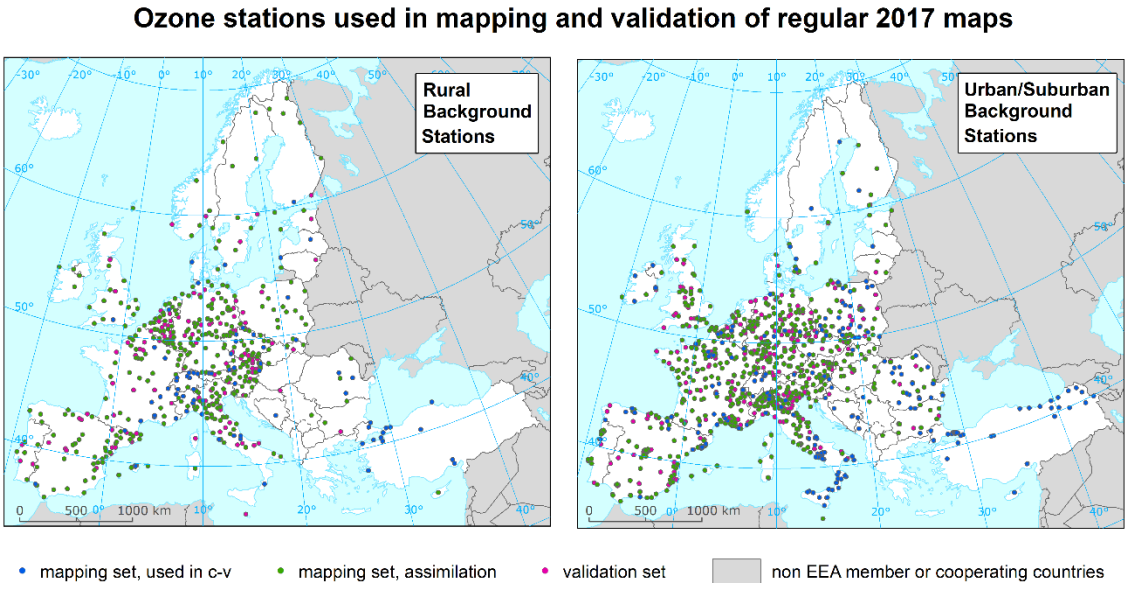


*Figure 3.6 Spatial distribution of $NO_2$ background stations used in mapping and validation, 2017*

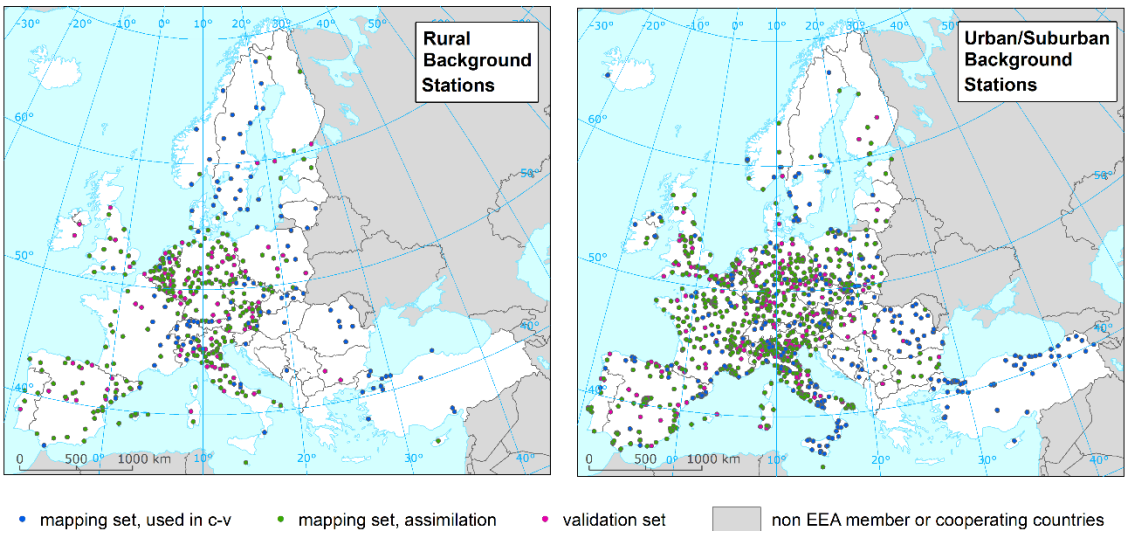


### 3.1.2 Chemical transport modelling data

**CAMS Forecast and Reanalysis Modelling Data**

We use the CAMS Ensemble Forecast and Interim Reanalysis modelling data in the RIMM air quality mapping methodology. We have downloaded the CAMS Ensemble Forecast and Interim Reanalysis for 2017 from the CAMS data archive (Copernicus, 2019). The forecast data is downloaded in GRIB2 format and then subjected to post-processing to create a complete time series of the data in NetCDF format. The interim reanalysis data is available for download as NetCDF and required no post-processing.

The forecast and reanalysis products are available at hourly intervals and have a spatial resolution of 0.1 × 0.1°. All of the models used in the CAMS Ensemble products were ran using the TNO-MACC emissions representative of 2011 (Kuenen et al., 2014). The CAMS Ensemble modelling products are described in further detail in Section 2.2.

**EMEP MSC-W modelling data**

The chemical dispersion model used in this paper is the EMEP MSC-W (formerly called Unified EMEP) model (version rv4.17a), which is an Eulerian model. Simpson et al. (2012) and https://github.com/metno/emep-ctm describe the model in more detail. Emissions for the year 2016 (Mareckova et al., 2018) are used and the model is driven by ECMWF meteorology for the relevant year 2017. EMEP (2018) provides details on the EMEP modelling for 2017. The resolution of this model run is 0.1° x 0.1°, i.e. circa 10x10 $km^2$. The model run for a year Y based on emission of a year Y-1 and meteorology of a year Y is available in the beginning of September of a year Y+1.

All modelling data have been aggregated into the annual statistics and converted to 1x1 $km^2$ grid resolution: the data in 0.1° x 0.1° resolution have been imported into *ArcGIS* and transformed into the ETRS89-LAEA5210 projection, subsequently converted into a 100x100 $m^2$ resolution raster grid and spatially aggregated into the reference EEA 1x1 $km^2$ grid. The pollutants and parameters used are the same as for the monitoring data

### *3.1.3 Other supplementary data*

**Altitude**

We use the altitude data field (in m) of Global Multi-resolution Terrain Elevation Data 2010 (GMTED2010), with an original grid resolution of 15x15 arcseconds coming from U.S. Geological Survey Earth Resources Observation and Science, see Danielson et al. (2011). The data were converted into the EEA reference grid in 1x1 $km^2$ grid resolution, as described in Horálek et al. (2020). Next to this, another aggregation has been executed based on the 1x1 $km^2$ grid cells, i.e., the floating average of the circle with a radius of 5 km around all relevant grid cells.

**Meteorological data**

The meteorological parameters used are *wind speed* (annual average for 2017, in $m.s^{-1}$) and *surface net solar radiation* (annual average of daily sum for 2017, $MWs.m^{-2}$). The daily data in resolution 15x15 arc-seconds were extracted from the Meteorological Archival and Retrieval System (MARS) of ECMWF. The data have been imported into ArcGIS as a point shapefile. Each point represents the centre of a grid cell. The shapefile has been converted into ETRS89-LAEA5210 projection, converted into a 100x100 $m^2$ resolution raster grid and spatially aggregated into the reference EEA 1x1 $km^2$ grid.

**Satellite data**

The annual average $NO_2$ dataset was constructed from data acquired by the *OMI* instrument onboard the Aura platform. The OMNO2d product generated by NASA was used as a basis, NASA (2019). The tropospheric column was used. All the orbits within a given day (typically observed between 13:00 and 14:00 local time) are mapped into a 0.25x0.25 degrees grid. For details, see Horálek et al. (2020). The parameter used is:

$NO_2$ – annual average tropospheric vertical column density (VCD) [number of $NO_2$ molecules per $cm^2$ of earth surface], year 2017 (aggregated from daily data).

**Population density**

Population density (in inhabitants.km$^{-2}$, census 2011) is based on Geostat 2011 grid dataset (Eurostat, 2014). The dataset is in 1x1 km$^2$ resolution, in the EEA reference grid. For regions not included in the Geostat 2011 dataset we use as alternative sources JRC (2009) and ORNL (EEA, 2008) data. For details, see Horálek et al. (2020). Next to the basic resolution of 1x1 km$^2$, the floating averaging of the circle with radius 5 km around all individual 1x1 km$^2$ grid cells has been prepared.

**Land cover**

CORINE Land Cover 2012 – grid 100 x 100 m$^2$, Version 18.5 (09/2016) is used (EEA, 2016). Like in Horálek et al. (2020), the 44 CLC classes have been re-grouped into the 8 more general classes. In this paper we use five of these general classes, namely High density residential areas (HDR), Low density residential areas (LDR), Agricultural areas (AGR), Natural areas (NAT), Traffic areas (TRA). For details, see Horálek et al. (2020). Two aggregations are used, i.e. into 1x1 km$^2$ grid and into the circle with radius of 5 km. For each general CLC class we spatially aggregated the high land use resolution into the 1x1 km EEA standard grid resolution. The aggregated grid square value represents for each general class the total area of this class as percentage of the total 1x1 km square area.

**Road data**

GRIP (i.e. Global Roads Inventory Dataset) vector road type data is used (Meijer et al., 2018). Based on the GRIP data, *ratio of area influenced by traffic* based on buffers around the roads is used. For details, see Horálek (2020).

### *3.1.4 Synthesis on the timing of observations*

The timing of availability of modelling products and observation datasets is summarized in Table 3.3. In the table, the availability of the EMEP, CAMS Ensemble Forecast (CAMS-FC), CAMS Ensemble Interim Reanalysis (CAMS-IRA) and CAMS Ensemble validated reanalysis (CAMS-VRA) modelling products is presented, together with the E2a and E1a AQ e-reporting observation datasets. The table shows that the earliest maps for the previous year (YY-1) could be produced with UTD observation (E2a) and CAMS Near real time production (CAMS-FC) as early as in January of the year YY (albeit with the major drawback of not relying upon validated data). The maps relying on validated observations could be produced in April of the next year (YY+1) based on either EMEP, CAMS-FC or CAMS-IRA model results.

*Table 3.3 Timing of availability of modelling products and observation datasets*

| | 01/YY | 02/YY | 03/YY | 04/YY | 05/YY | 06/YY | 07/YY | 08/YY | 09/YY | 10/YY | 11/YY | 12/YY |
|---|---|---|---|---|---|---|---|---|---|---|---|---|
| Model | CAMS-FC (YY-1) | | CAMS-IRA (YY-1) | | | | | | CAMS-VRA (YY-2)<br>EMEP (YY-1) | | | |
| Observations | E2a (YY-1) | | E1a* (YY-2) | | | | | | | | | |

*) EEA intends to provide the E1a data earlier.

## 3.2 Comparison Approach

It this report, the evaluation of the maps and their mutual comparison are executed primarily by applying the validation set of the stations not used in the mapping. In addition, the 'leave-one-out' cross-validation and the simple comparison between the measurement and mapped resp. modelled values is also used. All comparisons are done separately for rural and urban background stations. Traffic stations are not used in the comparisons, due to their limited impact in the 1x1 km$^2$ resolution maps. For the number of the stations used in the comparisons, see Section 3.1.1 (Tables 3.1 and 3.2).

The basic evaluation of the maps is based on the simple *point observation – grid prediction* comparison between point measurement data *at stations not used in mapping* (and model reanalysis) and gridded prediction values of the relevant RIMM map (or CAMS Ensemble model output, in Chapter 5). For comparisons of the validated maps in different variants (Section 4.2) and the RIMM mapping with the CAMS Ensemble model results (Chapter 5), for all pollutants, the "validation set" of the stations as applied in CAMS for 2017 data is used. The stations of this set have not been used in the reanalysis in CAMS. Similarly, for comparison purposes, they are not used in the creation of the RIMM spatial maps, which are analysed in Section 4.2 and Chapter 5 (i.e. regular maps). For comparisons of the interim maps (Section 4.1), a validation set is created using the stations with E1a data that are not included in the E2a data set (as applied in the interim mapping).

Additionally, the *point observation – point cross-validation prediction* is applied for comparisons of different RIMM variants (Chapter 4). This comparison is performed based on the *stations used in the RIMM mapping* (or a specific subset of these stations, see below), using the 'leave-one-out' cross-validation: The cross-validation method computes the spatial interpolation for each measurement point from all available information except from the point in question, i.e. it withholds one data point and then makes a prediction at the spatial location of that point. The prediction is compared with the measurement value. This procedure is repeated for all measurement points in the available set. Based on this, the quality of the predicted values is evaluated. The cross-validation analysis of Chapter 5 is based on all stations used in the RIMM mapping. For the comparisons of different variants of RIMM mapping (Chapter 4), the stations of the "validation set" of the stations as applied in CAMS (Section 4.1), resp. the stations used in the mapping apart from the stations of the CAMS "assimilation set" (Section 4.2) are applied. The reason for the exclusion of the CAMS assimilation set is to avoid the underestimation of the mapping uncertainty for the variant using the CAMS-Ensemble interim reanalysis: these stations have been already used in the reanalysis.

In Chapter 5, next to the evaluation based on the CAMS validation set, we also apply simple *point observation – grid prediction* comparison based on all stations. For RIMM (which uses all stations in mapping), we apply *point observation – grid cross-validation prediction*, for consistency resons.

For all comparisons, the main indicators used are *root mean squared error* (RMSE), *relative root mean squared error* (RRMSE) and *bias*:

$$RMSE = \sqrt{\frac{1}{N}\sum_{i=1}^{N}(\hat{Z}(s_i) - Z(s_i))^2} \qquad RRMSE = \frac{RMSE}{\frac{1}{N}\sum_{i=1}^{N} Z(s_i)} \cdot 100$$

$$Bias = \frac{1}{N}\sum_{i=1}^{N}(\hat{Z}(s_i) - Z(s_i)) \qquad (3.1)$$

where $Z(s_i)$ is the observed air quality indicator value at the $i^{th}$ point,

$\hat{Z}(s_i)$ is the estimated air quality indicator value at the $i^{th}$ point,

$N$ is the number of the observational points used in the validation set.

RMSE and bias are expressed in absolute units, *RRMSE* is expressed in percent.

Other indicators are the coefficient of determination $R^2$ and the regression equation parameters *slope* and *intercept*, following from the scatter plot between the predicted and the observed concentrations.

Lower RMSE and RRMSE and higher $R^2$ generally indicate better performance; bias closer to zero is also an indication of better performance. Furthermore, the slope should be as close to *1* as possible and the intercept as close to *0* as possible.

# 4 Comparison of RIMM Spatial Mapping Results Using EMEP and CAMS Modelling Results

## 4.1 Preliminary Maps

In this section, we examine the interim (also referred to as "preliminary") maps created based on the E2a (UTD) measurement data (Section 3.1.1) and CAMS Ensemble resp. EMEP modelling data (Section 3.1.2), together with other supplementary data (Section 3.1.3). The reason of this examination is a potential creation of spatial maps in preliminary version in the first months of the year subsequent to the mapped year, i.e. more than one year earlier compared to the official maps based on the validated E1a data. Such preliminary maps are compared with the official reported E1a data and with the maps created based on them. The analysis is performed for $PM_{10}$ annual average and $NO_2$ annual average, for 2017 data. Section 4.1.1 presents the analysis for $PM_{10}$, while Section 4.1.2 for $NO_2$.

For both pollutants, the RIMM spatial mapping procedure has been carried out using three different chemical transport model outputs as described in Section 3.1.2, namely the following variants:

- RIMM using EMEP model output, labelled (E)
- RIMM using CAMS Ensemble Forecast, labelled (C-FC)
- RIMM using CAMS Ensemble Interim Reanalysis, labelled (C-IRA)

The evaluation of the maps and their mutual comparison is based primarily on the E1a station data not included in the E2a date set. In addition, the evaluation based on the validation set as used in CAMS is executed, using the 'leave-one-out' cross-validation (see Section 3.2).

### *4.1.1 $PM_{10}$ annual average*

Table 4.1 presents the technical details of the interim spatial RIMM maps using different model outputs. It shows the estimated parameters of the multiple linear regression (c, $a_1$, $a_2$, …) and of the residual kriging (nugget, sill, range) and includes the statistical indicators of the regression part of the mapping.

*Table 4.1 Parameters of linear regression and spatial interpolation (ordinary kriging) in RIMM mapping of $PM_{10}$ annual average for 2017 preliminary maps in rural background, urban background and urban traffic areas for mapping variants using different CTM model outputs*

| Linear Regr. Model + OK of residuals | (E) EMEP | | | (C-F) CAMS-ENS forecast | | | (C-IR) CAMS-ENS int. rean. | | |
|---|---|---|---|---|---|---|---|---|---|
| | rural | urb. b. | urb. tr. | rural | urb. b. | urb. tr. | rural | urb. b. | urb. tr. |
| | coeff. | coeff. | coeff. | coeff. | coeff. | coeff. | coeff. | coeff. | coeff. |
| c (constant) | 7.83 | 2.01 | 2.23 | 7.85 | 1.53 | 1.94 | 5.85 | 0.80 | 1.88 |
| a1 (CTM model) | 0.368 | 0.397 | 0.409 | 0.561 | 0.594 | 0.581 | 0.835 | 0.839 | 0.547 |
| a2 (altitude_1km) | -0.0004 | | *n. sign.* | -0.0003 | | *n. sign.* | -0.0002 | | *n. sign.* |
| a3 (wind speed) | *n. sign.* | | -0.040 | *n. sign.* | | -0.068 | *n. sign.* | | -0.053 |
| a4 (rel. humidity) | -0.062 | | | -0.068 | | | -0.055 | | |
| a5 (CLC_NAT_1km) | -0.002 | | | -0.002 | | | -0.002 | | |
| **Adjusted $R^2$** | **0.47** | **0.15** | **0.30** | **0.49** | **0.21** | **0.37** | **0.60** | **0.40** | **0.37** |
| **St. Err. [µg.m$^{-3}$]** | **0.244** | **0.291** | **0.270** | **0.24** | **0.28** | **0.25** | **0.21** | **0.24** | **0.26** |
| Nugget | 0.022 | 0.018 | 0.010 | 0.018 | 0.020 | 0.005 | 0.019 | 0.013 | 0.003 |
| Sill | 0.054 | 0.058 | 0.045 | 0.046 | 0.054 | 0.040 | 0.038 | 0.042 | 0.041 |
| Range [km] | 900 | 210 | 290 | 230 | 220 | 290 | 280 | 260 | 410 |

Note: Grey empty cells indicate variables not used in the variant of the linear regression model.

Map 4.1 presents the final merged interim maps of the $PM_{10}$ annual average, as created using the three different models.

*Map 4.1 Interim concentration map of $PM_{10}$ annual average, 2017, RIMM methodology using E2a (UTD) measurement data and EMEP (top), CAMS-ENS forecast (middle) and CAMS-ENS interim reanalysis (bottom) model outputs*

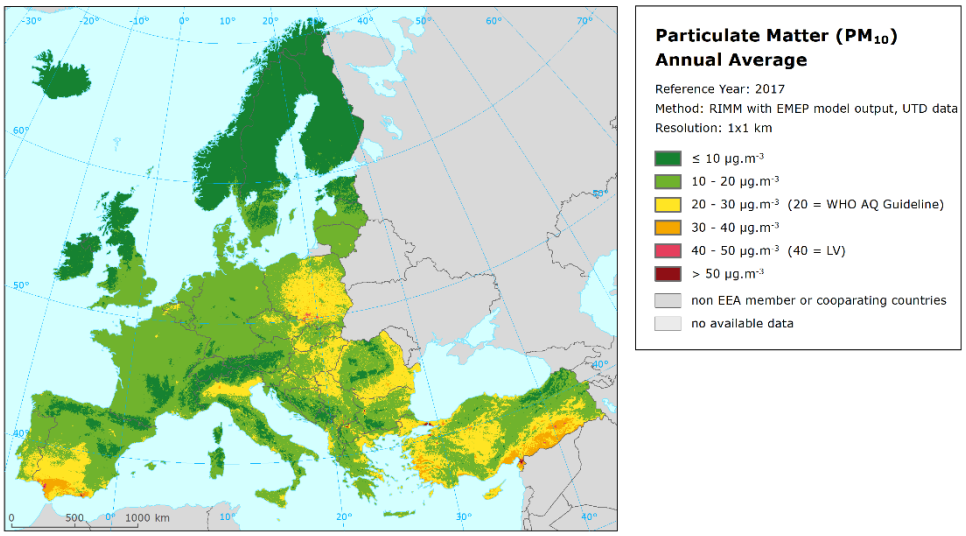


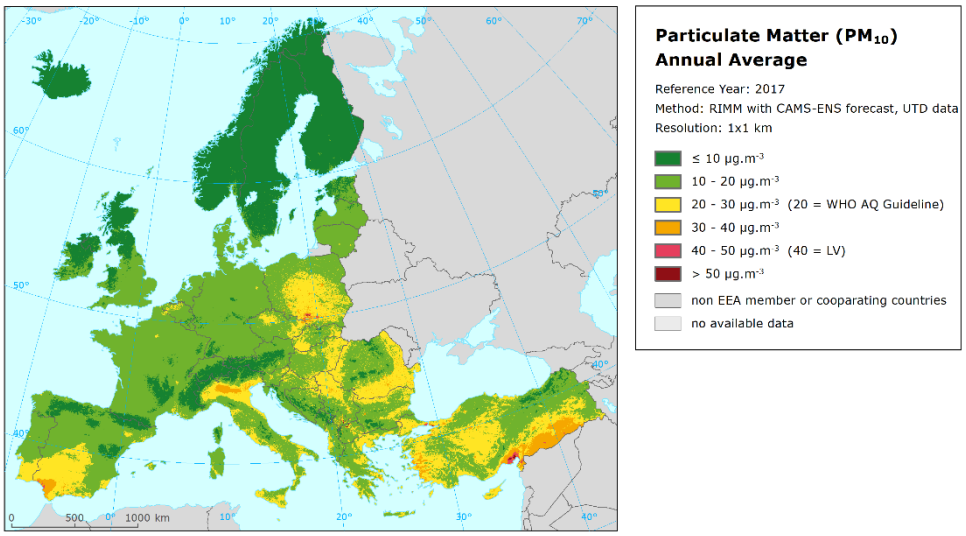


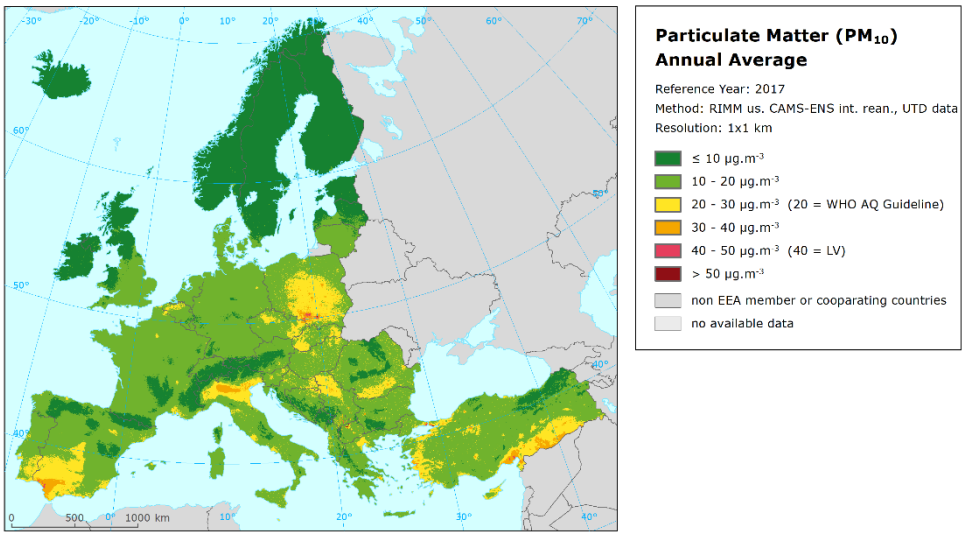

Table 4.2 presents the evaluation and comparison of the interim maps using three different models, based on the E1a station data not included in the E2a data set, for different areas types. Next to the analysis for the entire mapping area, we have executed the comparison separately for two distinct areas: for areas covered by the E2a data (i.e. for entire area without Italy, Bulgaria, Romania, Serbia, Baltic countries, Cyprus and Turkey) and for areas not covered by the E2a data (i.e. for Italy, Bulgaria, Romania, Serbia, Baltic countries, Cyprus and Turkey). Additionally, for areas not covered by the E2a data, we show separately the urban results for areas outside Turkey and for Turkey, due to much higher uncertainty for Turkey compared to the other areas (similarly like in regular maps, Horálek et al., 2020).

*Table 4.2 Comparison of different model used in interim RIMM spatial mapping showing RMSE, RRMSE, bias, $R^2$ and linear regression from validation scatter plots for $PM_{10}$ annual mean in rural background (top) and urban background (bottom) areas, 2017. Validation set of stations has not been used in mapping. Units: $\mu g.m^{-3}$ except RRMSE and $R^2$.*

| Model used in RIMM spatial mapping | | Rural background areas – entire area | | | | |
|---|---|---|---|---|---|---|
| | | RMSE | RRMSE | Bias | $R^2$ | Regr. eq. |
| (E) | EMEP | 5.0 | 29.6% | -0.3 | 0.626 | y = 0.609x + 6.29 |
| (C-FC) | CAMS Ensemble forecast | 4.6 | 27.2% | 0.8 | 0.692 | y = 0.694x + 6.00 |
| (C-IRA) | CAMS Ensemble interim reanalysis | 4.5 | 26.6% | -0.2 | 0.700 | y = 0.651x + 5.71 |
| | | Rural background areas covered by E2a data | | | | |
| | | RMSE | RRMSE | Bias | $R^2$ | Regr. eq. |
| (E) | EMEP | 2.6 | 17.5% | 0.4 | 0.804 | y = 0.737x + 4.14 |
| (C-FC) | CAMS Ensemble forecast | 2.6 | 17.8% | 0.4 | 0.807 | y = 0.769x + 3.61 |
| (C-IRA) | CAMS Ensemble interim reanalysis | 2.6 | 17.6% | 0.3 | 0.811 | y = 0.790x + 3.22 |
| | | Rural background areas not covered by E2a data | | | | |
| | | RMSE | RRMSE | Bias | $R^2$ | Regr. eq. |
| (E) | EMEP | 7.0 | 32.9% | -2.6 | 0.564 | y = 0.573x + 6.39 |
| (C-FC) | CAMS Ensemble forecast | 5.8 | 27.6% | 0.2 | 0.643 | y = 0.616x + 8.29 |
| (C-IRA) | CAMS Ensemble interim reanalysis | 5.7 | 26.8% | -1.8 | 0.716 | y = 0.595x + 6.804 |
| | | | | | | |
| Model used in RIMM spatial mapping | | Urban background areas – entire area | | | | |
| | | RMSE | RRMSE | Bias | $R^2$ | Regr. eq. |
| (E) | EMEP | 12.9 | 43.0% | -5.0 | 0.378 | y = 0.315x + 15.54 |
| (C-FC) | CAMS Ensemble - forecast | 12.2 | 40.7% | -4.0 | 0.430 | y = 0.325x + 16.24 |
| (C-IRA) | CAMS Ensemble - interim reanalysis | 13.8 | 46.1% | -5.9 | 0.302 | y = 0.272x + 15.92 |
| | | Urban background areas covered by E2a data | | | | |
| | | RMSE | RRMSE | Bias | $R^2$ | Regr. eq. |
| (E) | EMEP | 5.5 | 22.5% | -1.0 | 0.687 | y = 0.682x + 6.75 |
| (C-F) | CAMS Ensemble - forecast | 5.8 | 23.5% | -1.0 | 0.658 | y = 0.658x + 7.35 |
| (C-IR) | CAMS Ensemble - interim reanalysis | 6.2 | 25.5% | -1.4 | 0.611 | y = 0.661x + 6.88 |
| | | Urban background areas not covered by E2a data | | | | |
| | | RMSE | RRMSE | Bias | $R^2$ | Regr. eq. |
| (E) | EMEP | 16.4 | 48.0% | -7.9 | 0.281 | y = 0.227x + 18.38 |
| (C-FC) | CAMS Ensemble - forecast | 15.3 | 45.0% | -6.2 | 0.336 | y = 0.222x + 20.32 |
| (C-IRA) | CAMS Ensemble - interim reanalysis | 17.5 | 51.3% | -9.2 | 0.222 | y = 0.186x + 18.48 |
| | | Urban background areas not covered by E2a data, apart from TR | | | | |
| | | RMSE | RRMSE | Bias | $R^2$ | Regr. eq. |
| (E) | EMEP | 8.0 | 30.3% | -3.3 | 0.215 | y = 0.268x + 15.94 |
| (C-F) | CAMS Ensemble - forecast | 6.5 | 24.6% | -1.1 | 0.379 | y = 0.383x + 15.11 |
| (C-IR) | CAMS Ensemble - interim reanalysis | 7.0 | 26.7% | -3.4 | 0.431 | y = 0.431x + 11.53 |
| | | Urban background areas not covered by E2a data, Turkey | | | | |
| | | RMSE | RRMSE | Bias | $R^2$ | Regr. eq. |
| (E) | EMEP | 25.3 | 50.3% | -16.8 | 0.000 | not significant regression |
| (C-FC) | CAMS Ensemble - forecast | 29.0 | 57.7% | -21.4 | 0.002 | not significant regression |
| (C-IRA) | CAMS Ensemble - interim reanalysis | 26.4 | 52.4% | -17.7 | 0.001 | not significant regression |

Note: Areas not covered by E2a data are comprised of IT, BG, RO, RS, LT, LV, EE, CY and TR.

Lower RMSE and RRMSE and higher $R^2$ generally indicate better performance; bias closer to zero is also an indication of better performance. Furthermore, the slope should be as close to *1* as possible and the intercept as close to *0* as possible. The table areas highlighted by green shows the statistics of the RIMM variant that provides the best performance. For the green highlighting, the ad hoc criterion of more than ca. 5% difference (in terms of RMSE, RRMSE and $R^2$) and 0.2 µg.m$^{-3}$ (in terms of RMSE and bias) for result distinguishing has been applied.

Looking at the statistics, one can state that the results are quite satisfactory in general. Nevertheless, the performance of the interim map varies between different areas (see also below discussion of Map 4.2). As expected, the mapping skills are poorer in the areas with no E2a data, both for rural and for urban areas.

In the more detailed analysis of areas not covered by the E2a data, large uncertainties in urban areas has been found, whatever the modelled map used, for the area of Turkey, namely RRMSE of 50% – 58% and bias of between -14 µg.m$^{-3}$ and -25 µg.m$^{-3}$. The uncertainties in urban areas for areas outside Turkey are considerable smaller.

It can be seen that in the areas covered by the E2a data, all three variants give quite similar results. In the areas not covered by the E2a data, the variants using CAMS Ensemble model results give better results compared to the variant using EMEP; the best results in terms of bias are given by the (C-FC) variant.

Figure 4.1 shows the scatter plots of predicted mapped values against the E1a measurement data at the stations of the validation set (for the entire area).

*Figure 4.1 Correlation between RIMM using EMEP (left), CAMS Ensemble Forecast (middle) or CAMS Ensemble Interim Reanalysis (right) mapping values (y-axis) versus measurements from rural (top), resp. urban/suburban (bottom) background stations (x-axis) from the validation set for $PM_{10}$ annual average 2017.*

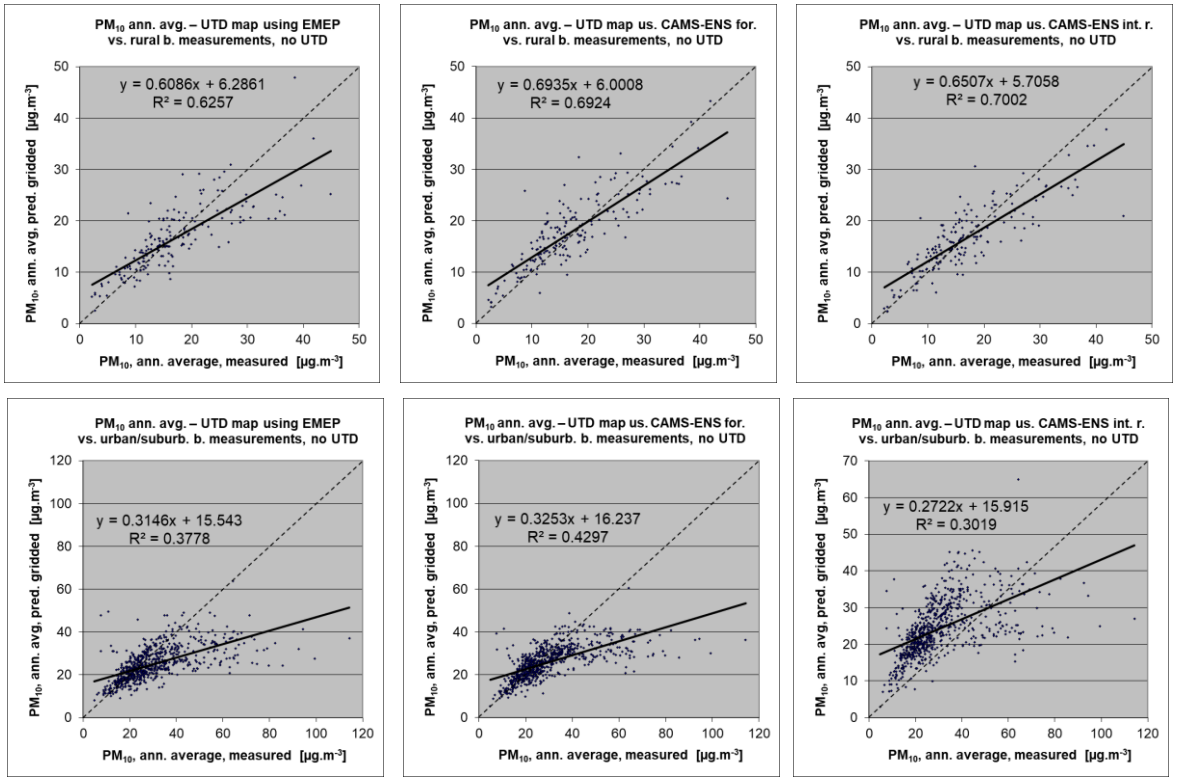

It can be seen that the results are better in the rural areas compared to the urban background areas.

Table 4.3 presents the additional evaluation of the interim maps in three variants, based on the validation set as used in CAMS (i.e. subset of the stations used in the mapping, see Section 3.2), using cross-validation, separately for rural and urban background areas. This validation applies for areas covered by the E2a (UTD) data only. As the E2a data only are used in the validation, the reservation mentioned in Section 3.1.1 does not apply here and the evaluation applies both for the final map and for the mapping procedure.

*Table 4.3 Comparison of different models used in interim RIMM spatial mapping showing RMSE, RRMSE, bias, $R^2$ and linear regression from cross-validation scatter plots based on the CAMS validation set of the stations for $PM_{10}$ annual mean in rural background (top) and urban background (bottom) areas, 2017. Units: µg.m$^{-3}$ except RRMSE and $R^2$.*

| Model used in RIMM spatial mapping | | Rural background areas | | | | |
|---|---|---|---|---|---|---|
| | | RMSE | RRMSE | Bias | $R^2$ | Regr. eq. |
| (E) | EMEP | 3.9 | 23.7% | -1.3 | 0.649 | y = 0.530x + 6.41 |
| (C-FC) | CAMS Ensemble forecast | 3.3 | 20.0% | -1.0 | 0.755 | y = 0.619x + 5.25 |
| (C-IRA) | CAMS Ensemble interim reanalysis | 3.0 | 18.2% | -1.1 | 0.810 | y = 0.669x + 4.34 |
| | | | | | | |
| **Model used in RIMM spatial mapping** | | **Urban background areas** | | | | |
| | | **RMSE** | **RRMSE** | **Bias** | **$R^2$** | **Regr. eq.** |
| (E) | EMEP | 3.1 | 15.9% | 0.2 | 0.706 | y = 0.787x + 4.30 |
| (C-FC) | CAMS Ensemble - forecast | 3.0 | 15.3% | 0.4 | 0.735 | y = 0.823x + 3.82 |
| (C-IRA) | CAMS Ensemble - interim reanalysis | 3.0 | 15.3% | 0.1 | 0.739 | y = 0.860x + 2.85 |

The results presented in Table 4.3 confirm that in the areas covered by the E2a (UTD) data, the quality of the spatial interim map is quite satisfactory.

Map 4.2 shows difference maps between the interim RIMM maps (in different variants) and the reference RIMM map (Horálek et al., 2020). One can see that the areas with poor coverage of E2a stations (see Figure 3.1) gives higher differences, e.g., a large areas of the Balkans, Italy and rural areas in Scandinavia.

Based on the results presented in this section, it can be concluded that the areas without E2a stations (especially Turkey, see the more detailed analysis above, but also other areas like the Balkans and Italy) show too high uncertainties to be visualised in the interim RIMM map (in all variants).

Potentially, the lack of E2a stations in these areas could be substituted by so-called pseudo stations, i.e. estimates in the points of stations with E1a data from a year Y-1 and lack of E2a data in a given year Y. Such an estimate would be done based on the relation between E2a data and validated E1a data from year Y-1 in the points of stations with both E2a data of a year Y and E1a data of a year Y-1. It is recommended to investigate such an approach.

*Map 4.2 Difference map of $PM_{10}$ annual average, 2017, interim RIMM maps using EMEP (top), CAMS Ensemble Forecast (middle) and CAMS Ensemble Interim Reanalysis (bottom) model outputs minus reference RIMM map*

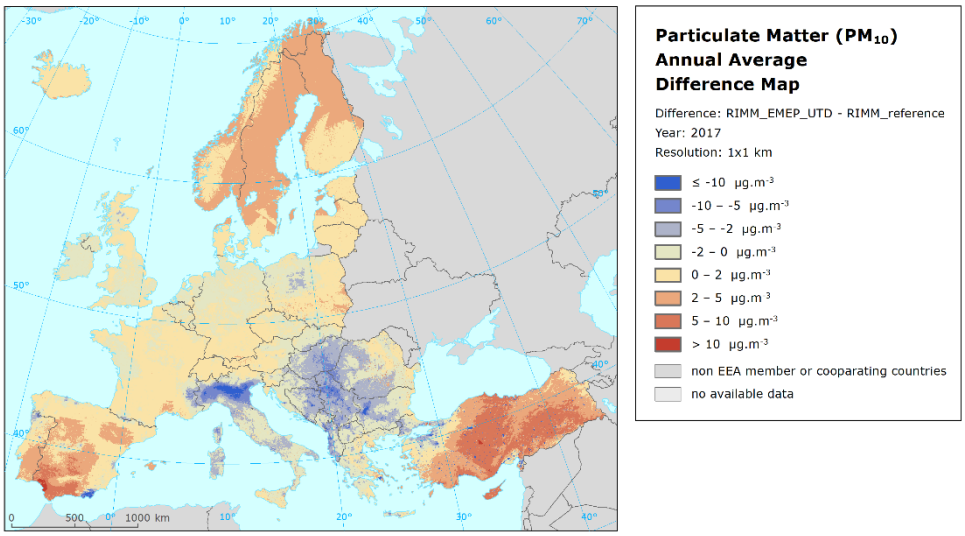


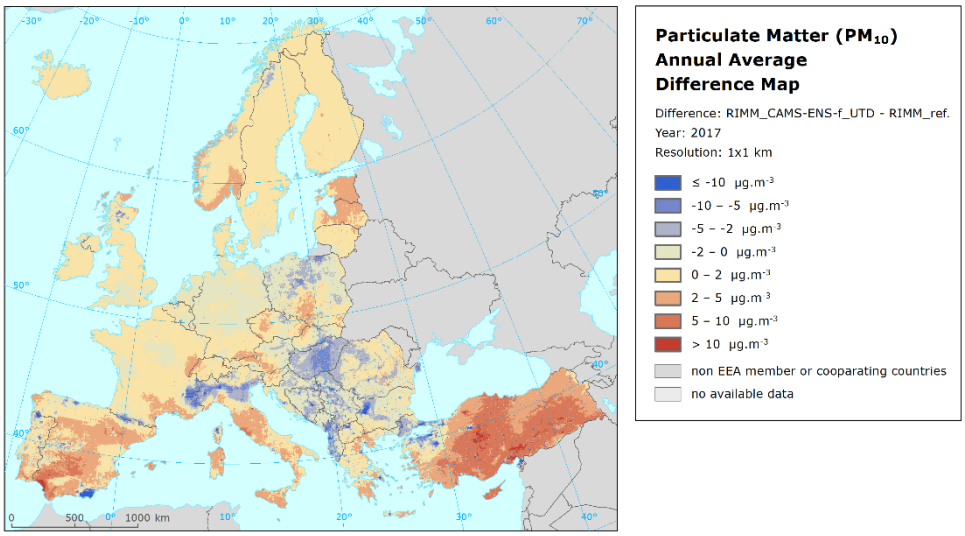


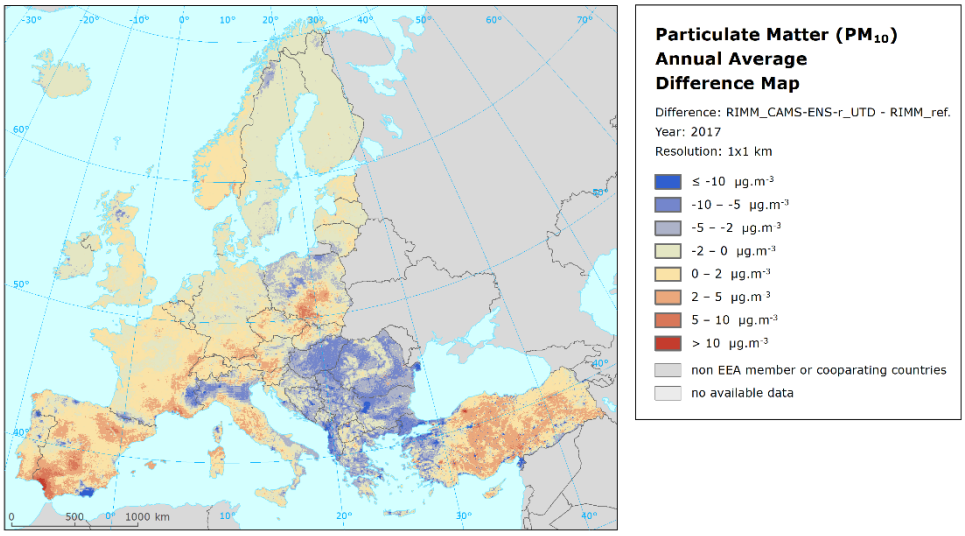

### 4.1.2 $NO_2$ annual average

Similar analysis as for $PM_{10}$ has been conducted for $NO_2$ as well. Table 4.4 presents the technical details of the interim spatial RIMM maps of $NO_2$ using different model outputs.

*Table 4.4 Parameters of linear regression and spatial interpolation (ordinary kriging) in RIMM mapping of $NO_2$ annual average for preliminary 2017 maps in rural background, urban background and urban traffic areas for mapping variants using different CTM model outputs*

| Linear Regr. Model + OK of residuals | (E) EMEP | | | (C-F) CAMS-ENS forecast | | | (C-IR) CAMS-ENS int. rean. | | |
|---|---|---|---|---|---|---|---|---|---|
| | rural | urb. b. | urb. tr. | rural | urb. b. | urb. tr. | rural | urb. b. | urb. tr. |
| | coeff. | coeff. | coeff. | coeff. | coeff. | coeff. | coeff. | coeff. | coeff. |
| c (constant) | 7.76 | 17.87 | 22.89 | 7.49 | 17.69 | 22.59 | 4.44 | 11.37 | 16.79 |
| a1 (CTM model) | 0.402 | 0.316 | 0.389 | 0.548 | 0.606 | 0.678 | 0.716 | 0.908 | 0.982 |
| a2 (altitude_1km) | -0.00856 | | | -0.00864 | | | -0.00827 | | |
| a3 (altitude_5km_r) | 0.00893 | | | 0.00897 | | | 0.00841 | | |
| a4 (wind speed) | -1.020 | -2.118 | -1.489 | -1.037 | -1.915 | -1.236 | -0.717 | -1.209 | -0.597 |
| a5 (population density) | 0.0026 | 0.0003 | | 0.0030 | 0.0002 | | 0.0025 | 0.0002 | |
| a6 (OMI satellite) | 1.029 | 1.006 | 1.046 | 0.524 | *n.sign.* | *n.sign.* | 0.544 | *n.sign.* | *n.sign.* |
| a7 (LC_NAT_1km) | | -0.0375 | | | -0.0462 | | | -0.0455 | |
| a8 (LC_AGR_1km) | | -0.0274 | | | -0.0333 | | | -0.0278 | |
| a9 (LC_TRA_1km) | | 0.1069 | | | 0.1073 | | | 0.0763 | |
| a10 (LC_LDR_5km_r) | 0.0583 | 0.0500 | 0.2173 | 4.5796 | 0.0480 | 0.2228 | *n. sign.* | *n.sign.* | 0.1747 |
| a11 (LC_HDR_5km_r) | | *n.sign.* | 0.1601 | | 0.0786 | 0.2123 | | *n.sign.* | 0.1416 |
| a12 (LC_NAT_5km_r) | -0.0408 | | | -0.0379 | | | -0.0334 | | |
| **Adjusted $R^2$** | **0.776** | **0.599** | **0.401** | **0.776** | **0.604** | **0.384** | **0.804** | **0.676** | **0.436** |
| **St. Err. [µg.m$^{-3}$]** | **2.36** | **4.76** | **9.50** | **2.36** | **4.73** | **9.63** | **2.21** | **4.28** | **9.22** |
| Nugget | 5 | 16 | 61 | 5 | 15 | 51 | 4 | 14 | 56 |
| Sill | 5 | 19 | 91 | 5 | 18 | 95 | 4 | 15 | 85 |
| Range [km] | 580 | 0 | 160 | 580 | 230 | 320 | 470 | 250 | 150 |

Note: Grey empty cells indicate variables not used in the variant of the linear regression model.

Map 4.3 presents the final merged interim maps of the $NO_2$ annual average, as created using the three different models.

Table 4.5 presents the evaluation and comparison of the interim maps using three different models, for different areas resp. station types. Like for $PM_{10}$, next to the analysis for the entire mapping area, separate comparison for two distinct areas we have been executed: first, for areas covered by E2a data (i.e. without Italy, Bulgaria, Romania, Serbia, Cyprus and Turkey) and for areas not covered by the E2a data (i.e. for Italy, Bulgaria, Romania, Serbia , Cyprus and Turkey). Additionally, like in the case of $PM_{10}$, for areas not covered by the E2a data, we present separately the urban results for areas outside Turkey and for Turkey, due to much higher uncertainty for Turkey compared to another areas.

*Map 4.3 Interim concentration map of $NO_2$ annual average, 2017, RIMM methodology using EMEP (top), CAMS Ensemble Forecast (middle) and CAMS Ensemble Interim Reanalysis (bottom) model outputs*

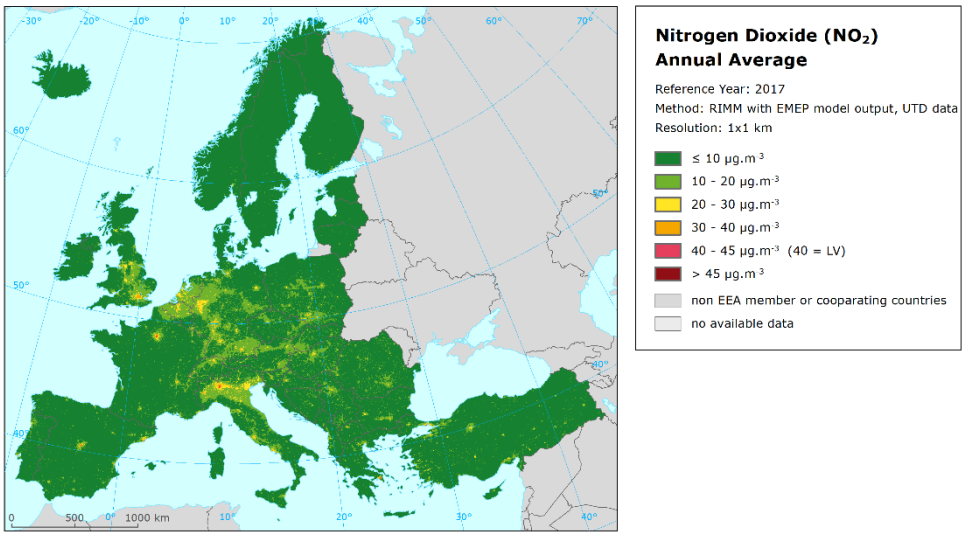


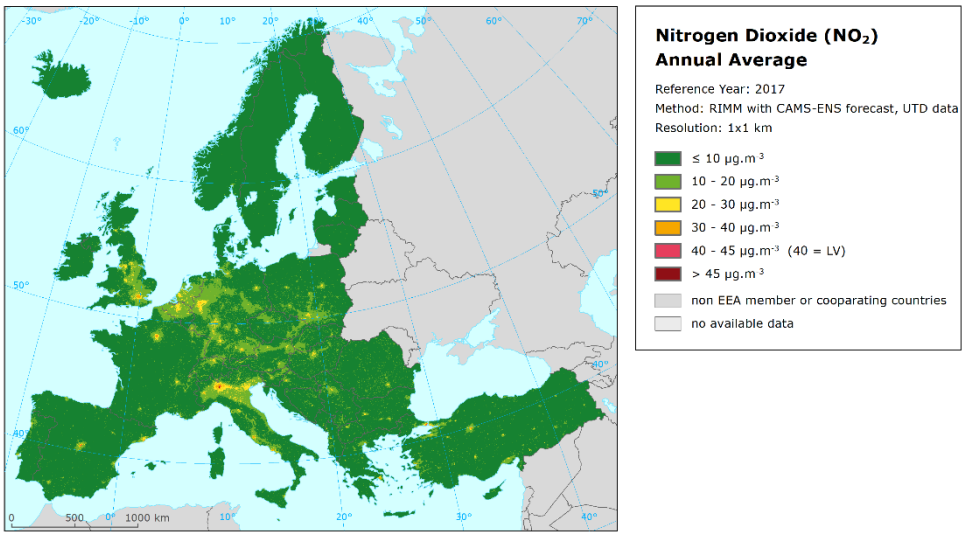


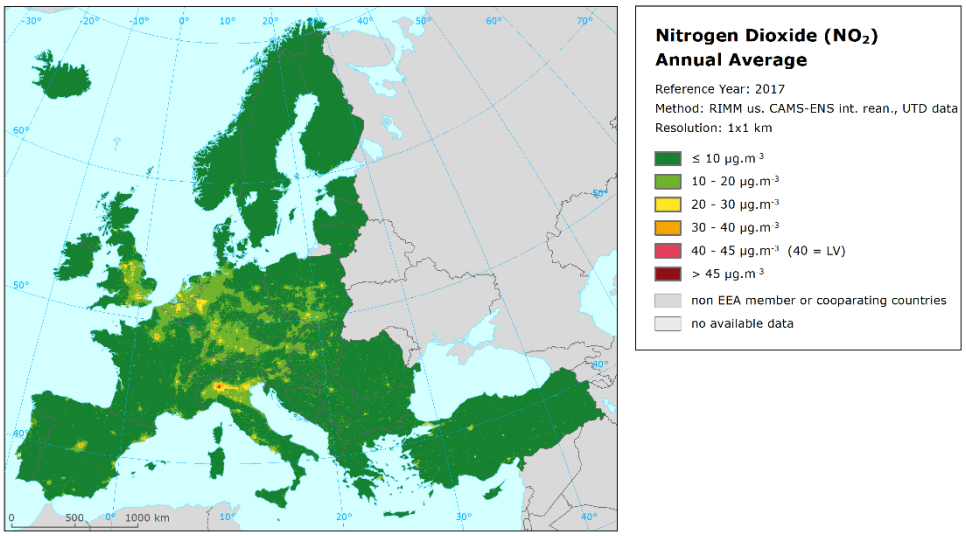

*Table 4.5 Comparison of different models used in interim RIMM spatial mapping showing RMSE, RRMSE, bias, $R^2$ and linear regression from validation scatter plots for $NO_2$ annual mean in rural background (top) and urban background (bottom) areas, 2017. Validation set of stations has not been used in mapping. Units: $\mu g.m^{-3}$ except RRMSE and $R^2$.*

| Model used in RIMM spatial mapping | | Rural background areas – entire area | | | | |
|---|---|---|---|---|---|---|
| | | RMSE | RRMSE | Bias | $R^2$ | Regr. eq. |
| (E) | EMEP | 4.0 | 45.2% | 1.0 | 0.705 | y = 0.718x + 3.50 |
| (C-FC) | CAMS Ensemble forecast | 3.8 | 42.9% | 0.8 | 0.730 | y = 0.750x + 3.03 |
| (C-IRA) | CAMS Ensemble interim reanalysis | 3.6 | 40.1% | 0.1 | 0.754 | y = 0.776x + 2.04 |
| | | Rural background areas covered by E2a data | | | | |
| | | RMSE | RRMSE | Bias | $R^2$ | Regr. eq. |
| (E) | EMEP | 2.8 | 42.2% | 0.6 | 0.821 | y = 0.887x + 1.35 |
| (C-FC) | CAMS Ensemble forecast | 2.7 | 41.5% | 0.3 | 0.814 | y = 0.819x + 1.45 |
| (C-IRA) | CAMS Ensemble interim reanalysis | 2.6 | 40.3% | 0.1 | 0.824 | y = 0.844x + 1.11 |
| | | Rural background areas not covered by E2a data | | | | |
| | | RMSE | RRMSE | Bias | $R^2$ | Regr. eq. |
| (E) | EMEP | 4.5 | 44.5% | 1.3 | 0.595 | y = 0.533x + 6.41 |
| (C-FC) | CAMS Ensemble forecast | 4.4 | 41.8% | 1.3 | 0.640 | y = 0.625x + 5.37 |
| (C-IRA) | CAMS Ensemble interim reanalysis | 4.2 | 38.5% | 0.0 | 0.668 | y = 0.698x + 3.30 |
| | | | | | | |
| Model used in RIMM spatial mapping | | Urban background areas – entire area | | | | |
| | | RMSE | RRMSE | Bias | $R^2$ | Regr. eq. |
| (E) | EMEP | 9.3 | 41.7% | -1.8 | 0.330 | y = 0.345x + 12.89 |
| (C-FC) | CAMS Ensemble - forecast | 9.0 | 40.2% | -1.6 | 0.373 | y = 0.395x + 11.95 |
| (C-IRA) | CAMS Ensemble - interim reanalysis | 9.9 | 44.0% | -3.4 | 0.325 | y = 0.381x + 10.52 |
| | | Urban background areas covered by E2a data | | | | |
| | | RMSE | RRMSE | Bias | $R^2$ | Regr. eq. |
| (E) | EMEP | 4.3 | 24.4% | 1.4 | 0.664 | y = 0.767x + 5.46 |
| (C-FC) | CAMS Ensemble - forecast | 4.2 | 23.7% | 1.2 | 0.669 | y = 0.747x + 5.67 |
| (C-IRA) | CAMS Ensemble - interim reanalysis | 4.1 | 23.3% | 0.2 | 0.651 | y = 0.727x + 5.01 |
| | | Urban background areas not covered by E2a data | | | | |
| | | RMSE | RRMSE | Bias | $R^2$ | Regr. eq. |
| (E) | EMEP | 10.8 | 44.1% | -3.1 | 0.266 | y = 0.470x + 10.54 |
| (C-FC) | CAMS Ensemble - forecast | 10.4 | 42.5% | -2.8 | 0.451 | y = 0.520x + 9.41 |
| (C-IRA) | CAMS Ensemble - interim reanalysis | 11.4 | 46.7% | -4.9 | 0.450 | y = 0.555x + 6.77 |
| | | Urban background areas not covered by E2a data, apart fromTR | | | | |
| | | RMSE | RRMSE | Bias | $R^2$ | Regr. eq. |
| (E) | EMEP | 7.3 | 32.6% | -1.3 | 0.415 | y = 0.290x + 14.27 |
| (C-FC) | CAMS Ensemble - forecast | 7.1 | 31.7% | -1.3 | 0.310 | y = 0.346x + 13.19 |
| (C-IRA) | CAMS Ensemble - interim reanalysis | 7.7 | 34.6% | -3.2 | 0.276 | y = 0.345x + 11.14 |
| | | Urban background areas not covered by E2a data, Turkey | | | | |
| | | RMSE | RRMSE | Bias | $R^2$ | Regr. eq. |
| (E) | EMEP | 20.5 | 59.5% | -11.7 | 0.074 | y = 0.098x + 19.34 |
| (C-FC) | CAMS Ensemble - forecast | 19.6 | 57.1% | -9.8 | 0.076 | y = 0.127x + 20.22 |
| (C-IRA) | CAMS Ensemble - interim reanalysis | 21.7 | 63.1% | -12.9 | 0.057 | y = 0.117x + 17.47 |

The results are quite satisfactory in general. Nevertheless, the performance of the interim map varies in different areas.

It can be seen that for the urban areas, the mapping skills are poorer in the areas with no E2a data. For rural areas, the uncertainty is quite similar in the areas covered and not covered by the E2a data. Comparing the different mapping variants, one can see quite similar results for all three variants, with slightly better performance of the variants using the CAMS Ensemble model outputs in the rural areas.

In a more detailed analysis for areas not covered by E2a data, large uncertainty of the map in urban areas for the area of Turkey has been ascertained for all three variants, namely RRMSE of 57% – 63% and bias of between -10 µg.m$^{-3}$ and -12 µg.m$^{-3}$. The mapping uncertainties in urban areas for areas outside Turkey are considerable smaller.

Figure 4.2 shows the scatter plots of predicted mapped values against the E1a measurement data at the stations of the validation set (for the entire area). It can be seen that the results are better in the rural areas compared to the urban background areas.

*Figure 4.2 Correlation between RIMM using EMEP (left), CAMS Ensemble Forecast (middle) or CAMS Ensemble Interim Reanalysis (right) mapping values (y-axis) versus measurements from rural (top), resp. urban/suburban (bottom) background stations (x-axis) from the validation set for $NO_2$ annual average 2017.*

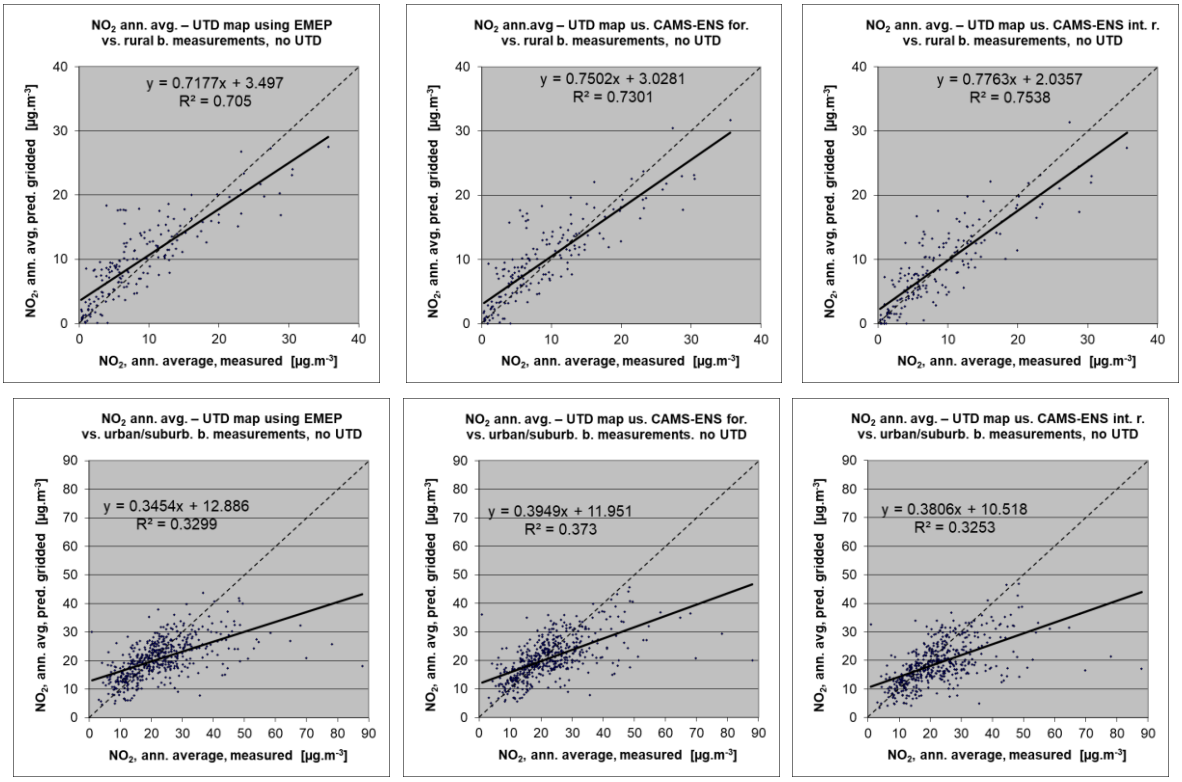


Table 4.6 presents the additional evaluation of the interim maps in three variants, based on the validation set as used in CAMS, using cross-validation, separately for rural and urban areas.

The results presented in Table 4.6 confirm that in the areas covered by the E2a (UTD) data, for which this table applies, the quality of the spatial interim map is satisfactory.

*Table 4.6 Comparison of different model used in interim RIMM spatial mapping showing RMSE, RRMSE, bias, $R^2$ and linear regression from cross-validation scatter plots based on the CAMS validation set of the stations for $NO_2$ annual mean in rural background (top) and urban background (bottom) areas, 2017. Units: $\mu g.m^{-3}$ except RRMSE and $R^2$.*

| Model used in RIMM spatial mapping | | Rural background areas | | | | |
|---|---|---|---|---|---|---|
| | | RMSE | RRMSE | Bias | $R^2$ | Regr. eq. |
| (E) | EMEP | 2.2 | 26.2% | 0.1 | 0.689 | y = 0.767x + 2.08 |
| (C-FC) | CAMS Ensemble forecast | 2.3 | 26.7% | 0.1 | 0.678 | y = 0.756x + 2.24 |
| (C-IRA) | CAMS Ensemble interim reanalysis | 2.6 | 30.3% | 0.5 | 0.616 | y = 0.744x + 2.74 |
| | | | | | | |
| **Model used in RIMM spatial mapping** | | **Urban background areas** | | | | |
| | | RMSE | RRMSE | Bias | $R^2$ | Regr. eq. |
| (E) | EMEP | 4.4 | 21.5% | -0.1 | 0.675 | y = 0.702x + 6.01 |
| (C-FC) | CAMS Ensemble - forecast | 4.5 | 21.8% | -0.2 | 0.665 | y = 0.668x + 6.61 |
| (C-IRA) | CAMS Ensemble - interim reanalysis | 4.5 | 21.8% | -0.6 | 0.670 | y = 0.693x + 5.71 |

Map 4.4 shows difference maps between the interim maps (in different variants) and the reference RIMM map (Horálek et al., 2020).

The differences shown in Map 4.4 are not so distinct as in the case of $PM_{10}$. However, one can see noticeable differences in some areas with no E2a data, e.g. in Italy and Turkey. One can see the different results for (C-IRA) variant in the Balkan area, compared to both (E) and (C-FC) variants.

Like in the case of $PM_{10}$, there is a need to improve the estimation of the areas with lack of the E2a stations. It is recommended to test the feasibility of an approach based on so-called pseudo stations, similarly like for $PM_{10}$.

### *4.1.3 Conclusion*

Preliminary/interim spatial interpolation (RIMM) air quality maps based on the UTD (E2a) measurement data can be constructed as early as March of the following year for the year in question (i.e. more than one year earlier than the validated maps), using any of the examined models, when available. The CAMS Ensemble Forecast is available in near real time, and so the entire year of model data is available in January of the following year, the CAMS Ensemble Interim Reanalysis is available in March of the following year, EMEP (based on emission of year Y-1) is available in September of the following year. In order to offer the earliest production date, the CAMS Ensemble Forecast could be a relevant candidate for the use in the potential interim mapping.

Due to the **lack of the E2a data in some areas, the quality of the interim maps in these areas is poorer** compared to the main part of Europe. Potentially, the lack of E2a stations in these areas could be substituted by so-called pseudo stations, i.e., by the estimates at the locations of E1a stations with no E2a data, based on the relation between E2a data and validated E1a data from year Y-1. It is recommended to investigate such an approach.

We have evaluated here the mapping techniques using preliminary observations and models, but an important decision lies within EEA to give the green light for potential production of exposure maps not relying on observations validated by the member states. Such potential interim maps should have to be treated as preliminary only and could not substitute the regular maps based on the official submitted data.

*Map 4.4 Difference map of $NO_2$ annual average, 2017, interim RIMM map using EMEP (top), CAMS Ensemble Forecast (middle) and CAMS Ensemble Interim Reanalysis (bottom) model outputs minus reference RIMM map*

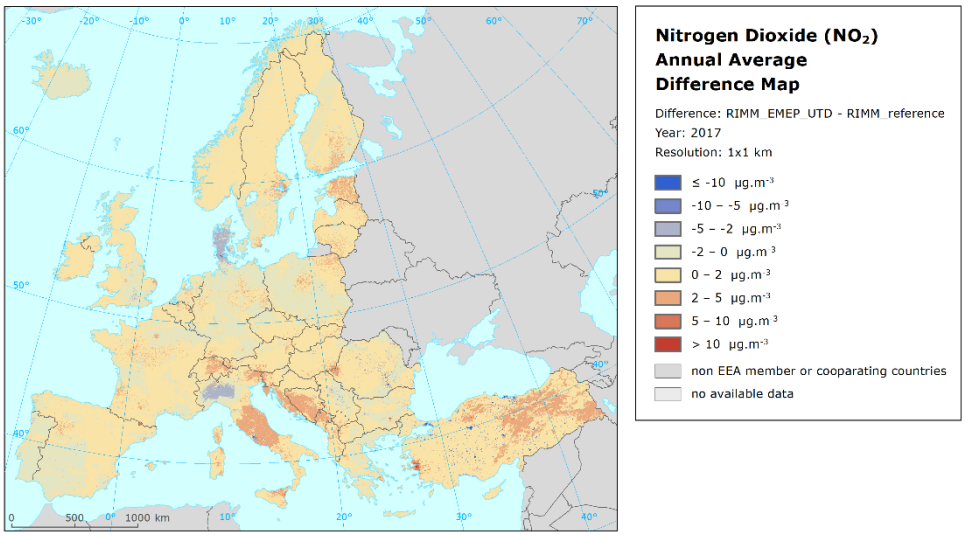


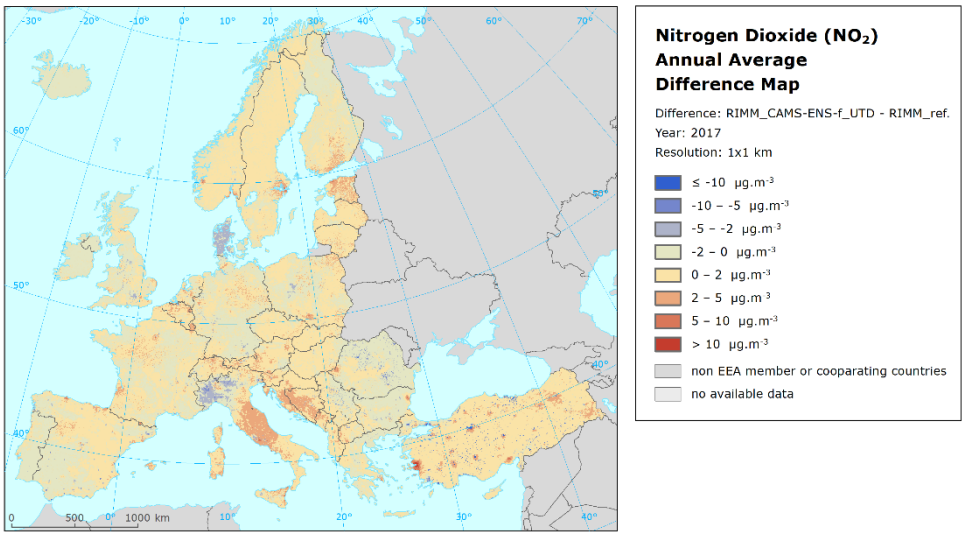


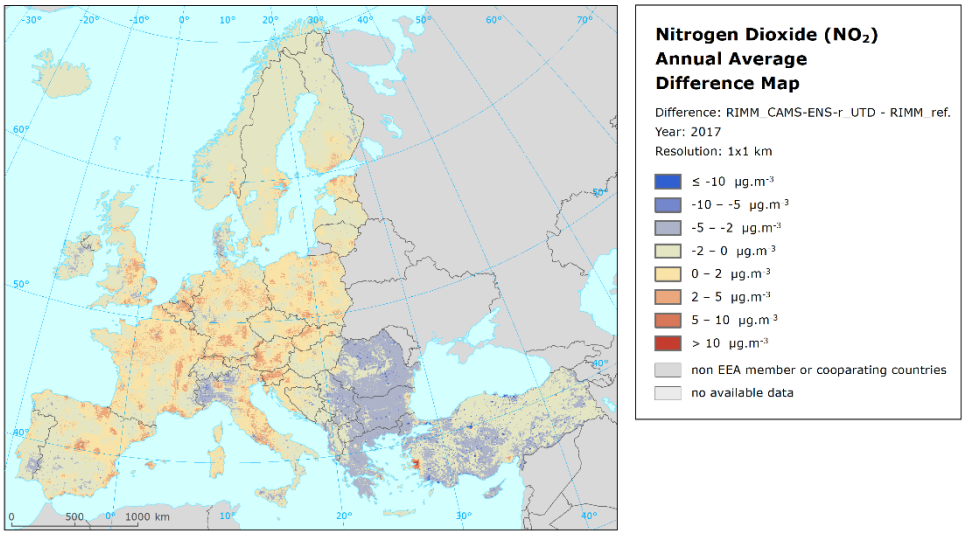

## 4.2 Validated Maps

This section examines and compares the performance of the RIMM spatial mapping results using three different model outputs (i.e., the EMEP, the CAMS Ensemble Forecast and the CAMS Ensemble Interim Reanalysis), with the aim to conclude whether the use of the CAMS Ensemble modelling data instead of the EMEP model output improves the mapping results. The analysis is based on 2017 data, with it being the most recent year with all data needed available. Contrary to Section 4.1, we use here exclusively the E1a measurements as the data official reported by the EEA's member, cooperating and other reporting countries.

In the mapping procedure, all stations apart from the CAMS validation set (see Section 3.2) are used. Both the mapping procedure and the data used are the same as in the reference RIMM maps (Horálek et al., 2020), apart from this skipping of the validation set's stations, and the different model used in the two of three variants.

The mapping results are evaluated and mutually compared primarily based on the CAMS validation set of stations (see above). In addition, evaluation based on the stations used in the mapping – apart from the CAMS assimilation set – is executed, using the 'leave-one-out' cross-validation (see Section 3.2).

The analysis is performed for four pollutants, i.e. $PM_{10}$ (annual average), $PM_{2.5}$ (annual average), ozone (SOMO35) and $NO_2$ (annual average).

### *4.2.1 $PM_{10}$ annual average*

Table 4.7 presents the technical details of the spatial RIMM maps using different model outputs. It shows the estimated parameters of the multiple linear regression (c, $a_1$, $a_2$, …) and of the residual kriging (nugget, sill, range) and includes the statistical indicators of the regression part of the mapping. In general, adjusted $R^2$ shows a ratio of a variability estimated by the regression. One can see better regression relation for the rural areas compared to the urban (both background and the traffic) areas.

*Table 4.7 Parameters of linear regression and spatial interpolation (ordinary kriging) in RIMM mapping of $PM_{10}$ annual average for 2017 in rural background, urban background and urban traffic areas for mapping variants using different CTM model outputs*

| Linear Regr. Model + OK of residuals | (E) EMEP | | | (C-F) CAMS-ENS forecast | | | (C-IR) CAMS-ENS int. rean. | | |
|---|---|---|---|---|---|---|---|---|---|
| | rural | urb. b. | urb. tr. | rural | urb. b. | urb. tr. | rural | urb. b. | urb. tr. |
| | coeff. | coeff. | coeff. | coeff. | coeff. | coeff. | coeff. | coeff. | coeff. |
| c (constant) | 4.27 | 1.76 | 2.21 | 4.44 | 1.13 | 2.01 | 4.32 | 1.19 | 2.06 |
| a1 (CTM model) | 0.605 | 0.556 | 0.447 | 0.761 | 0.822 | 0.572 | 0.872 | 0.767 | 0.538 |
| a2 (altitude_1km) | -0.0003 | | *n. sign.* | -0.0003 | | *n. sign.* | -0.0003 | | *n. sign.* |
| a3 (wind speed) | -0.038 | | -0.051 | -0.059 | | -0.070 | -0.059 | | -0.072 |
| a4 (rel. humidity) | -0.029 | | | -0.034 | | | -0.036 | | |
| a5 (CLC_NAT_1km) | -0.002 | | | -0.002 | | | -0.002 | | |
| **Adjusted $R^2$** | **0.71** | **0.27** | **0.42** | **0.71** | **0.31** | **0.45** | **0.77** | **0.25** | **0.41** |
| **St. Err. [µg.m$^{-3}$]** | **0.247** | **0.380** | **0.287** | **0.24** | **0.37** | **0.28** | **0.22** | **0.39** | **0.29** |
| Nugget | 0.028 | 0.035 | 0.019 | 0.021 | 0.032 | 0.014 | 0.023 | 0.033 | 0.014 |
| Sill | 0.055 | 0.086 | 0.050 | 0.052 | 0.079 | 0.046 | 0.041 | 0.073 | 0.046 |
| Range [km] | 970 | 740 | 210 | 520 | 630 | 370 | 320 | 550 | 370 |

Note: Grey empty cells indicate variables not used in the variant of the linear regression model.

Table 4.8 shows the comparison of the spatial mapping performance using different model outputs. The table shows the statistics based on the validation set of the stations. Again, lower RMSE and RRMSE and higher $R^2$ indicate better performance; bias closer to zero is also an indication of better performance; the slope should be as close to *1* as possible and the intercept as close to *0* as possible.

*Table 4.8 Comparison of different models used in RIMM spatial mapping showing RMSE, RRMSE, bias, $R^2$ and linear regression from validation scatter plots for $PM_{10}$ annual mean in rural background (top) and urban background (bottom) areas, 2017. Validation set of stations has not been used in mapping. Units: $\mu g.m^{-3}$ except RRMSE and $R^2$.*

| Model used in RIMM spatial mapping | | Rural background areas | | | | |
|---|---|---|---|---|---|---|
| | | RMSE | RRMSE | Bias | $R^2$ | Regr. eq. |
| (E) | EMEP | 3.2 | 19.7% | -1.3 | 0.704 | y = 0.638x + 4.67 |
| (C-FC) | CAMS Ensemble forecast | 3.1 | 19.0% | -0.9 | 0.698 | y = 0.692x + 4.14 |
| (C-IRA) | CAMS Ensemble interim reanalysis | 2.9 | 17.8% | -0.9 | 0.736 | y = 0.721x + 3.72 |
| | | | | | | |
| **Model used in RIMM spatial mapping** | | **Urban background areas** | | | | |
| | | RMSE | RRMSE | Bias | $R^2$ | Regr. eq. |
| (E) | EMEP | 3.4 | 16.9% | 0.1 | 0.747 | y = 0.837x + 3.34 |
| (C-FC) | CAMS Ensemble - forecast | 3.4 | 17.3% | 0.3 | 0.736 | y = 0.832x + 3.59 |
| (C-IRA) | CAMS Ensemble - interim reanalysis | 3.4 | 17.3% | 0.1 | 0.746 | y = 0.877x + 2.59 |

By comparing the results of the three models applied in the mapping process, one can see quite similar performance of all the three variants, with slightly better results of (C-IRA) in rural areas (although only 52 rural stations are available for testing).

Figure 4.3 shows the validation scatter plots, for both rural and urban background areas.

*Figure 4.3 Correlation between RIMM using EMEP (left), CAMS Ensemble Forecast (middle) or CAMS Ensemble Interim Reanalysis (right) mapping values (y-axis) versus measurements from rural (top), resp. urban/suburban (bottom) background stations (x-axis) from the validation set for $PM_{10}$ annual average 2017.*

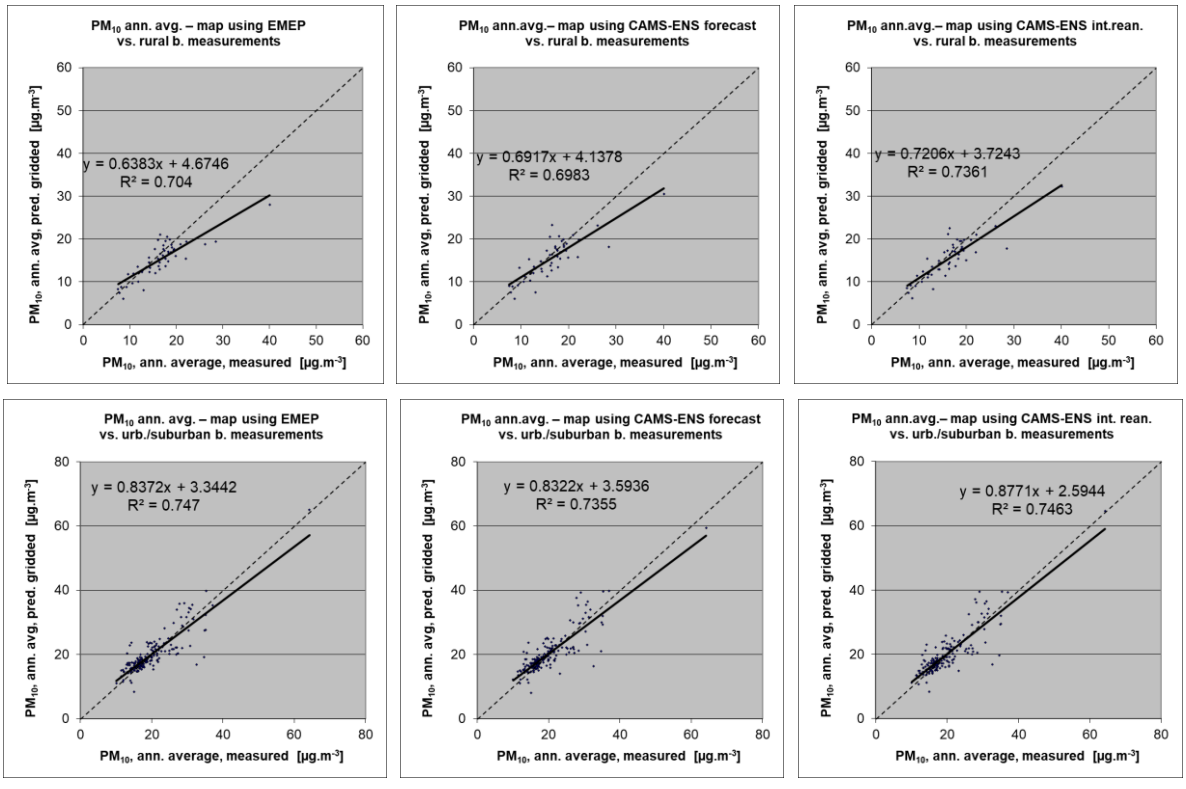

Table 4.9 presents the additional comparison of the maps in three variants, using the cross-validation based on the station used in mapping, apart from the CAMS assimilation set. The reason for not using the CAMS assimilation set is to prevent the underestimation of the uncertainty for the CAMS variants (see Section 3.2). It can be seen that all three variants of the maps give quite similar results.

*Table 4.9 Comparison of different models used in RIMM spatial mapping showing RMSE, RRMSE, bias, $R^2$ and linear regression from cross-validation scatter plots based on the stations used in the mapping apart from the CAMS "assimilation set" for $PM_{10}$ annual mean in rural background (top) and urban background (bottom) areas, 2017. Units: µg.m$^{-3}$ except RRMSE and $R^2$.*

| Model used in RIMM spatial mapping | | Rural background areas | | | | |
|---|---|---|---|---|---|---|
| | | RMSE | RRMSE | Bias | $R^2$ | Regr. eq. |
| (E) | EMEP | 5.4 | 32.1% | 0.8 | 0.655 | y = 0.887x + 2.77 |
| (C-FC) | CAMS Ensemble forecast | 5.2 | 30.6% | 1.0 | 0.690 | y = 0.912x + 2.47 |
| (C-IRA) | CAMS Ensemble interim reanalysis | 5.5 | 32.4% | 0.9 | 0.666 | y = 0.924x + 2.16 |
| | | | | | | |
| **Model used in RIMM spatial mapping** | | **Urban background areas** | | | | |
| | | RMSE | RRMSE | Bias | $R^2$ | Regr. eq. |
| (E) | EMEP | 9.4 | 32.0% | -0.8 | 0.592 | y = 0.631x + 10.08 |
| (C-FC) | CAMS Ensemble - forecast | 9.5 | 32.5% | -0.8 | 0.582 | y = 0.628x + 10.11 |
| (C-IRA) | CAMS Ensemble - interim reanalysis | 9.5 | 32.4% | -1.0 | 0.586 | y = 0.632x + 9.84 |

Map 4.5 presents the RIMM spatial maps for $PM_{10}$ annual average created using different model outputs. Annex, Map A.2 presents differences between the spatial maps using different model outputs.

Comparing the results, it should be noted that the ensemble character of both CAMS Ensemble models leads to smoothing of high values. This leads into reduced occurrence of high estimates in RIMM maps that are based on model output and emission data, not on measurements (e.g. Almeria region).

*Map 4.5 Concentration map of $PM_{10}$ annual average, 2017, RIMM methodology using EMEP (top), CAMS Ensemble Forecast (middle) and CAMS Ensemble Interim Reanalysis (bottom) model outputs*

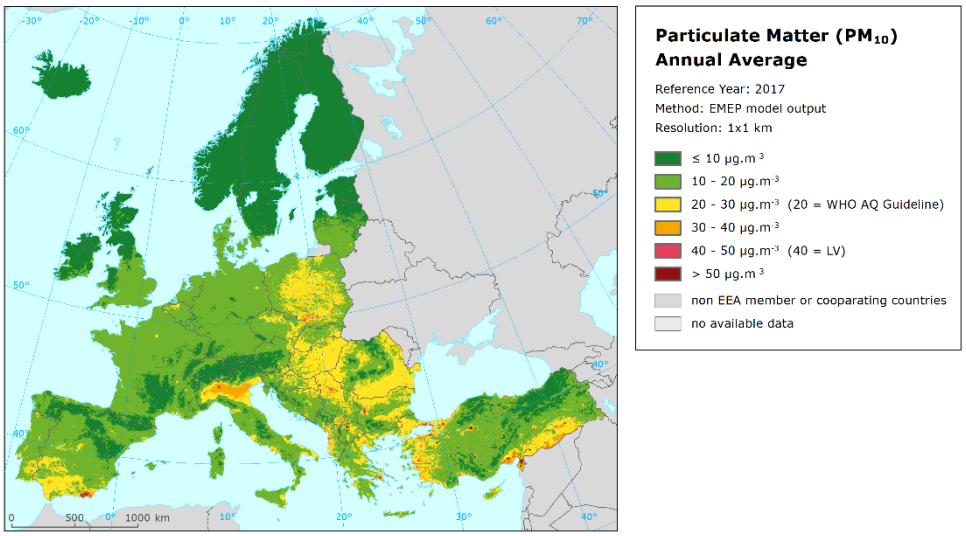


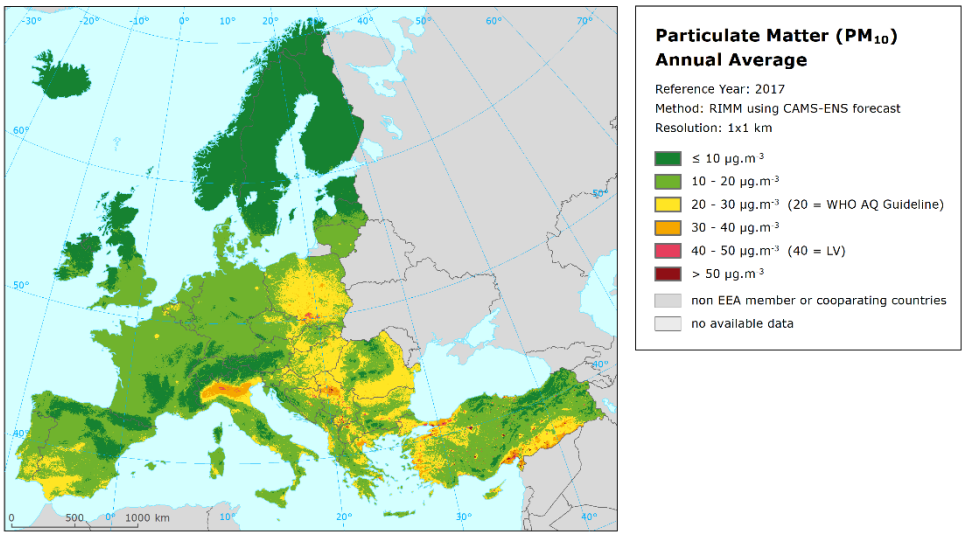


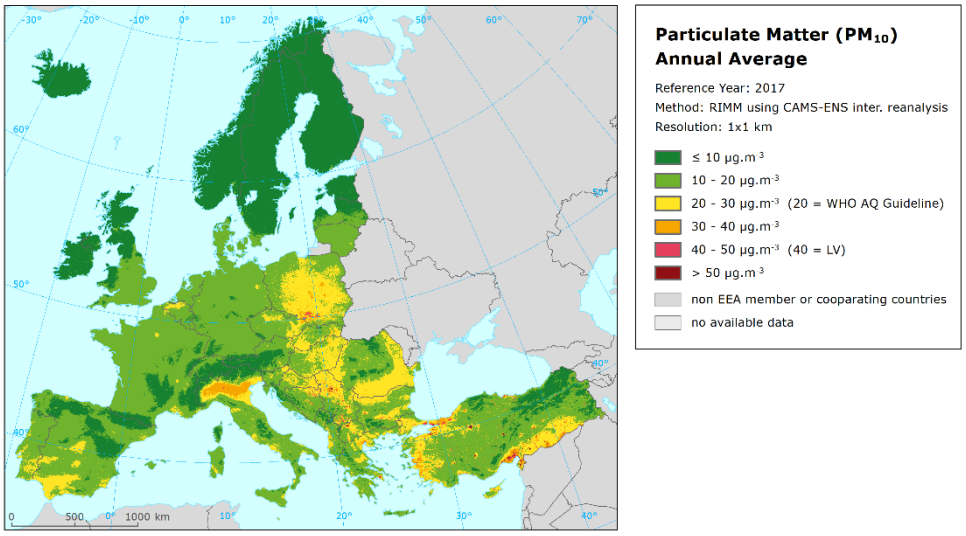

### 4.2.2 $PM_{2.5}$ annual average

Table 4.10 presents the technical details of the spatial RIMM maps using different model outputs.

*Table 4.10 Parameters of linear regression and spatial interpolation (ordinary kriging) in RIMM mapping of $PM_{2.5}$ annual average for 2017 in rural background, urban background and urban traffic areas for mapping variants using different CTM model outputs*

| Linear Regr. Model + OK of residuals | (E) EMEP | | | (C-F) CAMS-ENS forecast | | | (C-IR) CAMS-ENS int. rean. | | |
|---|---|---|---|---|---|---|---|---|---|
| | rural | urb. b. | urb. tr. | rural | urb. b. | urb. tr. | rural | urb. b. | urb. tr. |
| | coeff. | coeff. | coeff. | coeff. | coeff. | coeff. | coeff. | coeff. | coeff. |
| c (constant) | 0.84 | 1.48 | 0.66 | 0.40 | 0.68 | 0.54 | 0.11 | 0.35 | 1.12 |
| a1 (CTM model) | 0.761 | 0.530 | 0.839 | 0.967 | 0.912 | 0.865 | 1.059 | 1.015 | 0.591 |
| a2 (altitude_1km) | -0.00010 | | | -0.00011 | | | -0.00012 | | |
| a3 (wind speed) | *n. sign.* | | | *n. sign.* | | | *n. sign.* | | |
| a4 (CLC_NAT_1km) | -0.0024 | | | -0.0025 | | | -0.0021 | | |
| **Adjusted $R^2$** | **0.641** | **0.271** | **0.587** | **0.664** | **0.456** | **0.584** | **0.708** | **0.526** | **0.496** |
| **St. Err. [$\mu g.m^{-3}$]** | **0.31** | **0.37** | **0.31** | **0.30** | **0.32** | **0.31** | **0.28** | **0.30** | **0.35** |
| Nugget | 0.054 | 0.018 | 0.028 | 0.053 | 0.016 | 0.024 | 0.049 | 0.016 | 0.029 |
| Sill | 0.083 | 0.112 | 0.075 | 0.087 | 0.078 | 0.070 | 0.077 | 0.070 | 0.083 |
| Range [km] | 410 | 920 | 360 | 410 | 490 | 360 | 410 | 490 | 360 |

Note: Grey empty cells indicate variables not used in the variant of the linear regression model.

Table 4.11 shows the comparison of the spatial mapping performance using different model outputs.

*Table 4.11 Comparison of different models used in RIMM spatial mapping showing RMSE, RRMSE, bias, $R^2$ and linear regression from validation scatter plots for $PM_{2.5}$ annual mean in rural background (top) and urban background (bottom) areas, 2017. Validation set of stations has not been used in mapping. Units: $\mu g.m^{-3}$ except RRMSE and $R^2$.*

| Model used in RIMM spatial mapping | | Rural background areas | | | | |
|---|---|---|---|---|---|---|
| | | RMSE | RRMSE | Bias | $R^2$ | Regr. eq. |
| E | EMEP | 1.5 | 14.7% | 0.0 | 0.859 | y = 0.706x + 3.02 |
| C-FC | CAMS Ensemble forecast | 1.5 | 14.2% | 0.1 | 0.885 | y = 0.69x + 3.24 |
| C-IRA | CAMS Ensemble interim reanalysis | 1.3 | 12.1% | 0.2 | 0.916 | y = 0.74x + 2.86 |

| Model used in RIMM spatial mapping | | Urban background areas | | | | |
|---|---|---|---|---|---|---|
| | | RMSE | RRMSE | Bias | $R^2$ | Regr. eq. |
| E | EMEP | 2.3 | 17.8% | -0.2 | 0.743 | y = 0.811x + 2.20 |
| C-FC | CAMS Ensemble - forecast | 2.3 | 18.0% | -0.3 | 0.733 | y = 0.752x + 2.92 |
| C-IRA | CAMS Ensemble - interim reanalysis | 2.3 | 17.7% | -0.3 | 0.744 | y = 0.789x + 2.43 |

Note: In rural areas, the validation set consists of 20 stations only.

One can see quite similar results for all three variants, with slightly improved results for (C-IRA) in the rural areas. However, it should be noted that in the rural areas, the validation is based on 20 stations only.

Figure 4.4 shows the validation scatter plots, for both rural and urban background areas.

*Figure 4.4 Correlation between RIMM using EMEP (left), CAMS Ensemble Forecast (middle) or CAMS Ensemble Interim Reanalysis (right) mapping values (y-axis) versus measurements from rural (top), resp. urban/suburban (bottom) background stations (x-axis) from the validation set for $PM_{2.5}$ annual average 2017.*

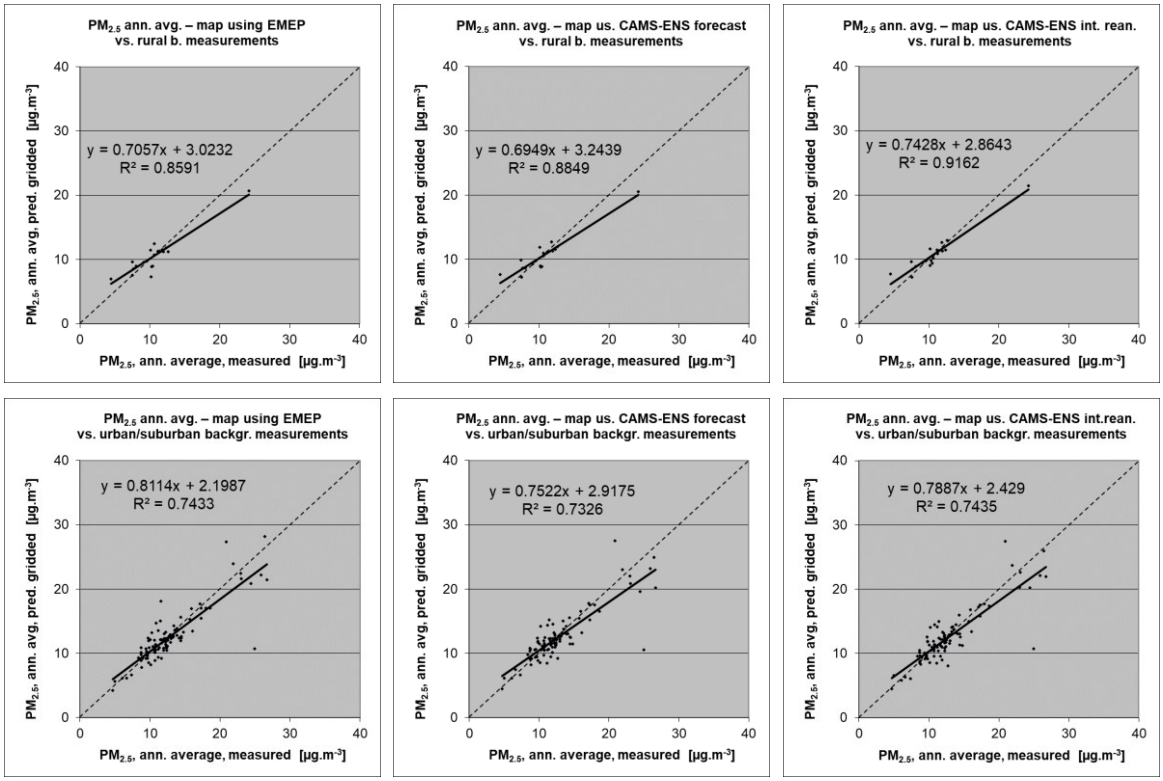


Table 4.12 presents the additional comparison of the maps in three variants, using the cross-validation based on the station used in mapping, apart from the CAMS assimilation set (see Section 3.2). It can be seen that all three variants of the maps give quite similar results.

*Table 4.12 Comparison of different models used in RIMM spatial mapping showing RMSE, RRMSE, bias, $R^2$ and linear regression from cross-validation scatter plots based on the stations used in the mapping apart from the CAMS "assimilation set" for $PM_{2.5}$ annual mean in rural background (top) and urban background (bottom) areas, 2017. Units: µg.m$^{-3}$ except RRMSE and $R^2$.*

| Model used in RIMM spatial mapping | | Rural background areas | | | | |
|---|---|---|---|---|---|---|
| | | RMSE | RRMSE | Bias | $R^2$ | Regr. eq. |
| (E) | EMEP | 2.8 | 24.2% | -0.2 | 0.803 | y = 0.775x + 2.43 |
| (C-FC) | CAMS Ensemble forecast | 2.8 | 24.1% | -0.1 | 0.805 | y = 0.763x + 2.58 |
| (C-IRA) | CAMS Ensemble interim reanalysis | 2.8 | 24.3% | -0.3 | 0.807 | y = 0.750x + 2.60 |
| | | | | | | |
| **Model used in RIMM spatial mapping** | | **Urban background areas** | | | | |
| | | RMSE | RRMSE | Bias | $R^2$ | Regr. eq. |
| (E) | EMEP | 2.9 | 17.8% | 0.1 | 0.819 | y = 0.838x + 2.73 |
| (C-FC) | CAMS Ensemble - forecast | 2.9 | 17.7% | 0.1 | 0.823 | y = 0.868x + 2.27 |
| (C-IRA) | CAMS Ensemble - interim reanalysis | 3.0 | 18.0% | 0.1 | 0.816 | y = 0.866x + 2.29 |

Map 4.6 presents the RIMM spatial maps for $PM_{2.5}$ annual average created using different model outputs. Annex, Map A.4 presents the differences between the spatial maps using different model outputs.

*Map 4.6 Concentration map of $PM_{2.5}$ annual average, 2017, RIMM methodology using EMEP (top), CAMS-ENS Forecast (middle) and CAMS-ENS Interim Reanalysis (bottom) model outputs*

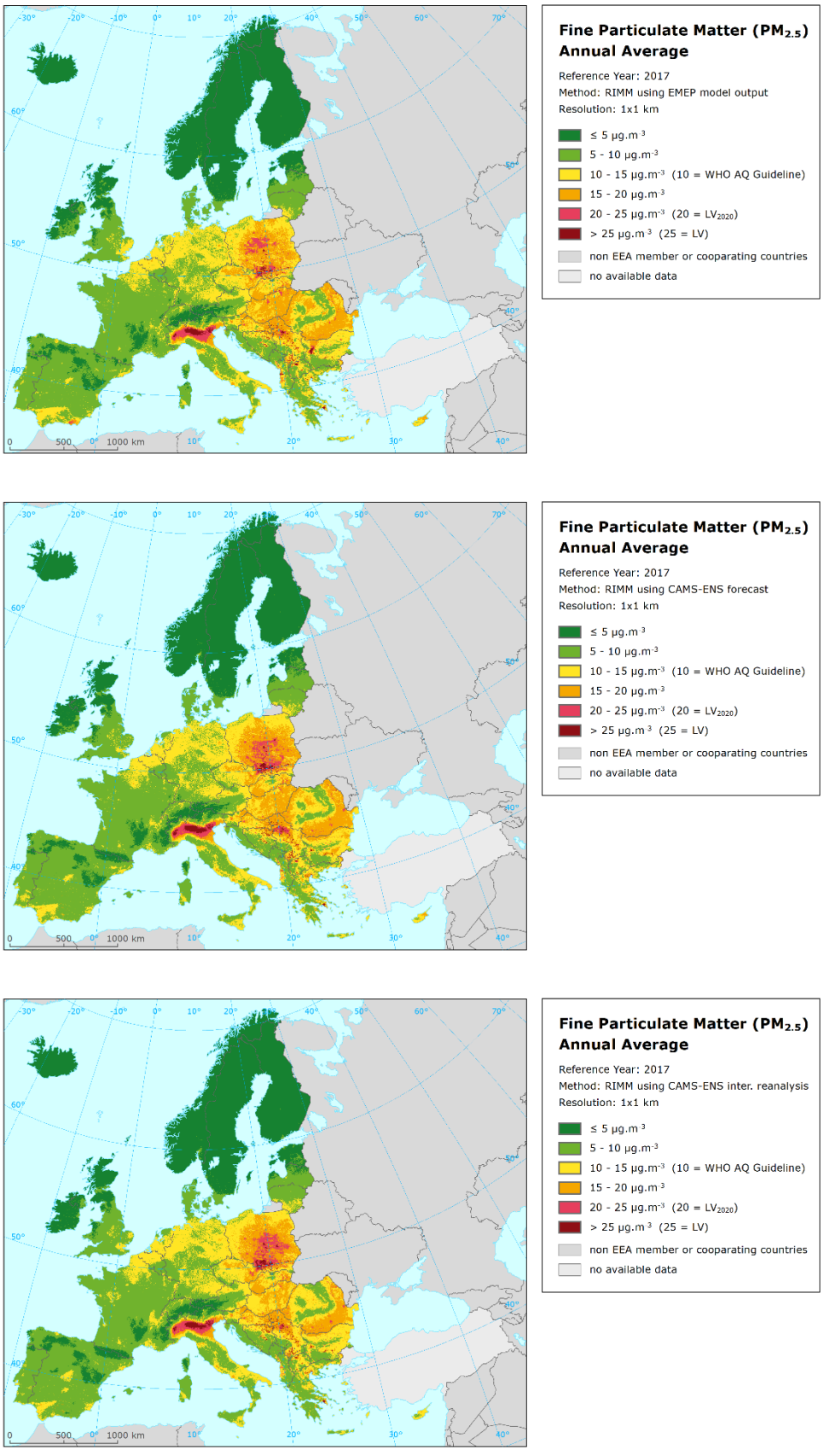

### 4.2.3 Ozone – SOMO35

Table 4.13 presents the technical details of the spatial RIMM maps using different model outputs.

*Table 4.13 Parameters of linear regression and spatial interpolation (ordinary kriging) in RIMM mapping of ozone indicator SOMO35 for 2017 in rural background, urban background and urban traffic areas for mapping variants using different CTM model outputs*

| Linear Regr. Model + OK of residuals | (E) EMEP | | (C-F) CAMS-ENS forecast | | (C-IR) CAMS-ENS int. rean. | |
|---|---|---|---|---|---|---|
| | rural | urb. b. | rural | urb. b. | rural | urb. b. |
| | coeff. | coeff. | coeff. | coeff. | coeff. | coeff. |
| c (constant) | -3138 | -1667 | -813 | 2195 | 144 | 2412 |
| a1 (CTM model) | 0.706 | 0.601 | 1.024 | 0.758 | 1.063 | 0.796 |
| a2 (altitude_1km) | 0.619 | | 3.046 | | 2.380 | |
| a3 (wind speed) | | *n. sign.* | | -508.1 | | -397.1 |
| a4 (s. solar radiation) | 345.7 | 195.5 | *n. sign.* | *n. sign.* | *n. sign.* | *n. sign.* |
| **Adjusted $R^2$** | **0.680** | **0.533** | **0.694** | **0.565** | **0.730** | **0.553** |
| **St. Err. [µg.m$^{-3}$]** | **1674** | **1716** | **1637** | **1656** | **1538** | **1680** |
| Nugget | 0 | 7.0E+05 | 0 | 6.0E+05 | 0 | 7.0E+05 |
| Sill | 2.3E+06 | 2.3E+06 | 2.3E+06 | 2.3E+06 | 2.0E+06 | 1.8E+06 |
| Range [km] | 20 | 740 | 20 | 740 | 20 | 740 |

Note: Grey empty cells indicate variables not used in the variant of the linear regression model.

Table 4.14 shows the comparison of the spatial mapping performance using different model outputs.

*Table 4.14 Comparison of different models used in RIMM spatial mapping showing RMSE, RRMSE, bias, $R^2$ and linear regression from validation scatter plots for ozone indicator SOMO35 in rural background (top) and urban background (bottom) areas, 2017. Validation set of stations has not been used in mapping. Units: µg.m$^{-3}$ except RRMSE and $R^2$.*

| | | Rural background areas | | | | |
|---|---|---|---|---|---|---|
| | | RMSE | RRMSE | Bias | $R^2$ | Regr. eq. |
| (E) | EMEP | 1445 | 27.4% | -74 | 0.734 | y = 0.721x + 1395 |
| (C-FC) | CAMS Ensemble forecast | 1425 | 27.1% | -119 | 0.743 | y = 0.732x + 1293 |
| (C-IRA) | CAMS Ensemble interim reanalysis | 1442 | 27.4% | -240 | 0.742 | y = 0.734x + 1141 |
| | | | | | | |
| | | Urban background areas | | | | |
| | | RMSE | RRMSE | Bias | $R^2$ | Regr. eq. |
| (E) | EMEP | 1351 | 31.3% | 136 | 0.781 | y = 0.835x + 754 |
| (C-FC) | CAMS Ensemble forecast | 1358 | 31.4% | 126 | 0.777 | y = 0.829x + 767 |
| (C-IRA) | CAMS Ensemble interim reanalysis | 1341 | 31.1% | 167 | 0.786 | y = 0.833x + 794 |

Very similar results can be seen for all three variants, both in the rural and urban background areas.

Figure 4.5 shows the validation scatter plots, for both rural and urban background areas.

Table 4.15 presents the additional comparison of the maps in three variants, using the cross-validation based on the station used in mapping, apart from the CAMS assimilation set (see Section 3.2). It can be seen that all three variants of the maps give quite similar results.

*Figure 4.5 Correlation between RIMM using EMEP (left), CAMS Ensemble Forecast (middle) or CAMS Ensemble Interim Reanalysis (right) mapping values (y-axis) versus measurements from rural (top), resp. urban/suburban (bottom) background stations (x-axis) from the validation set for ozone indicator SOMO35, 2017.*

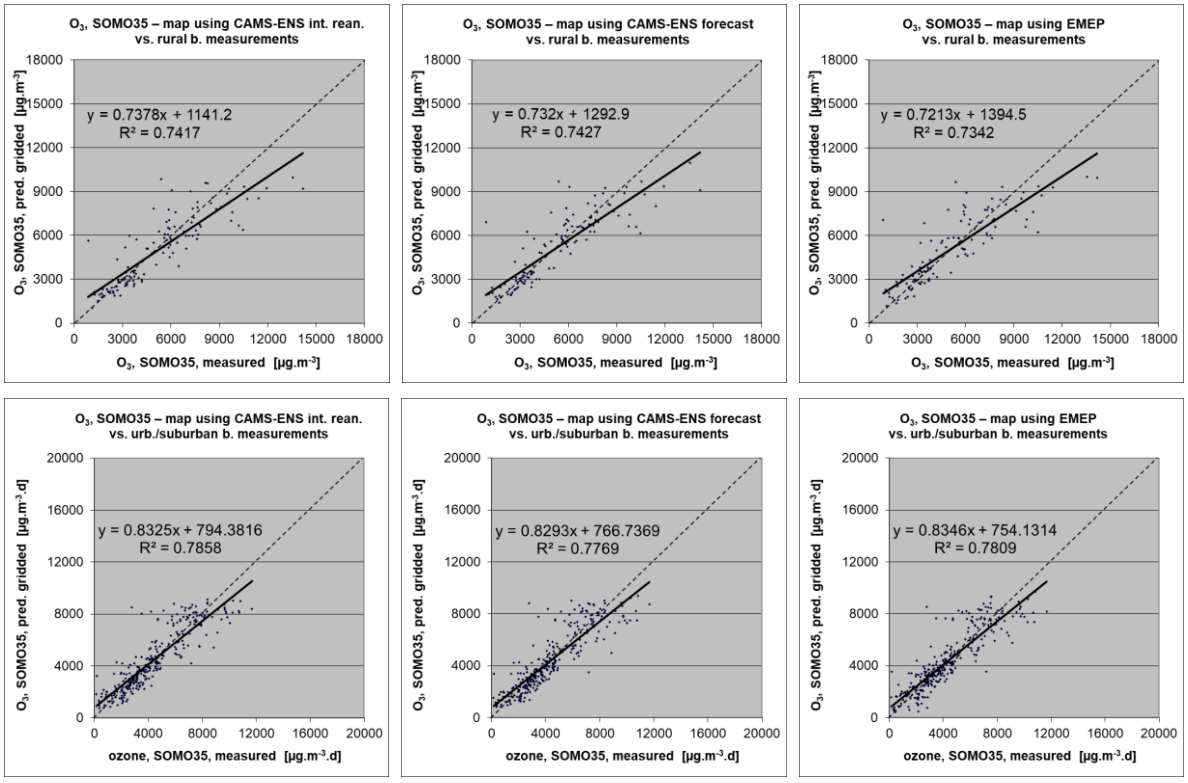


*Table 4.15 Comparison of different models used in RIMM spatial mapping showing RMSE, RRMSE, bias, $R^2$ and linear regression from cross-validation scatter plots based on the stations used in the mapping apart from the CAMS "assimilation set" for ozone indicator SOMO35 in rural background (top) and urban background (bottom) areas, 2017. Units: µg.m$^{-3}$ except RRMSE and $R^2$.*

| Model used in RIMM spatial mapping | | Rural background areas | | | | |
|---|---|---|---|---|---|---|
| | | RMSE | RRMSE | Bias | $R^2$ | Regr. eq. |
| (E) | EMEP | 1921 | 29.9% | -158 | 0.582 | y = 0.562x + 2655 |
| (C-FC) | CAMS Ensemble forecast | 1988 | 30.9% | -173 | 0.553 | y = 0.523x + 2893 |
| (C-IRA) | CAMS Ensemble interim reanalysis | 1964 | 30.6% | -117 | 0.560 | y = 0.551x + 277 |
| | | | | | | |
| **Model used in RIMM spatial mapping** | | **Urban background areas** | | | | |
| | | RMSE | RRMSE | Bias | $R^2$ | Regr. eq. |
| (E) | EMEP | 1938 | 46.5% | 0 | 0.556 | y = 0.589x + 1713 |
| (C-FC) | CAMS Ensemble - forecast | 1967 | 47.2% | -67 | 0.543 | y = 0.573x + 1710 |
| (C-IRA) | CAMS Ensemble - interim reanalysis | 1951 | 46.8% | -19 | 0.549 | y = 0.562x + 1806 |

Based on the results presented in Table 4.14, Figure 4.5 and Table 4.15, we can state that the spatial mapping using all three different models gives quite similar statistical results.

Map 4.7 presents the RIMM spatial maps for SOMO35 created using different model outputs. Annex, Map A.6 presents the differences between the spatial maps using different model outputs.

*Map 4.7 Concentration map of ozone indicator SOMO35, 2017, RIMM methodology using EMEP (top), CAMS Ensemble Forecast (middle) and CAMS Ensemble Interim Reanalysis (bottom) model outputs*

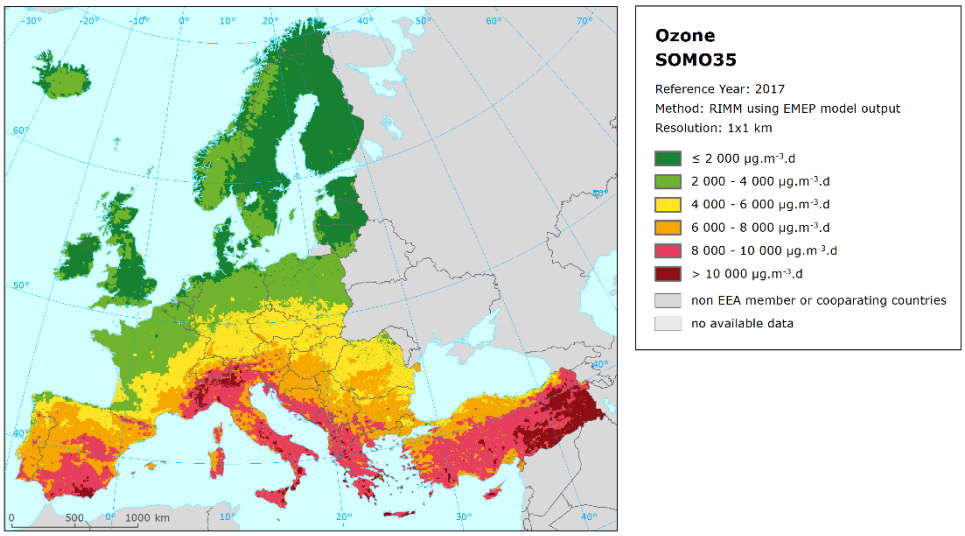


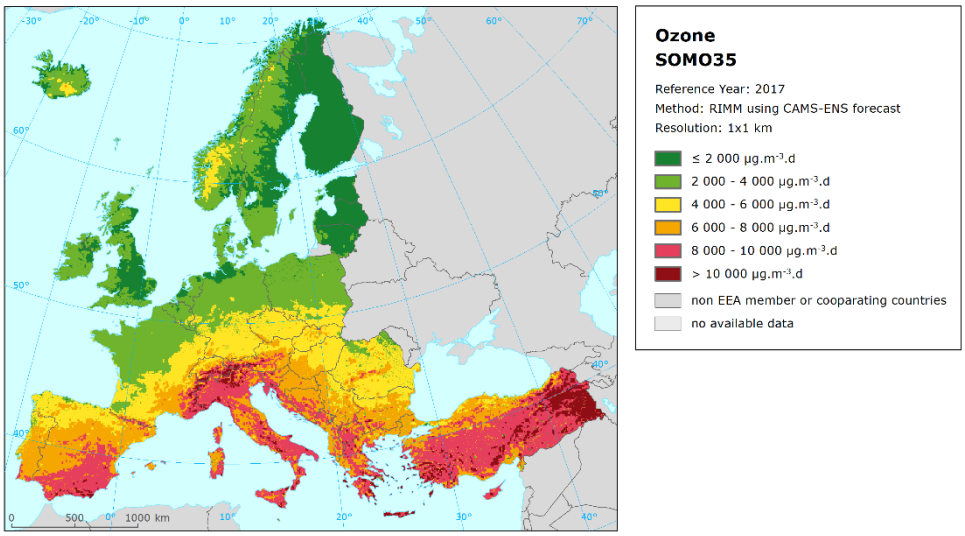


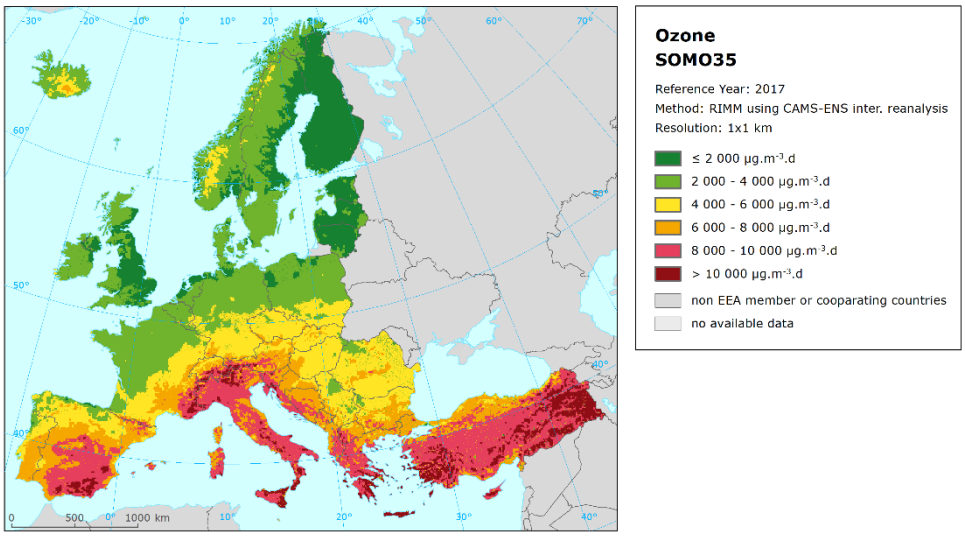

### 4.2.4 $NO_2$ annual average

Table 4.16 presents the technical details of the spatial RIMM maps using different model outputs.

*Table 4.16 Parameters of linear regression and spatial interpolation (ordinary kriging) in RIMM mapping of $NO_2$ annual average for 2017 in rural background, urban background and urban traffic areas for mapping variants using different CTM model outputs*

| Linear Regr. Model + OK of residuals | (E) EMEP | | | (C-F) CAMS-ENS forecast | | | (C-IR) CAMS-ENS int. rean. | | |
|---|---|---|---|---|---|---|---|---|---|
| | rural | urb. b. | urb. tr. | rural | urb. b. | urb. tr. | rural | urb. b. | urb. tr. |
| | coeff. | coeff. | coeff. | coeff. | coeff. | coeff. | coeff. | coeff. | coeff. |
| c (constant) | 7.59 | 24.25 | 27.98 | 7.19 | 24.80 | 27.84 | 4.26 | 22.62 | 24.87 |
| a1 (CTM model) | 0.511 | 0.146 | 0.224 | 0.691 | 0.570 | 0.397 | 0.781 | 0.474 | 0.594 |
| a2 (altitude_1km) | -0.01000 | | | -0.01049 | | | -0.01041 | | |
| a3 (altitude_5km_r) | 0.00995 | | | 0.01071 | | | 0.01026 | | |
| a4 (wind speed) | -1.026 | -3.275 | -2.313 | -0.988 | -3.078 | -2.173 | -0.652 | -2.954 | -1.768 |
| a5 (population density) | 0.0025 | 0.0003 | | 0.0024 | 0.0003 | | 0.0023 | 0.0003 | |
| a6 (OMI satellite) | 1.073 | 1.367 | 1.520 | 0.401 | *n.sign.* | 0.886 | 0.472 | 0.555 | 0.668 |
| a7 (LC_NAT_1km) | | -0.0889 | | | -0.0949 | | | -0.0928 | |
| a8 (LC_AGR_1km) | | -0.0424 | | | -0.0540 | | | -0.0451 | |
| a9 (LC_TRA_1km) | | 0.1024 | | | 0.1028 | | | 0.0994 | |
| a10 (LC_LDR_5km_r) | *n.sign.* | 0.0426 | 0.1872 | *n.sign.* | *n.sign.* | 0.1918 | *n.sign.* | *n.sign.* | 0.1697 |
| a11 (LC_HDR_5km_r) | | 0.1799 | 0.3570 | | 0.1021 | 0.3792 | | 0.1474 | 0.3442 |
| a12 (LC_NAT_5km_r) | -0.0445 | | | -0.0407 | | | -0.0329 | | |
| **Adjusted $R^2$** | **0.800** | **0.416** | **0.382** | **0.800** | **0.435** | **0.376** | **0.823** | **0.429** | **0.390** |
| **St. Err. [µg.m$^{-3}$]** | **2.64** | **7.28** | **10.11** | **2.64** | **7.16** | **10.16** | **2.48** | **7.20** | **10.04** |
| Nugget | 0 | 14 | 41 | 1 | 14 | 41 | 0 | 13 | 41 |
| Sill | 7 | 30 | 88 | 7 | 28 | 89 | 6 | 28 | 84 |
| Range [km] | 12 | 270 | 400 | 23 | 240 | 400 | 12 | 260 | 400 |

Note: Grey empty cells indicate variables not used in the variant of the linear regression model.

Table 4.17 shows the comparison of the spatial mapping performance using different model outputs.

*Table 4.17 Comparison of different models used in RIMM spatial mapping showing RMSE, RRMSE, bias, $R^2$ and linear regression from validation scatter plots for $NO_2$ annual mean in rural background (top) and urban background (bottom) areas, 2017. Validation set of stations has not been used in mapping. Units: µg.m$^{-3}$ except RRMSE and $R^2$.*

| Model used in RIMM spatial mapping | | Rural background areas | | | | |
|---|---|---|---|---|---|---|
| | | RMSE | RRMSE | Bias | $R^2$ | Regr. eq. |
| E | EMEP | 2.7 | 27.8% | -0.3 | 0.777 | y = 0.856x + 1.09 |
| C-FC | CAMS Ensemble forecast | 2.7 | 27.8% | -0.2 | 0.778 | y = 0.871x + 1.04 |
| C-IRA | CAMS Ensemble interim reanalysis | 2.9 | 30.3% | 0.2 | 0.739 | y = 0.852x + 1.59 |

| Model used in RIMM spatial mapping | | Urban background areas | | | | |
|---|---|---|---|---|---|---|
| | | RMSE | RRMSE | Bias | $R^2$ | Regr. eq. |
| E | EMEP | 5.2 | 24.8% | 1.0 | 0.620 | y = 0.761x + 5.86 |
| C-FC | CAMS Ensemble - forecast | 5.2 | 24.8% | 0.9 | 0.635 | y = 0.762x + 5.67 |
| C-IRA | CAMS Ensemble - interim reanalysis | 5.0 | 24.0% | 0.7 | 0.622 | y = 0.764x + 5.89 |

Figure 4.6 shows the validation scatter plots, for both rural and urban background areas. Looking at the results presented in Table 4.17 and Figure 4.6, one can conclude that the spatial mapping using EMEP and CAMS Ensemble Forecast gives quite similar statistical results. The spatial mapping using CAMS Ensemble Interim Reanalysis gives slightly worse result compared to the other two method variants in the rural areas.

*Figure 4.6 Correlation between RIMM using EMEP (left), CAMS Ensemble Forecast (middle) or CAMS Ensemble Interim Reanalysis (right) mapping values (y-axis) versus measurements from rural (top), resp. urban/suburban (bottom) background stations (x-axis) from the validation set for $NO_2$ annual average 2017.*

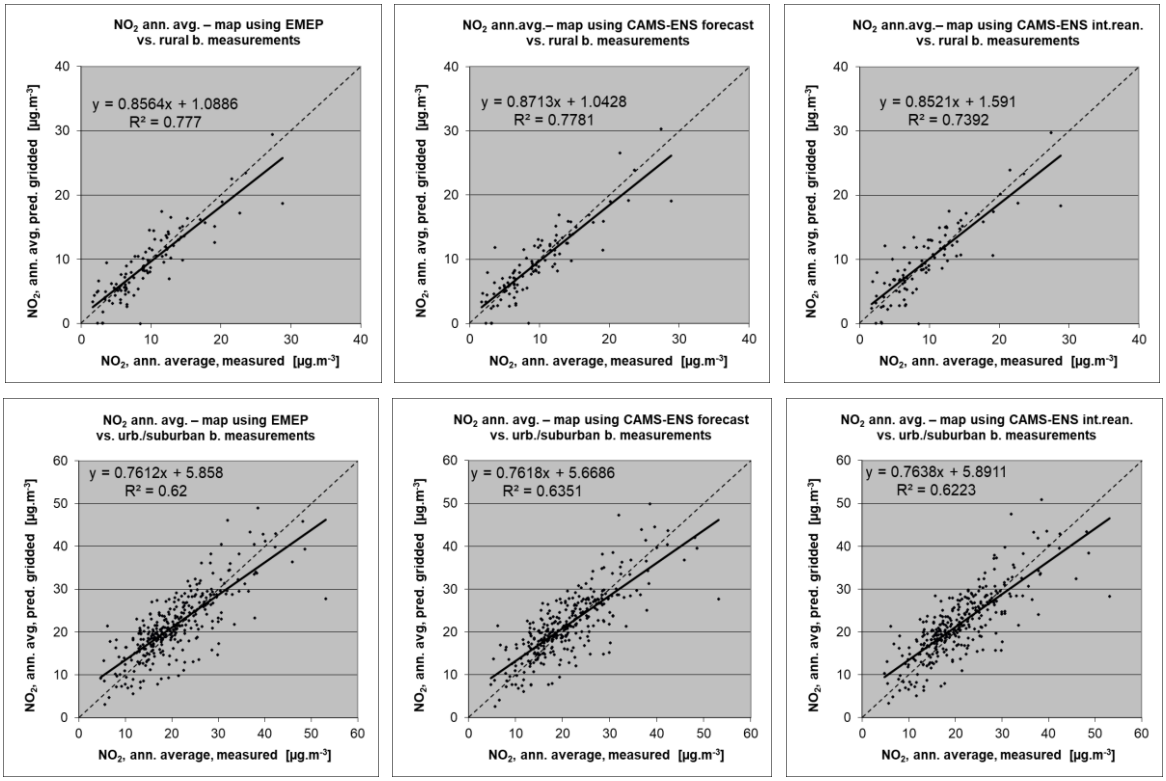


Map 4.8 presents the RIMM spatial maps for $NO_2$ annual average created using different model outputs. Annex, Map A.8 presents the differences between the spatial maps using different model outputs.

*Map 4.8 Concentration map of $NO_2$ annual average, 2017, RIMM methodology using EMEP (top), CAMS Ensemble Forecast (middle) and CAMS Ensemble Interim Reanalysis (bottom) model outputs*

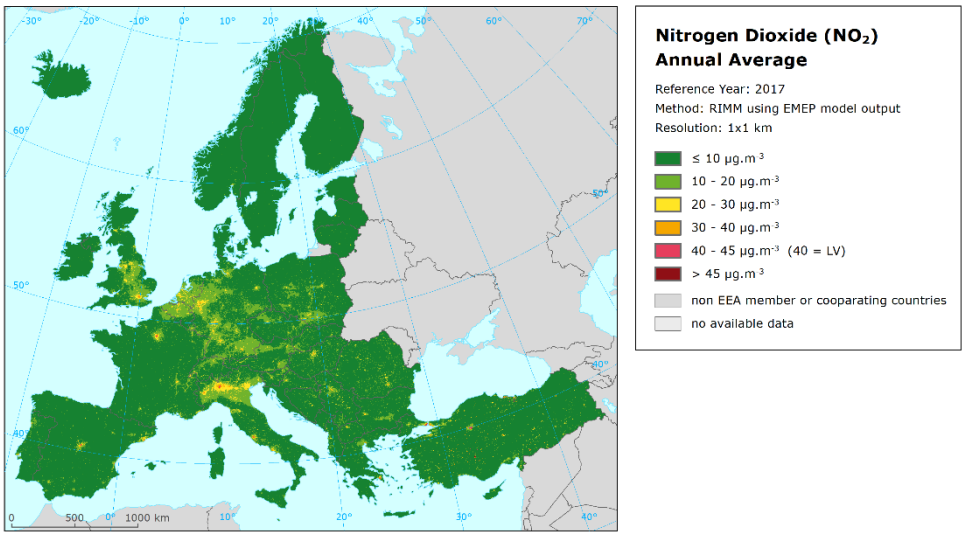


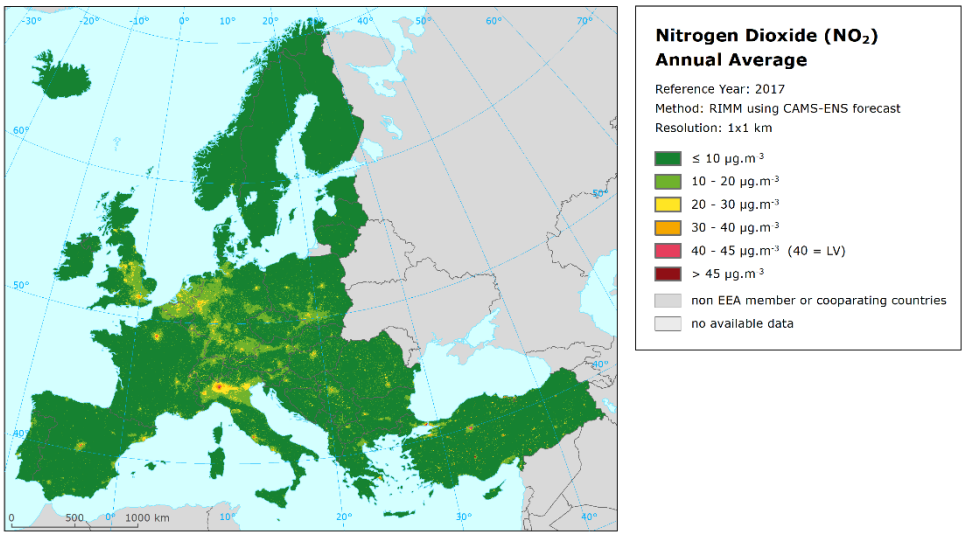


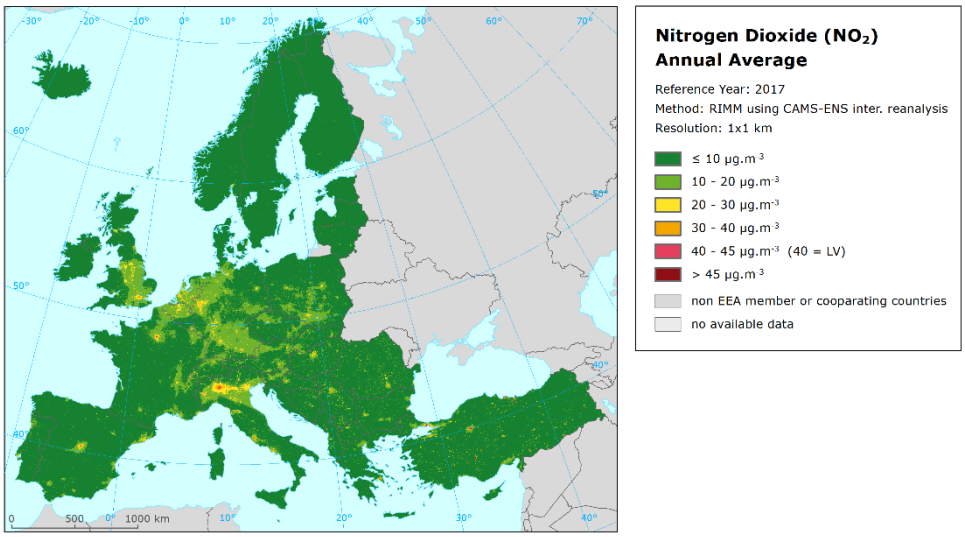

### *4.2.5 Conclusion*

Based on the evaluation of the results presented, **it is not possible to conclude that any of the three model datasets gives definitively better results compared to the others**. The margins of difference in the statistical measures used are so small that many of the differences are likely not statistically significant. **Such results do not give strong reasons for a potential change of the model used in the mapping**.

Considering the use of different model outputs in spatial mapping, several remarks can be done, in addition to those of Horálek et al. (2014). The ensemble character of both CAMS Ensemble models leads into smoothing, which reduces in spatial PM maps the occurrence of high values not based on measurements (which may have either negative or positive effect, in dependence of the quality of the model and its underlying emissions). Another note is the double counting of station data in the reanalysis and in the data fusion mapping, which would cause a more difficult and necessarily reduced uncertainty analysis, if CAMS Ensemble Interim Reanalysis is used. The most relevant issue for regular mapping probably is that the use of the EMEP model assures better year-to-year consistency of the final maps, compared to the ensemble-based CAMS modelling products (based on different model applied in different years). This leads into the recommendation for the continued use of the EMEP model data in the spatial mapping.

Be it also noted that the use of the CAMS Ensemble Forecast in the mapping does not give in general poorer results compared to the use of the CAMS Ensemble Interim Reanalysis, although it does not use any data assimilation. (Be aware that the comparison has been applied outside the stations used in the data assimilation.)

# 5 Comparison of RIMM Spatial Mapping Results with CAMS Ensemble Modelling Results

In this chapter, the comparison of the RIMM spatial mapping results (as routinely produced under ETC/ATNI, i.e. using EMEP) with the CAMS Ensemble modelling results is executed. Namely, the following estimates have been compared:

- RIMM spatial mapping (using EMEP model output), labelled (R)
- CAMS Ensemble Forecast, labelled (C-FC)
- CAMS Ensemble Interim Reanalysis, labelled (C-IRA)

The aim of this comparison is to verify the assumption that the RIMM spatial interpolated maps where the main input are AQ concentration data measured at monitoring stations, are better suited for exposure calculations.

The main comparison performed is between the RIMM spatial mapping and the CAMS Ensemble Interim Reanalysis. The CAMS Ensemble Forecast is included in the comparison for illustration only: since it does not include any information about observations (only raw model simulations), its quality is naturally poorer compared to products utilizing measurement data.

Be it noted that we did not include in the comparison the CAMS Ensemble Validated Reanalysis (which has the highest quality out of the CAMS modelling products), as its data for 2017 was not available in the time of analysis.

The comparison has been executed by two approaches, i.e.,

- Using all stations, without distinguishing whether used or not used in the mapping resp. modelling
- Using the “validation set” of the stations as used in CAMS. In this case, the Validation set of stations is not used in the mapping resp. modelling

In the first approach, all stations as listed in Table 3.2 and shown in Figures 3.3–3.6 are applied for the comparison (apart from Turkish stations in the case of $PM_{2.5}$). In this case, the routine spatial RIMM maps (Horálek et al., 2020) created based on all stations are used in the comparison. The reason for not using the Turkish $PM_{2.5}$ stations in the comparison and for not presenting the area of Turkey in the spatial $PM_{2.5}$ map is the lack of the rural $PM_{2.5}$ stations in Turkey for 2017, see Map 3.4 and Horálek et al. (2020).

In the second approach, only the validation set of the stations as listed in Table 3.2 and shown in Figures 3.3–3.6 is applied for the comparison. In this case, the spatial RIMM maps created without the validation set of the stations (as analysed in Section 4.2) are used in the comparison.

The comparison has been executed for four pollutants and their indicators, i.e. $PM_{10}$ annual average, $PM_{2.5}$ annual average, ozone indicator SOMO35 and $NO_2$ annual average.

## 5.1 $PM_{10}$ annual average

Table 5.1 shows the comparison of the RIMM spatial mapping results (as routinely produced, i.e. based on all stations) with two different CAMS Ensemble model results. The scores are calculated against observations from all stations. The agreement of the mapped resp. modelled values with the measurement data is mutually compared. Next to the simple validation (i.e. simple comparison between the mapped resp. modelled and measurement values), cross-validation is also used in the case of the RIMM spatial results (see Section 3.2). The reason is that in the simple validation of RIMM, the mapping results are compared with the same measurement data, which has already been used in the mapping. Thus, the uncertainty estimated based on such simple comparison is underestimated.

The table row highlighted by green shows the statistics that provide the best performance, apart from the simple validation of RIMM (highlighted by blue).

*Table 5.1 Comparison of different mapping methods showing RMSE, RRMSE, bias, $R^2$ and linear regression from simple (RIMM, CAMS Ensemble Forecast, CAMS Ensemble Interim Reanalysis) or cross-validation (RIMM) scatter plots for $PM_{10}$ annual mean in rural background (top) and urban background (bottom) areas, 2017. Units: µg.m$^{-3}$ except RRMSE and $R^2$.*

| | | Rural background areas | | | | |
|---|---|---|---|---|---|---|
| | | RMSE | RRMSE | Bias | $R^2$ | Regr. eq. |
| R | RIMM Spatial Mapping | 3.7 | 23.1% | 0.3 | 0.735 | y = 0.877x + 2.28 |
| | RIMM Spatial Mapping - cross-validation | 4.1 | 25.7% | 0.6 | 0.684 | y = 0.854x + 2.88 |
| C-FC | CAMS Ensemble forecast | 7.0 | 43.8% | -4.9 | 0.542 | y = 0.350x + 5.37 |
| C-IRA | CAMS Ensemble interim reanalysis | 6.2 | 38.9% | -4.0 | 0.614 | y = 0.356x + 6.27 |
| | | | | | | |
| | | Urban background areas | | | | |
| | | RMSE | RRMSE | Bias | $R^2$ | Regr. eq. |
| R | RIMM Spatial Mapping | 6.1 | 24.0% | -0.4 | 0.783 | y = 0.732x + 6.37 |
| | RIMM Spatial Mapping - cross-validation | 7.5 | 29.6% | -0.4 | 0.666 | y = 0.693x + 7.40 |
| C-FC | CAMS Ensemble - forecast | 17.5 | 69.3% | -13.1 | 0.227 | y = 0.130x + 8.94 |
| C-IRA | CAMS Ensemble - interim reanalysis | 16.8 | 66.5% | -11.8 | 0.163 | y = 0.109x + 10.71 |

Looking at Table 5.1, one can see that the best results are given by the RIMM spatial mapping, both in rural and urban areas. Namely, it should be noted that the CAMS Ensemble results (both the Forecast and the Interim Reanalysis) are underestimated, especially in the urban, but also in the rural areas.

Figure 5.1 shows the cross-validation resp. validation scatter plots for RIMM and CAMS Ensemble Interim Reanalysis results, for both rural and urban background areas.

Table 5.2 shows the comparison of the RIMM spatial mapping results (as used in Section 4.2, i.e. without the validation set of the stations) with two different CAMS Ensemble model results, based on the validation set of the stations. As the validation set of the stations was not used in the production of neither mapping nor modelling results, all the statistics are mutually comparable.

*Figure 5.1 Correlation between RIMM cross-validated (left) resp. CAMS Ensemble Interim Reanalysis (right) mapping values (y-axis) versus measurements from rural (top), resp. urban/suburban (bottom) background stations (x-axis) for $PM_{10}$ annual average 2017.*

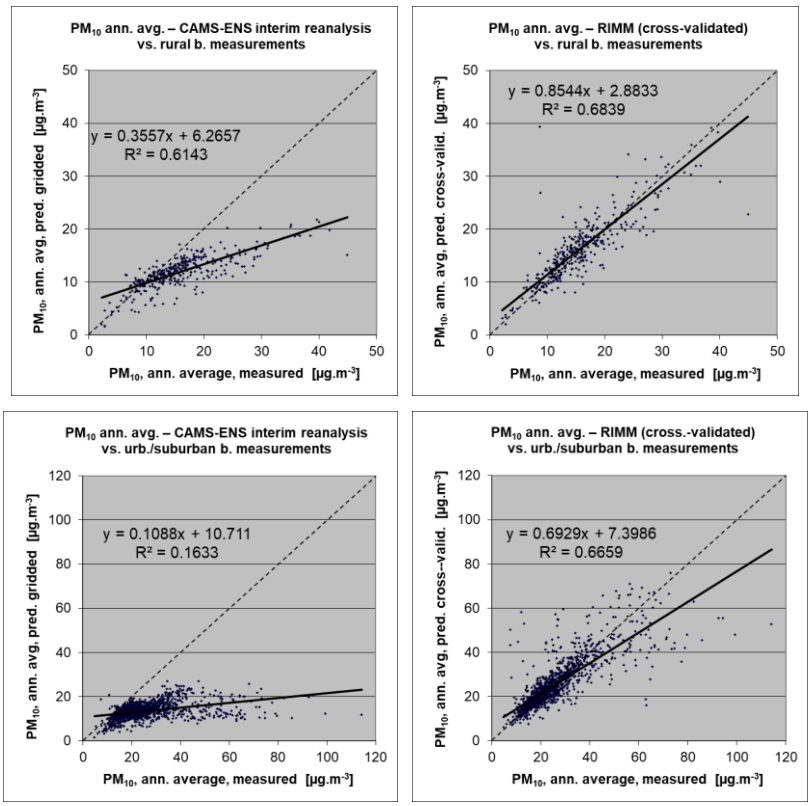


*Table 5.2 Comparison of different mapping methods showing RMSE, RRMSE, bias, $R^2$ and linear regression from simple scatter plots for $PM_{10}$ annual mean in rural background (top) and urban background (bottom) areas, 2017. Validation set of stations has not been used in mapping. Units: $\mu g.m^{-3}$ except RRMSE and $R^2$.*

| | | Rural background areas | | | | |
|---|---|---|---|---|---|---|
| | | RMSE | RRMSE | Bias | $R^2$ | Regr. eq. |
| R | RIMM Spatial Mapping | 3.2 | 19.7% | -1.3 | 0.704 | y = 0.638x + 4.67 |
| C-FC | CAMS Ensemble forecast | 7.2 | 43.9% | -5.5 | 0.250 | y = 0.226x + 7.27 |
| C-IRA | CAMS Ensemble interim reanalysis | 5.6 | 34.2% | -4.0 | 0.526 | y = 0.364x + 6.44 |
| | | | | | | |
| | | Urban background areas | | | | |
| | | RMSE | RRMSE | Bias | $R^2$ | Regr. eq. |
| R | RIMM Spatial Mapping | 3.4 | 16.9% | 0.1 | 0.747 | y = 0.837x + 3.34 |
| C-FC | CAMS Ensemble - forecast | 10.3 | 51.6% | -8.2 | 0.203 | y = 0.169x + 7.83 |
| C-IRA | CAMS Ensemble - interim reanalysis | 8.5 | 42.6% | -6.5 | 0.602 | y = 0.408x + 5.32 |

It can be seen that the RIMM spatial mapping clearly gives the best results, for both rural and urban areas, for all statistics.

Map 5.1 presents the concentration map of $PM_{10}$ annual average for 2017, based on RIMM spatial mapping (as routinely produced, Horálek et al., 2020), CAMS Ensemble Forecast and CAMS Ensemble Interim Reanalysis results. Annex, Map A.9 shows differences between the RIMM spatial map and the CAMS Ensemble Interim Reanalysis results. It can be clearly seen that the RIMM spatial map gives higher concentrations compared to the both CAMS Ensemble modelling results in a large part of Europe, especially in central and eastern Europe, Po valley, southern Spain and large areas of Turkey.

*Map 5.1 Concentration map of $PM_{10}$ annual average, 2017, created by routine spatial interpolation RIMM methodology (top), CAMS Ensemble Forecast model (middle) and CAMS Ensemble Interim Reanalysis model (bottom).*

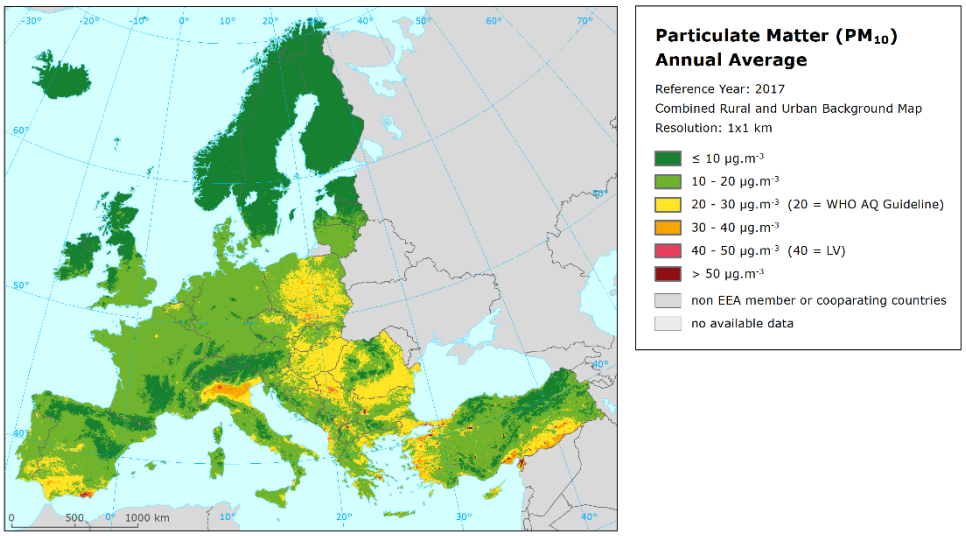


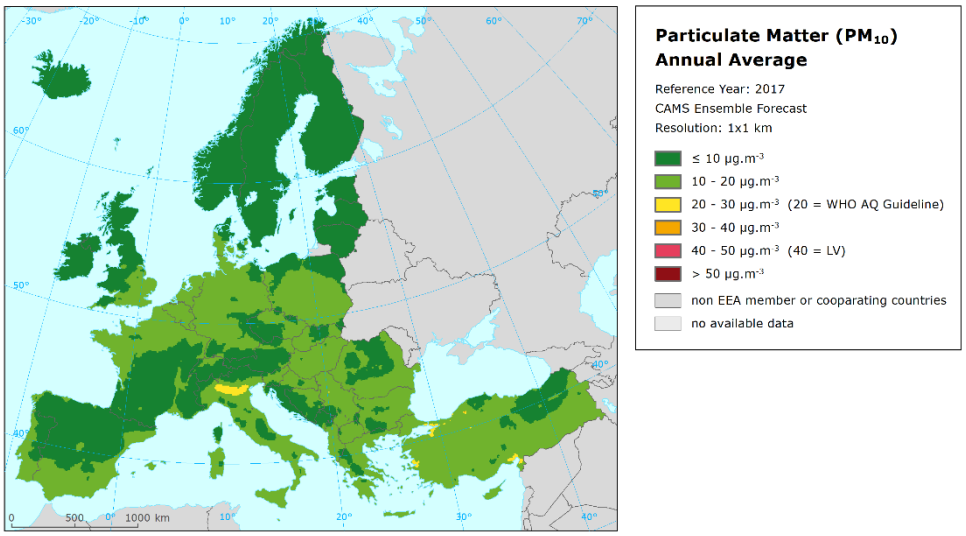


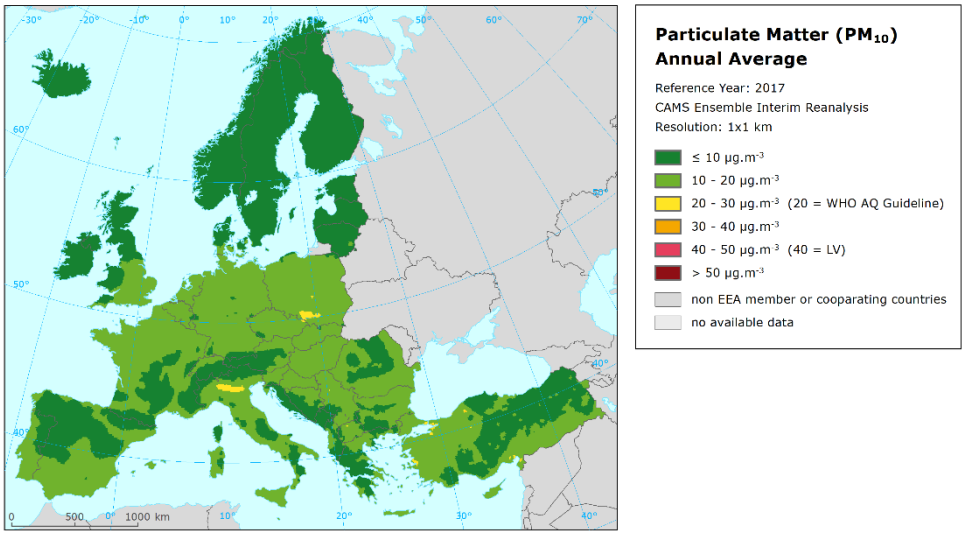

## 5.2 $PM_{25}$ annual average

Table 5.3 shows the comparison of the RIMM spatial mapping results (as routinely produced) with two different CAMS Ensemble model results, based on all stations.

The table row highlighted by green shows the statistics that provide the best performance, apart from the simple validation of RIMM (highlighted by blue).

*Table 5.3 Comparison of different mapping methods showing RMSE, RRMSE, bias, $R^2$ and linear regression from simple scatter plots for $PM_{2.5}$ annual mean in rural background (top) and urban background (bottom) areas, 2017. Units: µg.m$^{-3}$ except RRMSE and $R^2$.*

| | | Rural background areas | | | | |
|---|---|---|---|---|---|---|
| | | RMSE | RRMSE | Bias | $R^2$ | Regr. eq. |
| R | RIMM Spatial Mapping | 1.9 | 17.8% | -0.2 | 0.887 | y = 0.786x + 2.03 |
| | RIMM Spatial Mapping - cross-validation | 2.3 | 21.2% | 0.0 | 0.827 | y = 0.758x + 2.58 |
| C-FC | CAMS Ensemble forecast | 4.5 | 42.0% | -2.7 | 0.645 | y = 0.399x + 3.75 |
| C-IRA | CAMS Ensemble interim reanalysis | 3.9 | 36.5% | -1.9 | 0.722 | y = 0.427x + 4.18 |
| | | | | | | |
| | | Urban background areas | | | | |
| | | RMSE | RRMSE | Bias | $R^2$ | Regr. eq. |
| R | RIMM Spatial Mapping | 2.2 | 14.9% | -0.1 | 0.881 | y = 0.881x + 1.65 |
| | RIMM Spatial Mapping - cross-validation | 2.7 | 18.3% | -0.1 | 0.822 | y = 0.849x + 2.14 |
| C-FC | CAMS Ensemble - forecast | 7.8 | 52.1% | -5.9 | 0.452 | y = 0.290x + 4.64 |
| C-IRA | CAMS Ensemble - interim reanalysis | 6.8 | 45.4% | -4.9 | 0.574 | y = 0.343x + 4.87 |

One can see that the best results are clearly given by the RIMM spatial mapping, both in rural and urban areas. Like for $PM_{10}$, the CAMS Ensemble results (both the forecast and the interim reanalysis) are underestimated, especially in the urban, but also in the rural areas.

Figure 5.2 shows the cross-validation resp. validation scatter plots for RIMM and CAMS Ensemble Interim Reanalysis results, for both rural and urban background areas.

*Figure 5.2 Correlation between RIMM cross-validated (left) resp. CAMS Ensemble Interim Reanalysis (right) mapping values (y-axis) versus measurements from rural (top), resp. urban/suburban (bottom) background stations (x-axis) for $PM_{2.5}$ annual average 2017.*

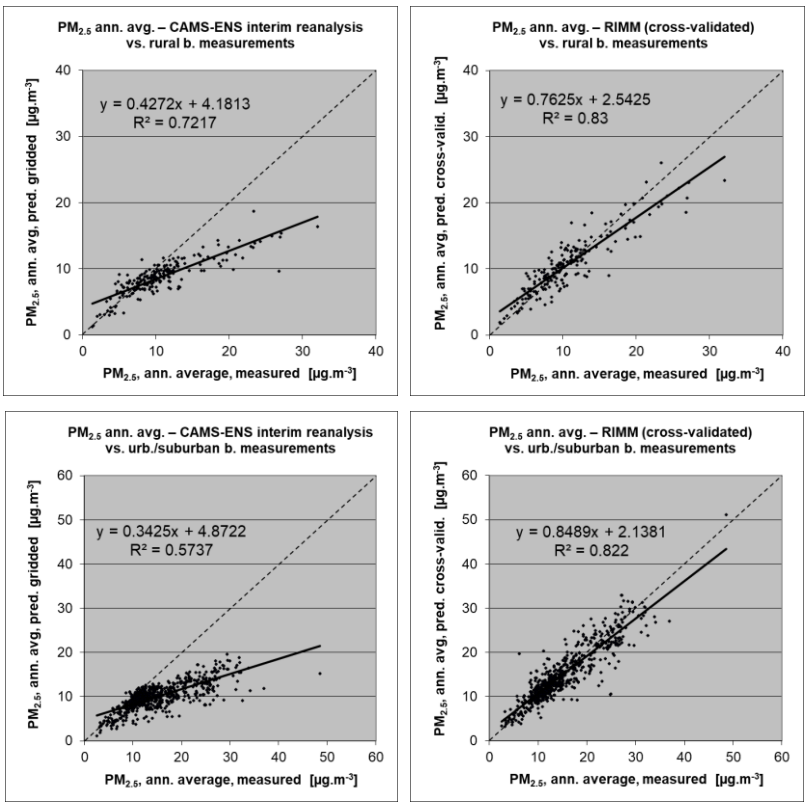


Table 5.4 shows the comparison of the RIMM spatial mapping results (as used in Section 4.2) with two different CAMS Ensemble model results, based on the validation set of the stations.

*Table 5.4 Comparison of different mapping methods showing RMSE, RRMSE, bias, $R^2$ and linear regression from simple scatter plots for $PM_{2.5}$ annual mean in rural background (top) and urban background (bottom) areas, 2017. Validation set of stations has not been used in mapping. Units: $\mu g.m^{-3}$ except RRMSE and $R^2$.*

| | | Rural background areas | | | | |
|---|---|---|---|---|---|---|
| | | RMSE | RRMSE | Bias | $R^2$ | Regr. eq. |
| R | RIMM Spatial Mapping | 1.5 | 14.7% | 0.0 | 0.859 | y = 0.706x + 3.02 |
| C-FC | CAMS Ensemble forecast | 3.9 | 36.9% | -2.3 | 0.358 | y = 0.206x + 6.06 |
| C-IRA | CAMS Ensemble interim reanalysis | 2.9 | 27.2% | -1.3 | 0.677 | y = 0.357x + 5.50 |
| | | | | | | |
| | | Urban background areas | | | | |
| | | RMSE | RRMSE | Bias | $R^2$ | Regr. eq. |
| R | RIMM Spatial Mapping | 2.3 | 17.8% | -0.2 | 0.743 | y = 0.811x + 2.20 |
| C-FC | CAMS Ensemble - forecast | 5.9 | 46.0% | -4.4 | 0.193 | y = 0.181x + 6.14 |
| C-IRA | CAMS Ensemble - interim reanalysis | 4.6 | 36.2% | -3.2 | 0.460 | y = 0.304x + 5.76 |

The statistics presented in Table 5.4 confirm the results of Table 5.3. It can be stated that the RIMM spatial mapping gives the best results, for both rural and urban areas, for all statistics.

Map 5.2 presents the concentration map of $PM_{2.5}$ annual average for 2017, based on RIMM spatial mapping (as routinely produced), CAMS Ensemble Forecast and CAMS-ENS Interim Reanalysis results.

*Map 5.2 Concentration map of $PM_{2.5}$ annual average, 2017, created by routine spatial interpolation RIMM methodology (top), CAMS Ensemble Forecast model (middle) and CAMS Ensemble Interim Reanalysis model (bottom).*

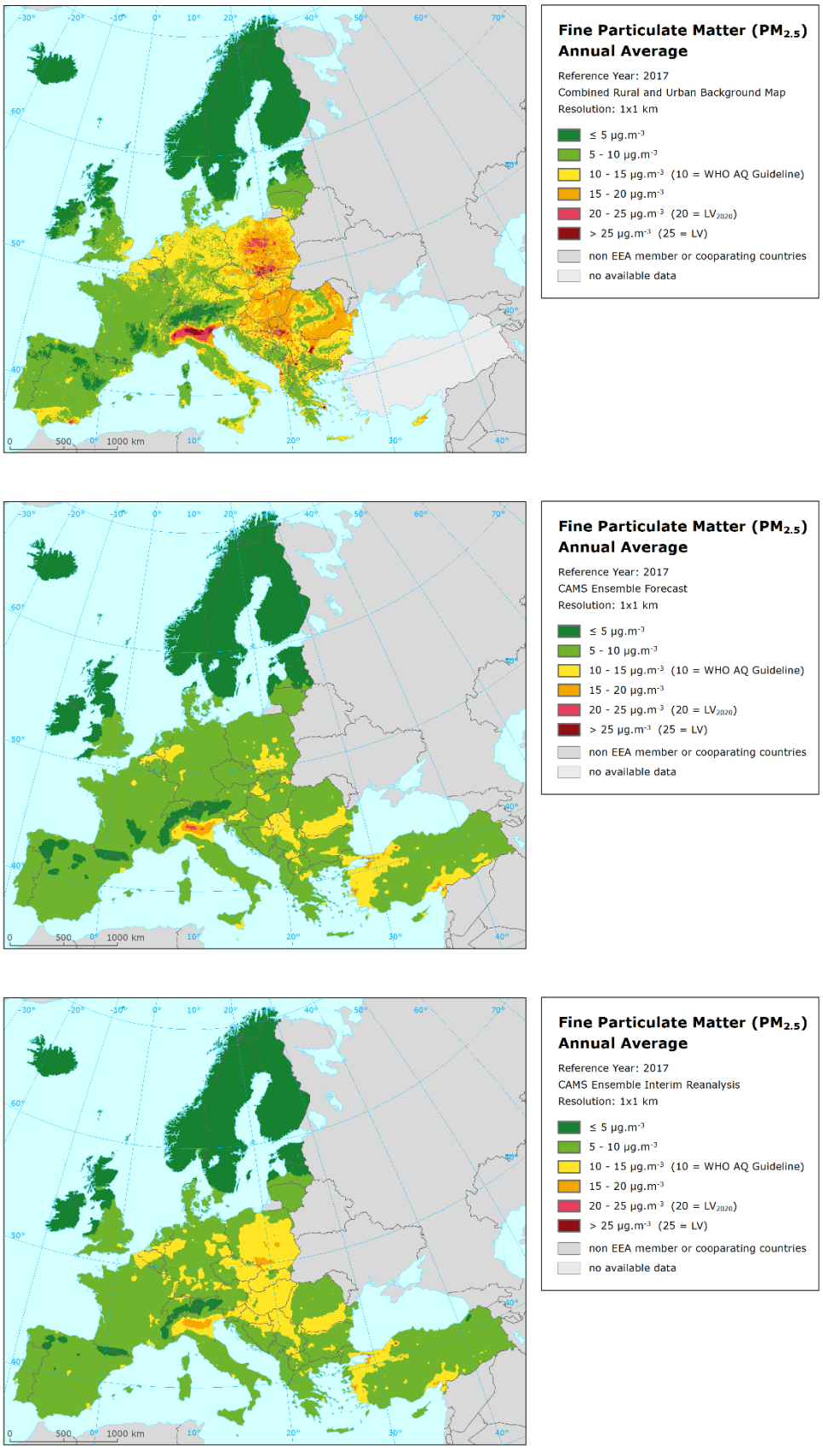

Annex, Map A.10 shows differences between the RIMM spatial map and the CAMS Ensemble Interim Reanalysis results.

Similarly to the case of $PM_{10}$, although to the less extent, the RIMM spatial map gives higher concentrations compared to both CAMS Ensemble modelling results in a large part of Europe, especially in the central and eastern Europe, in the Po valley and in southern Spain.

## 5.3 Ozone – SOMO35

Table 5.5 shows the comparison of the RIMM spatial mapping results (as routinely produced) with two different CAMS Ensemble model results, based on all stations.

The table row highlighted by green shows the statistics that provide the best performance, apart from the simple validation of RIMM (highlighted by blue).

*Table 5.5 Comparison of different mapping methods showing RMSE, RRMSE, bias, $R^2$ and linear regression from simple or cross-validation (RIMM) scatter plots for ozone indicator SOMO35 in rural background (top) and urban background (bottom) areas, 2017. Units: µg.m$^{-3}$ except RRMSE and $R^2$.*

| | | Rural background areas | | | | |
|---|---|---|---|---|---|---|
| | | RMSE | RRMSE | Bias | $R^2$ | Regr. eq. |
| R | RIMM Spatial Mapping | 1495 | 27.5% | -188 | 0.743 | y = 0.721x + 1331 |
| | RIMM Spatial Mapping - cross-validation | 1609 | 29.5% | -190 | 0.701 | y = 0.696x + 1466 |
| C-FC | CAMS Ensemble forecast | 2125 | 39.0% | -508 | 0.501 | y = 0.505x + 2189 |
| C-IRA | CAMS Ensemble interim reanalysis | 2309 | 42.4% | -1383 | 0.604 | y = 0.550x + 1067 |
| | | | | | | |
| | | Urban background areas | | | | |
| | | RMSE | RRMSE | Bias | $R^2$ | Regr. eq. |
| R | RIMM Spatial Mapping | 1036 | 24.0% | 72 | 0.828 | y = 0.839x + 769 |
| | RIMM Spatial Mapping - cross-validation | 1336 | 31.0% | 130 | 0.720 | y = 0.780x + 1078 |
| C-FC | CAMS Ensemble forecast | 1848 | 42.8% | 750 | 0.555 | y = 0.647x + 2276 |
| C-IRA | CAMS Ensemble interim reanalysis | 1667 | 38.6% | -255 | 0.570 | y = 0.634x + 1326 |

In Table 5.5 one can see that the best results are given by the RIMM spatial mapping, both in rural and urban areas. The difference is smaller than for $PM_{10}$ and $PM_{2.5}$.

Figure 5.3 shows the cross-validation resp. validation scatter plots for RIMM and CAMS Ensemble Interim Reanalysis results, for both rural and urban background areas.

*Figure 5.3 Correlation between RIMM cross-validated (left) resp. CAMS Ensemble Interim Reanalysis (right) mapping values (y-axis) versus measurements from rural (top), resp. urban/suburban (bottom) background stations (x-axis) for ozone indicator SOMO35 for 2017.*

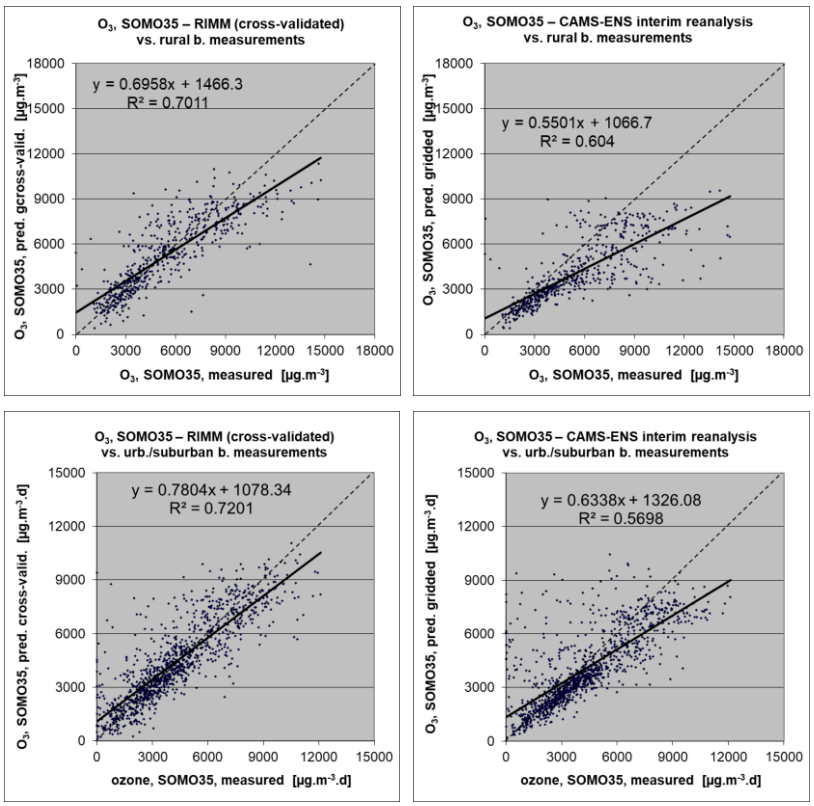


Table 5.6 shows the comparison of the RIMM spatial mapping results (as used in Section 4.2) with two different CAMS Ensemble model results, based on the validation set of the stations.

*Table 5.6 Comparison of different mapping methods showing RMSE, RRMSE, bias, $R^2$ and linear regression from simple scatter plots for ozone indicator SOMO35 in rural background (top) and urban background (bottom) areas, 2017. Validation set of stations has not been used in mapping. Units: µg.m$^{-3}$ except RRMSE and $R^2$.*

| | | Rural background areas | | | | |
|---|---|---|---|---|---|---|
| | | RMSE | RRMSE | Bias | $R^2$ | Regr. eq. |
| R | RIMM Spatial Mapping | 1445 | 27.4% | -74 | 0.734 | y = 0.721x + 1395 |
| C-F | CAMS Ensemble forecast | 2091 | 39.7% | -460 | 0.471 | y = 0.504x + 2151 |
| C-IRA | CAMS Ensemble interim reanalysis | 2404 | 45.6% | -1460 | 0.535 | y = 0.515x + 1094 |
| | | | | | | |
| | | Urban background areas | | | | |
| | | RMSE | RRMSE | Bias | $R^2$ | Regr. eq. |
| R | RIMM Spatial Mapping | 1351 | 31.3% | 136 | 0.781 | y = 0.835x + 754 |
| C-F | CAMS Ensemble forecast | 1656 | 37.7% | 602 | 0.608 | y = 0.679x + 2010 |
| C-IRA | CAMS Ensemble interim reanalysis | 1463 | 33.3% | -452 | 0.675 | y = 0.690x + 908 |

It can be seen that the best results are given by the RIMM spatial mapping, both in rural and urban areas. The difference in the rural areas is more remarkable.

Map 5.3 presents the concentration map of ozone indicator SOMO35 for 2017, based on RIMM spatial mapping (as routinely produced), CAMS Ensemble Forecast and CAMS-ENS Interim Reanalysis results.

*Map 5.3 Concentration map of ozone indicator SOMO35, 2017, created by routine spatial interpolation RIMM methodology (top), CAMS Ensemble Forecast model (middle) and CAMS Ensemble Interim Reanalysis model (bottom).*

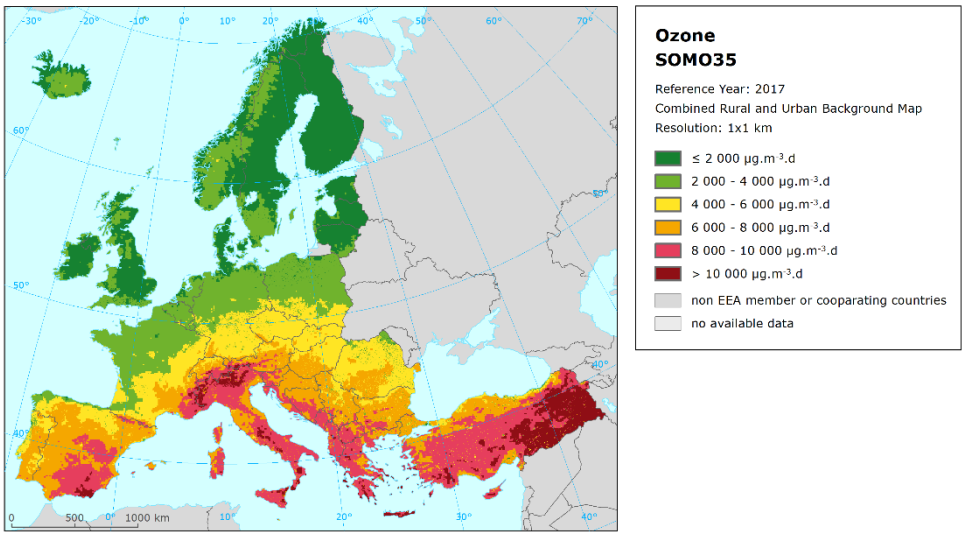


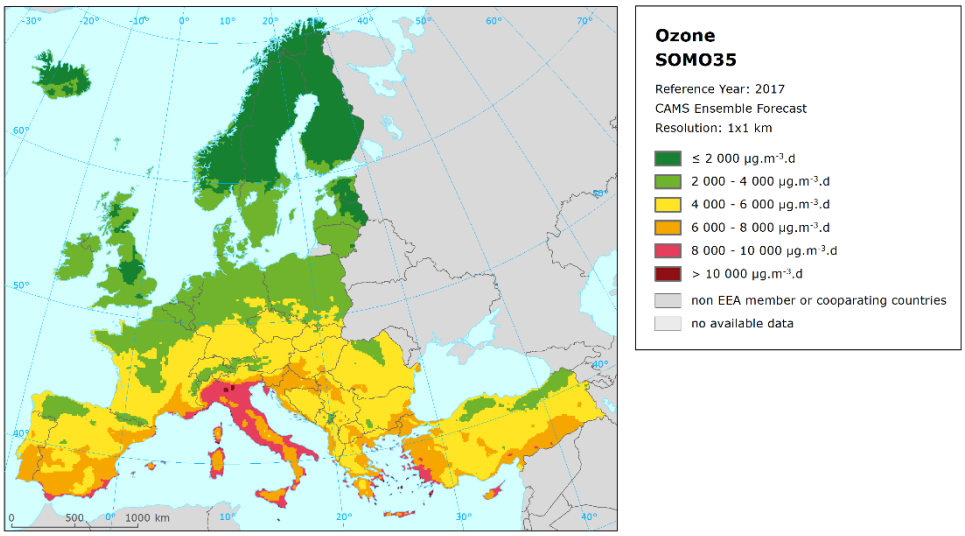


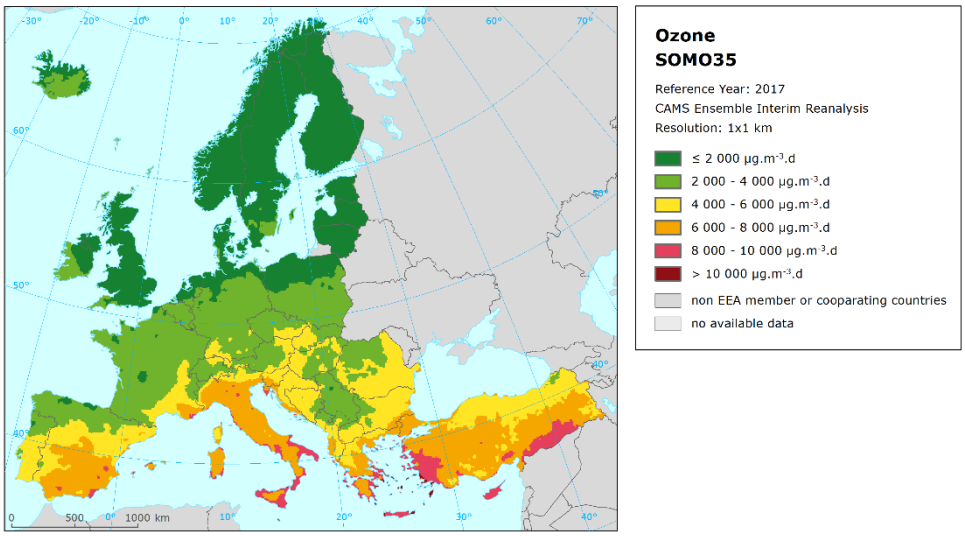

Annex, Map A.11 shows differences between the RIMM spatial map and the CAMS Ensemble Interim Reanalysis results.

Comparing the mapping results of SOMO35, one can see that the RIMM spatial map gives higher results in southern Europe and also in the mountainous areas like the Alps and the Pyrenees.

## 5.4 $NO_2$ annual average

Table 5.7 shows the comparison of the RIMM spatial mapping results (as routinely produced) with two different CAMS Ensemble model results, based on all stations.

Again, the table cells highlighted by green show the statistics that provide the best performance, apart from the simple validation of RIMM (highlighted by blue).

*Table 5.7 Comparison of different mapping methods showing RMSE, RRMSE, bias, $R^2$ and linear regression from simple or cross-validation (RIMM) scatter plots for $NO_2$ annual mean in rural background (top) and urban background (bottom) areas, 2017. Units: $\mu g.m^{-3}$ except RRMSE and $R^2$.*

| | | Rural background areas | | | | |
|---|---|---|---|---|---|---|
| | | RMSE | RRMSE | Bias | $R^2$ | Regr. eq. |
| R | RIMM Spatial Mapping | 2.8 | 32.5% | 0.3 | 0.785 | y = 0.878x + 1.31 |
| | RIMM Spatial Mapping - cross-validation | 2.9 | 33.7% | 0.5 | 0.769 | y = 0.851x + 1.76 |
| C-FC | CAMS Ensemble forecast | 3.8 | 43.8% | -1.4 | 0.643 | y = 0.698x + 1.23 |
| C-IRA | CAMS Ensemble interim reanalysis | 3.3 | 39.0% | -0.4 | 0.676 | y = 0.650x + 2.62 |
| | | | | | | |
| | | Urban background areas | | | | |
| | | RMSE | RRMSE | Bias | $R^2$ | Regr. eq. |
| R | RIMM Spatial Mapping | 4.6 | 22.4% | 0.5 | 0.749 | y = 0.781x + 5.02 |
| | RIMM Spatial Mapping - cross-validation | 5.9 | 28.4% | -0.5 | 0.602 | y = 0.680x + 6.14 |
| C-FC | CAMS Ensemble - forecast | 12.7 | 61.4% | -10.0 | 0.299 | y = 0.409x + 2.27 |
| C-IRA | CAMS Ensemble - interim reanalysis | 11.5 | 55.5% | -8.5 | 0.305 | y = 0.372x + 4.50 |

One can see that the best results are given by the RIMM spatial mapping, both in rural and urban areas. The difference in the urban areas is more sizeable, compared to the rural areas, which is caused mainly by the coarser resolution of the CAMS Ensemble results. It can be seen that the CAMS Ensemble results (both the forecast and the interim reanalysis) are clearly underestimated in the urban areas.

Figure 5.4 shows the cross-validation resp. validation scatter plots for RIMM and CAMS Ensemble Interim Reanalysis results, for both rural and urban background areas.

Table 5.6 shows the comparison of the RIMM spatial mapping results (as used in Section 4.2) with two different CAMS Ensemble model results, based on the validation set of the stations.

*Figure 5.4 Correlation between RIMM cross-validated (left) resp. CAMS Ensemble Interim Reanalysis (right) mapping values (y-axis) versus measurements from rural (top), resp. urban/suburban (bottom) background stations (x-axis) for $NO_2$ annual average 2017.*

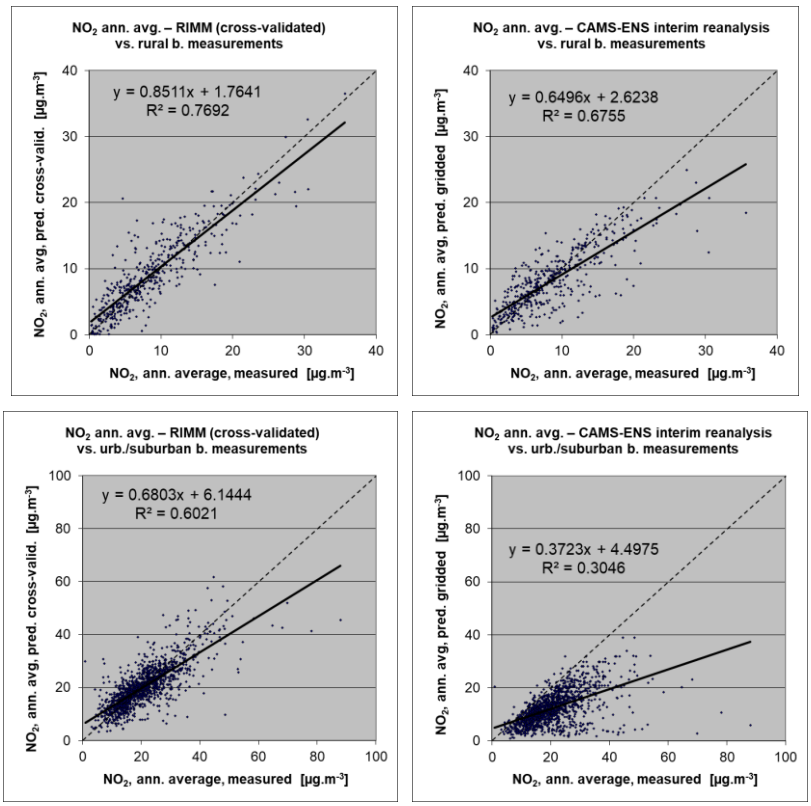


*Table 5.8 Comparison of different mapping methods showing RMSE, RRMSE, bias, $R^2$ and linear regression from simple scatter plots for $NO_2$ annual mean in rural background (top) and urban background (bottom) areas, 2017. Validation set of stations has not been used in mapping. Units: $\mu g.m^{-3}$ except RRMSE and $R^2$.*

| | | Rural background areas | | | | |
|---|---|---|---|---|---|---|
| | | RMSE | RRMSE | Bias | $R^2$ | Regr. eq. |
| R | RIMM Spatial Mapping | 2.7 | 27.8% | -0.3 | 0.777 | y = 0.856x + 1.09 |
| C-FC | CAMS Ensemble forecast | 3.5 | 37.0% | -1.1 | 0.637 | y = 0.726x + 1.54 |
| C-IRA | CAMS Ensemble interim reanalysis | 3.5 | 36.7% | 0.1 | 0.594 | y = 0.632x + 3.62 |
| | | | | | | |
| | | Urban background areas | | | | |
| | | RMSE | RRMSE | Bias | $R^2$ | Regr. eq. |
| R | RIMM Spatial Mapping | 5.2 | 24.8% | 1.0 | 0.620 | y = 0.761x + 5.86 |
| C-FC | CAMS Ensemble - forecast | 10.7 | 51.4% | -8.9 | 0.483 | y = 0.612x - 0.87 |
| C-IRA | CAMS Ensemble - interim reanalysis | 9.4 | 45.3% | -7.7 | 0.539 | y = 0.572x + 1.18 |

It can be seen that the best results are given by the RIMM spatial mapping, both in rural and urban areas. The difference in the urban areas is more remarkable.

Map 5.4 presents the concentration map of $NO_2$ annual average for 2017, based on RIMM spatial mapping (as routinely produced), CAMS Ensemble Forecast and CAMS Ensemble Interim Reanalysis results. Annex, Map A.12 shows differences between the RIMM spatial map and the CAMS Ensemble Interim Reanalysis results. Comparing the mapping results, one can see that the RIMM spatial map gives higher results in the Balkan area and Turkey, in the Po valley, in southern Spain and in general in the urban areas, while lower results in some rural areas in central and north-western Europe.

*Map 5.4 Concentration map of $NO_2$ annual average, 2017, created by routine spatial interpolation RIMM methodology (top), CAMS Ensemble Forecast model (middle) and CAMS Ensemble Interim Reanalysis model (bottom).*

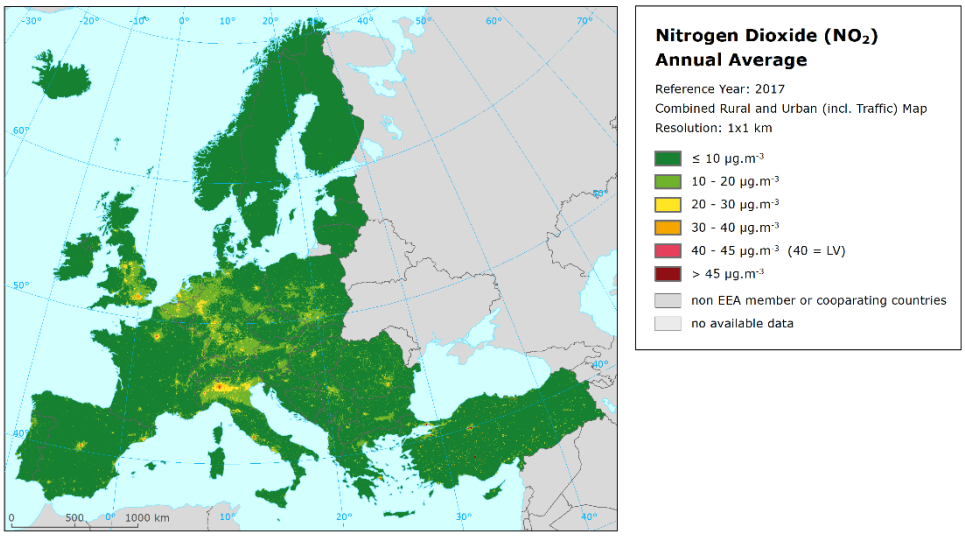


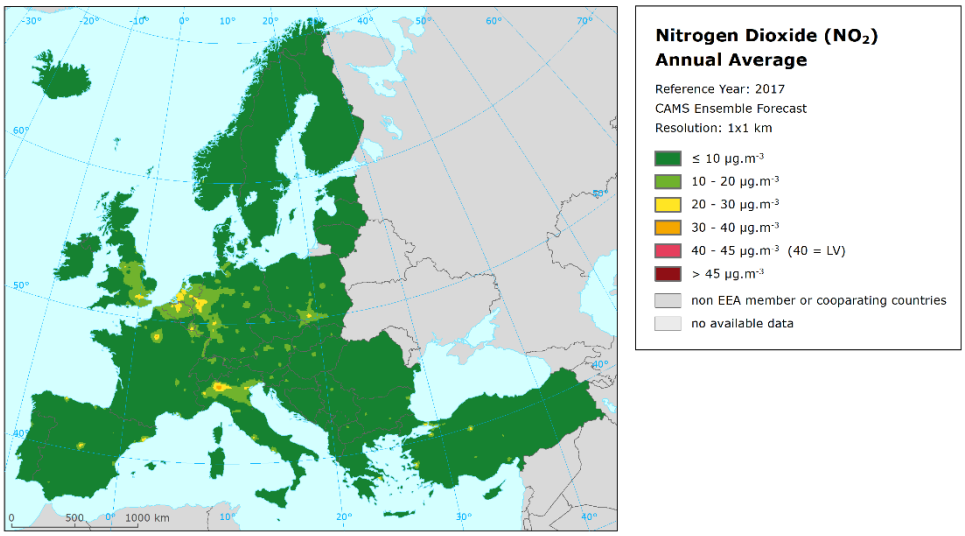


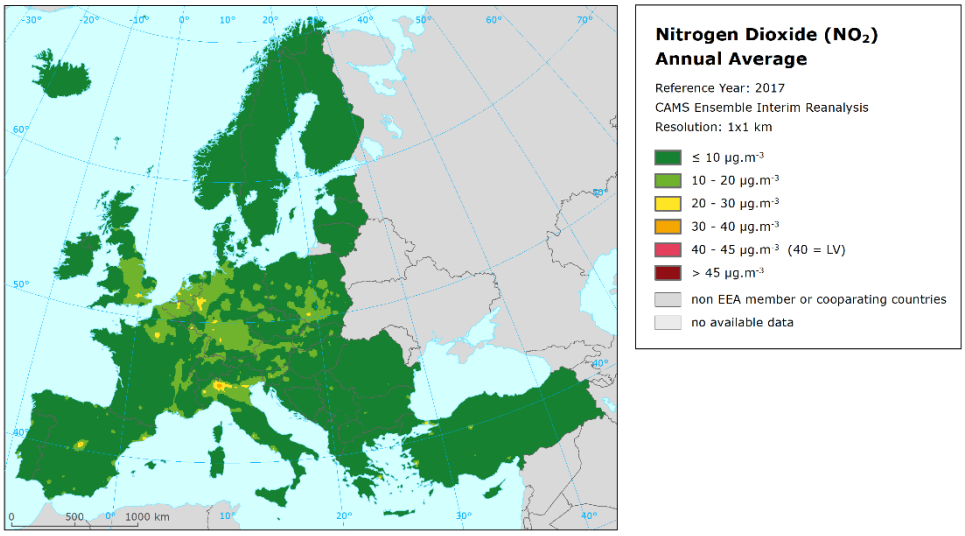

## 5.5 Conclusion

From the comparison of the RIMM spatial mapping results with the CAMS Ensemble modelling results, one can conclude that **the data fusion RIMM method gives better results, as expected, both in the rural and urban background areas**. This result is highly influenced by the finer resolution of the RIMM spatial maps. Among other reason for this, the introduction of additional ancillary data in the data fusion probably plays a role, as well as not fully reduced bias in some data assimilations methods (Denby et al., 2008), which are used in CAMS.

Based on this, we verify the assumption that **the RIMM spatial mapping** (where the main input is AQ concentration data measured at monitoring stations), **is better suited for exposure calculations**.

# 6 Conclusions and Recommendations

The report examines potential use of modelling outputs from the Copernicus Atmospheric Monitoring Service (CAMS) in the air quality spatial interpolation mapping. Specifically, the ensemble mean (i.e. the median of seven regional atmospheric dispersion models) forecast and interim reanalysis products have been examined. All the analysis has been performed for 2017 data.

Preliminary/interim spatial interpolation (RIMM) air quality maps based on the UTD (E2a) measurement data can be constructed approximately one year earlier than the validated maps, using any of the examined models. With respect to the availability, it is recommended to use the CAMS Ensemble Forecast in the potential interim mapping. (Potentially, alternatively might be used the CAMS Ensemble Analysis, which was not tested in this report.) Even though we have demonstrated the feasibility, potential production of indicator or exposure maps using UTD observations (i.e. not official submitted data) should be carefully considered. In addition, the evaluation of the mapping performances presented here is influenced by the lack of the E2a data in some areas, so that the quality of the interim maps in these areas is poorer compared to the main part of Europe. Potentially, the lack of E2a stations in these areas could be substituted by so-called pseudo stations, i.e. by the estimates at the locations of E1a stations with no E2a data, based on the relation between E2a data and validated E1a data from year Y-1. It is recommended to test the feasibility of such an approach.

Next to the evaluation of the potential interim maps, regular maps based on the validated E1a measurement data using three different chemical transport model outputs have been compared, i.e., using the CAMS Ensemble Forecast, the CAMS Ensemble Interim Reanalysis and the EMEP model outputs. Based on the evaluation of the results presented, it is not possible to conclude that any of the three model datasets gives definitively better results compared to the others. Depending on the pollutant and areas (urban/rural), one or another model provides better results. The margins of difference in the statistical measures used are so small that the differences are likely not statistically significant in many cases. Such results do not give strong reasons for a potential change of the model used in the mapping.

In addition, RIMM spatial mapping results have been compared with the examined CAMS Ensemble modelling results. From the comparison, one can conclude that the data fusion RIMM method gives better results, both in the rural and urban background areas, presumably because of the higher spatial resolution, introduction of additional ancillary data in the data fusion and not fully reduced bias in some data assimilation methods used in CAMS. Based on this, we verify the assumption that the RIMM spatial mapping (where the main input are AQ concentration data measured at monitoring stations), is better suited for exposure calculations (especially in urban areas) than the CAMS Ensemble Forecast and Interim Reanalysis. Be it noted that the comparison of the RIMM spatial maps with CAMS products is not complete and exhaustive, as the CAMS Validated Reanalysis model results have not been examined (due to not availability of these results for 2017 in the time of the analysis).

# 7 List of abbreviations

| | |
|---|---|
| AQ | Air quality |
| CAMS | Copernicus Atmospheric Monitoring Services |
| CLC | CORINE Land cover |
| CORINE | Co-ORdinated INformation on the Environment |
| CTM | Chemical transport model |
| ECMWF | European Centre for Medium-Range Weather Forecasts |
| EBAS | EMEP dataBASe |
| EEA | European Environmental Agency |
| EMEP | European Monitoring and Evaluation Programme |
| ETC/ACM | European Topic Centre on Air pollution and Climate change Mitigation |
| ETC/ATNI | European Topic Centre on Air pollution, Noise, Transport and Industrial pollution |
| GMTED | Global multi-resolution terrain elevation data |
| GRIP | Global Roads Inventory Dataset |
| JRC | Joint Research Centre |
| NASA | National Aeronautics and Space Administration |
| NILU | Norwegian Institute for Air Research |
| $NO_2$ | Nitrogen dioxide |
| $O_3$ | Ozone |
| OMI | Ozone Monitoring Instrument |
| $PM_{10}$ | Particulate Matter 10 micrometres or less in diameter |
| $PM_{2.5}$ | Particulate Matter 2.5 micrometres or less in diameter |
| RIMM | Regression – Interpolation – Merging Mapping |
| SOMO35 | Sum of Ozone Maximum daily 8-hour means Over 35 ppb (i.e. 70 $\mu g.m^{-3}$) |
| UTC | Coordinated Universal Time |
| UTD | Up-to-date |

# 8 References


Copernicus, 2019, *CAMS European air quality data archive* http://www.regional.atmosphere.copernicus.eu/?category=data_access).

Danielson, J. J. and Gesch, D. B., 2011, *Global multi-resolution terrain elevation data 2010 (GMTED2010)*, U.S. Geological Survey Open-File Report, pp. 2011–1073 (https://pubs.er.usgs.gov/publication/ofr20111073).

EEA, 2010, *ORNL Landscan 2008 Global Population Data conversion into EEA ETRS89-LAEA5210 1km grid* (by Hermann Peifer of EEA) (https://sdi.eea.europa.eu/catalogue/geoss/api/records/1d68d314-d07c-4205-8852-f74b364cd699).

EEA, 2016, *Corine land cover 2012 (CLC2012) raster data*, 100x100 $m^2$ gridded version 18 (09/2016 (https://sdi.eea.europa.eu/catalogue/srv/api/records/ff21ade0-a714-4725-86bb-279ee7a8a73e).

EEA, 2018, *Air Quality e-Reporting*, Air quality database, E2a dataset extracted by EEA in March 2018.

EEA, 2019, *Air Quality e-Reporting*, Air quality database (https://www.eea.europa.eu/data-and-maps/data/aqereporting-8).

EMEP, 2018, *Transboundary particular matter, photo-oxidants, acidifying and eutrophying components*, EMEP Report 1/2018 (http://emep.int/publ/reports/2018/EMEP_Status_Report_1_2018.pdf).

Denby, B., et al., 2008, 'Comparison of two data assimilation methods for assessing $PM_{10}$ exceedances on the European scale', *Atmospheric Environment* 42, pp. 7122–7134 (https://doi.org/10.1016/j.atmosenv.2008.05.058).

Horálek, J., et al., 2014, *Evaluation of Copernicus MACC-II ensemble products in the ETC/ACM spatial air quality mapping*, ETC/ACM Technical Paper 2013/9, http://www.eionet.europa.eu/etcs/etc-atni/products/etc-atni-reports/etcacm_tp_2013_9_aqmaps_with_maccproducts).

Horálek, J., et. al., 2020, *European air quality maps for 2017*, Eionet Report ETC/ATNI 2019/9 (https://doi.org/10.5281/zenodo.4309292).

JRC, 2009, *Population density disaggregated with Corine land cover 2000,* 100x100 $m^2$ grid resolution, EEA version (http://www.eea.europa.eu/data-and-maps/data/population-density-disaggregated-with-corine-land-cover-2000-2).

Kuenen, J. J. P., et al., 2014, 'TNO-MACC_II emission inventory; a multi-year (2003--2009) consistent high-resolution European emission inventory for air quality modelling', *Atmospheric Chemistry and Physics* 14, pp. 10963–10976, https://doi.org/10.5194/acp-14-10963-2014).

Meijer, J. R., et al., 2018, 'Global patterns of current and future road infrastructure', *Environmental Research Letters 13* 064006 (https://doi.org/10.1088/1748-9326/aabd42).

Marécal, V., et al., 2015, 'A regional air quality forecasting system over Europe: The MACC-II daily ensemble production', *Geoscientific Model Development* 8, pp. 2777–2813 (https://doi.org/10.5194/gmd-8-2777-2015).

Mareckova, K., et al., 2018, *Inventory Review 2018. Review of emission data reported under the LRTAP Convention and NEC Directive, Stage 1 and 2 review & Status of gridded and LPS data,* EEA/CEIP Technical Report 4/2018 (https://webdab01.umweltbundesamt.at/download/InventoryReport_2018_v2.pdf).

NASA, 2019, *OMNO2d level 3 satellite data* (https://acdisc.gsfc.nasa.gov/opendap/HDF-EOS5/Aura_OMI_Level3/OMNO2d.003).

NILU, 2018, *EBAS, database of atmospheric chemical composition and physical properties* (http://ebas.nilu.no).

Simpson, D., et al., 2012, 'The EMEP MSC-W chemical transport model – technical description', *Atmospheric Chemistry and Physics* 12, pp. 7825–7865, (https://doi.org/10.5194/acp-12-7825-2012).

# Annex
# Difference maps

This annex presents the maps showing differences between individual model results, for four pollutants $PM_{10}$, $PM_{2.5}$, ozone and $NO_2$, see Figures A1.1, A1.3, A1.5 and A1.7.

Next to this, it shows the maps showing differences between the RIMM spatial maps using different model results, again for four pollutants $PM_{10}$, $PM_{2.5}$, ozone and $NO_2$. See Figures A1.2, A1.4, A1.6 and A1.8.

Finally, it presents the maps showing differences between the RIMM spatial map (as routinely produced under ETC/ATNI, i.e. using EMEP) and the CAMS Ensemble Interim Reanalysis modelling results, see Figures A1.9–A1.12.

*Map A.1 Map showing difference in concentrations between CAMS-ENS Forecast and EMEP (top), CAMS-ENS Interim Reanalysis and EMEP (middle) or CAMS-ENS Forecast and CAMS-ENS Interim Reanalysis (bottom) model outputs for $PM_{10}$ annual average, 2017*

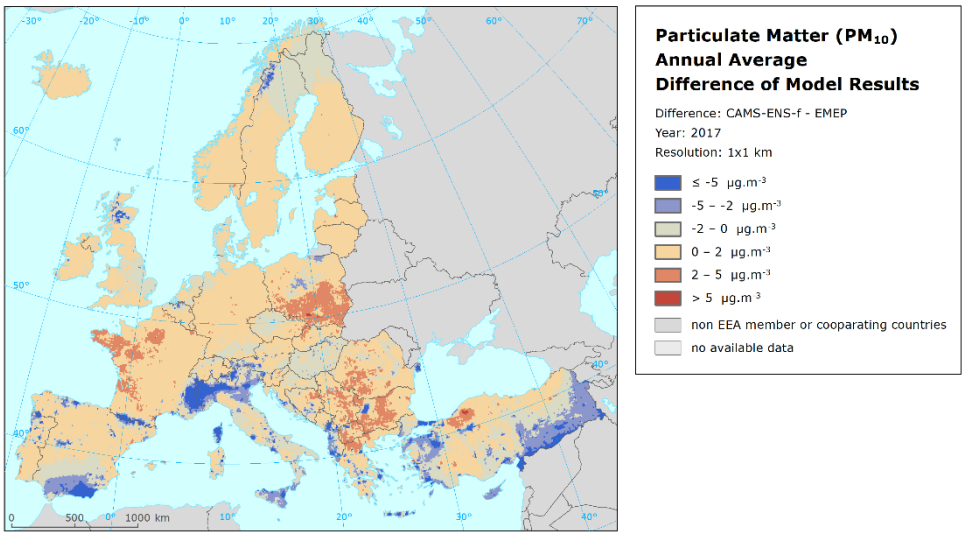


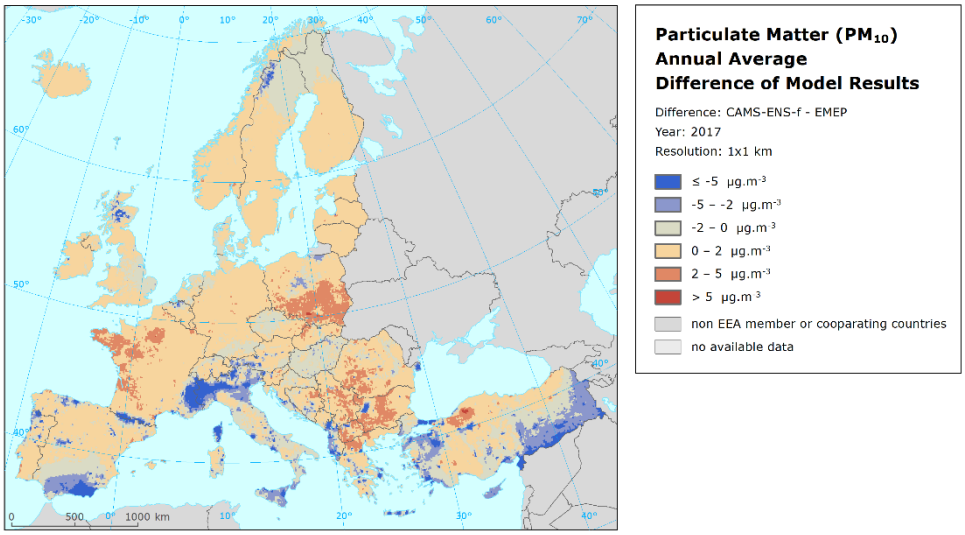


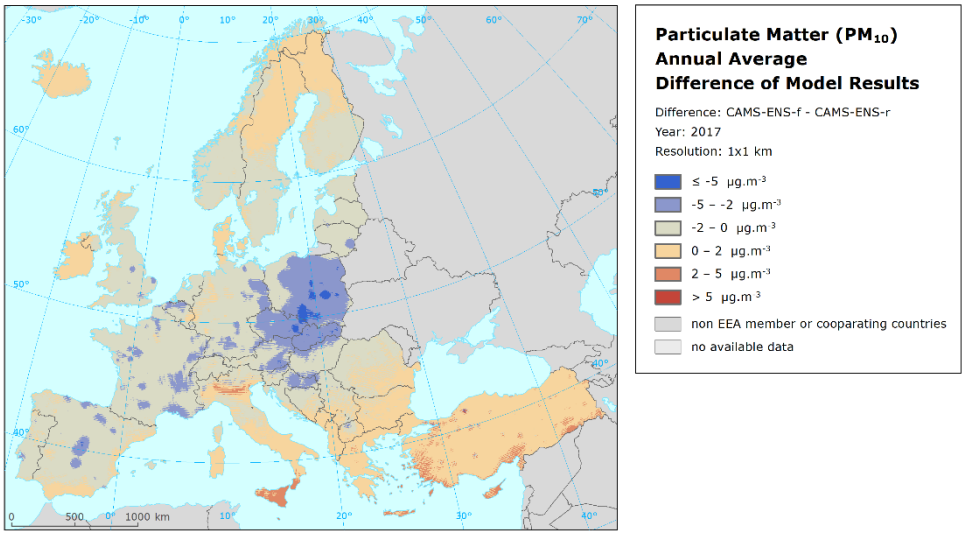

*Map A.2 Map showing difference in concentrations between RIMM using CAMS-ENS Forecast and RIMM using EMEP (top), RIMM using CAMS-ENS Interim Reanalysis and RIMM using EMEP (middle) or RIMM using CAMS-ENS Forecast and RIMM using CAMS-ENS Interim Reanalysis (bottom) model outputs for $PM_{10}$ annual average, 2017*

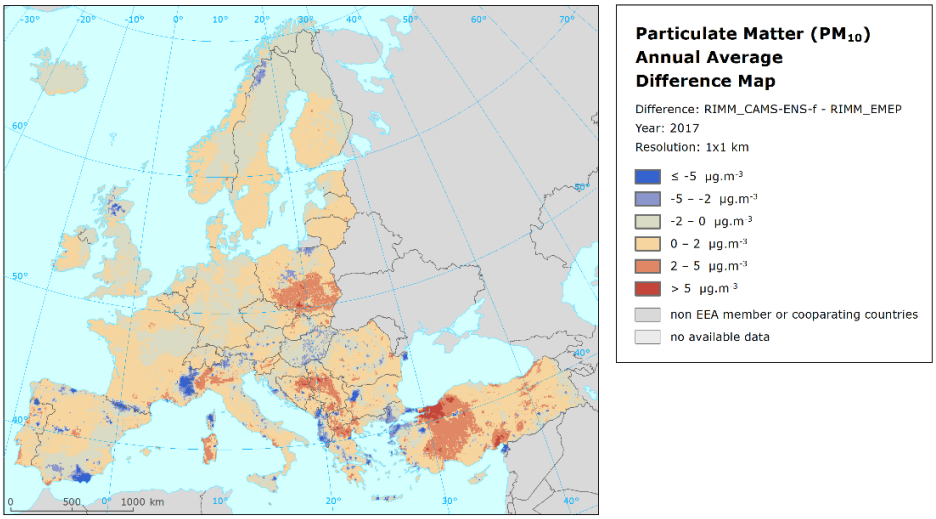


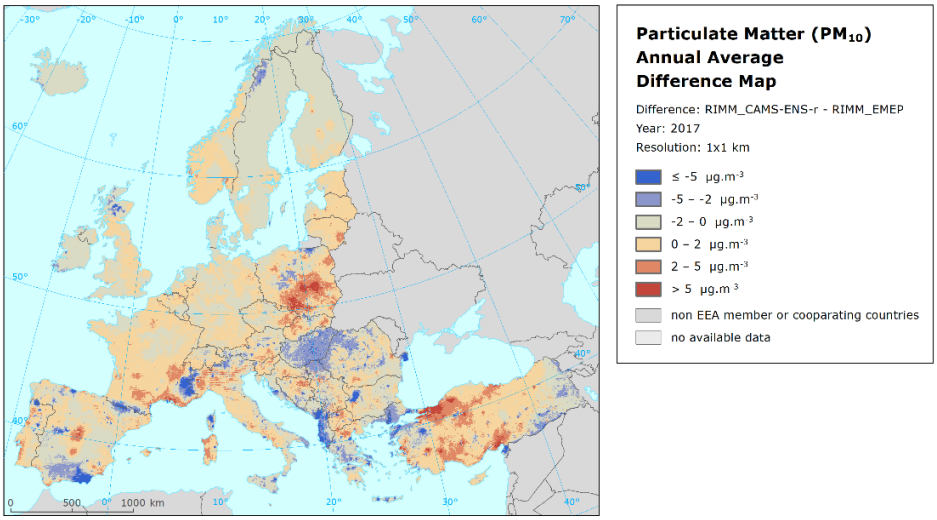


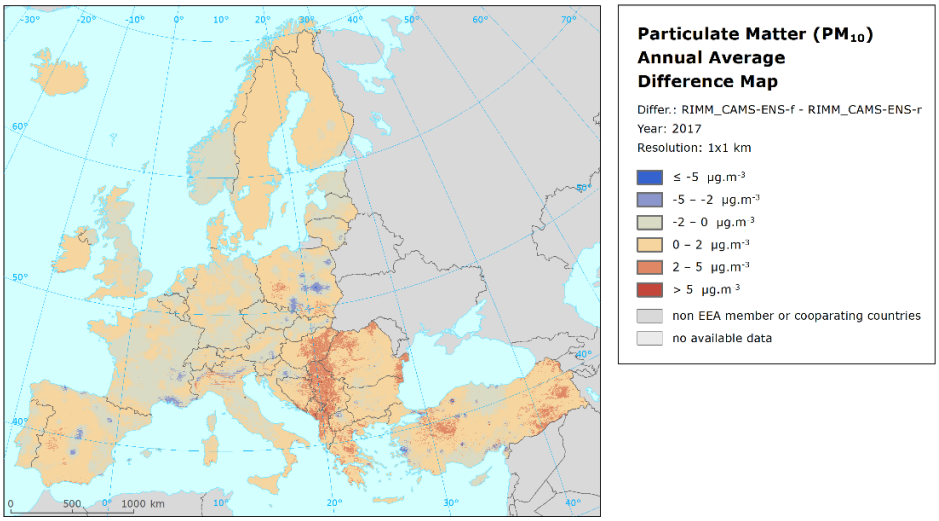

*Map A.3 Map showing difference in concentrations between CAMS-ENS Forecast and EMEP (top), CAMS-ENS Interim Reanalysis and EMEP (middle) or CAMS-ENS Forecast and CAMS-ENS Interim Reanalysis (bottom) model outputs for $PM_{2.5}$ annual average, 2017*

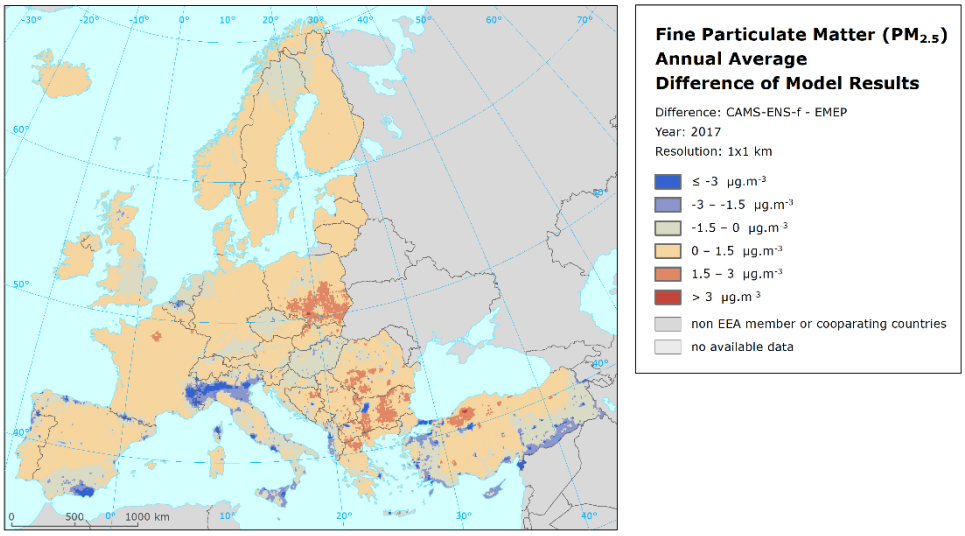


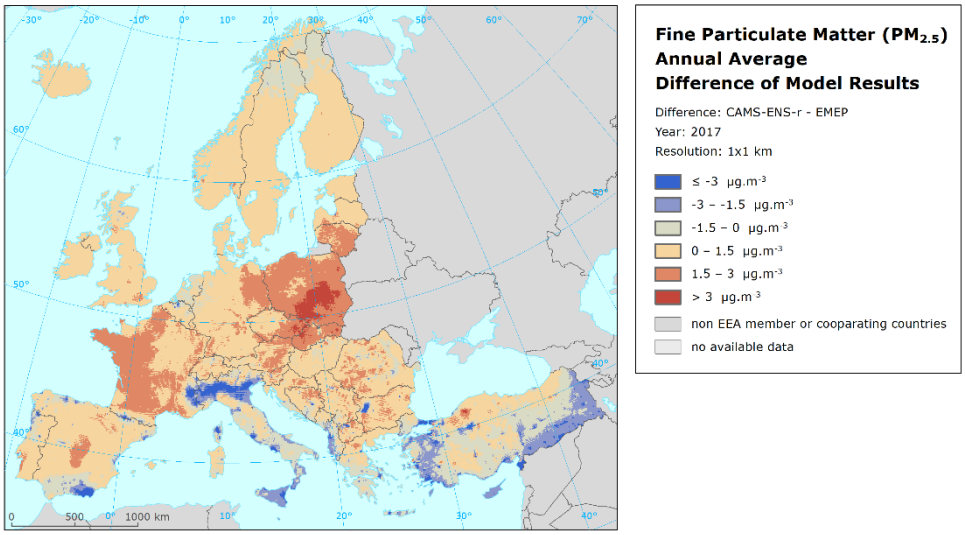


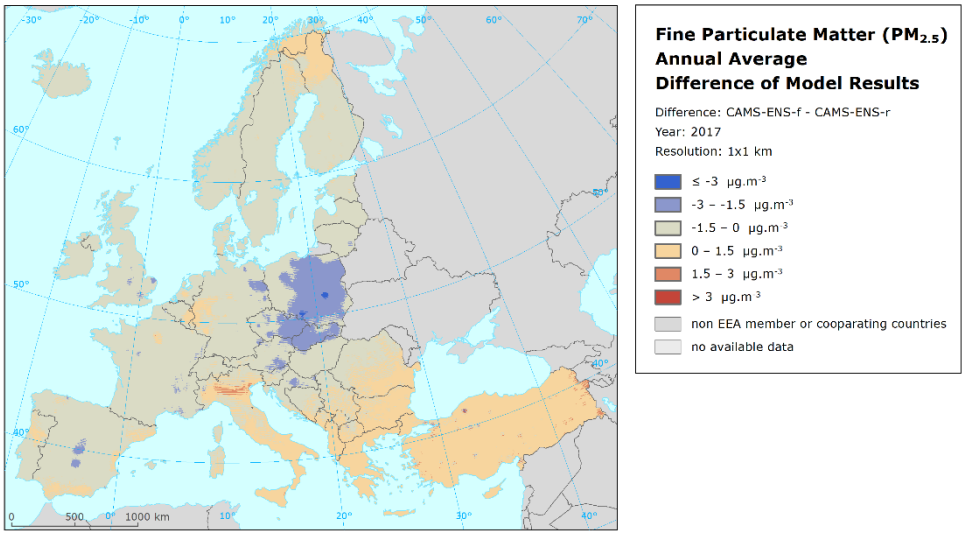

*Map A.4 Map showing difference in concentrations between RIMM using CAMS-ENS Forecast and RIMM using EMEP (top), RIMM using CAMS-ENS Interim Reanalysis and RIMM using EMEP (middle) or RIMM using CAMS-ENS Forecast and RIMM using CAMS-ENS Interim Reanalysis (bottom) model outputs for $PM_{2.5}$ annual average, 2017*

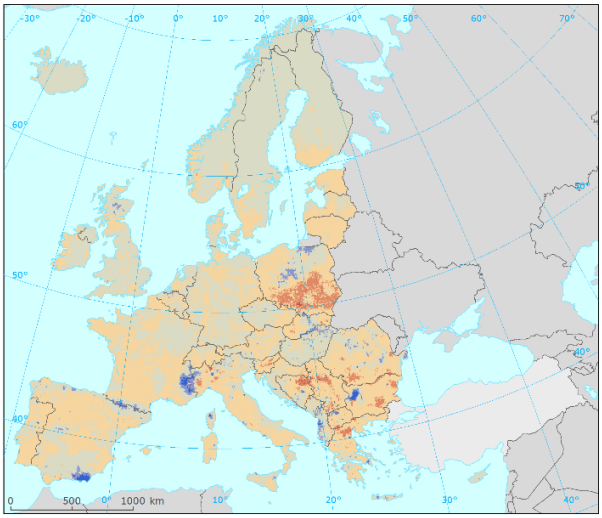


**Fine Particulate Matter ($PM_{2.5}$)**
**Annual Average**
**Difference Map**

Differ.: RIMM_CAMS-ENS-f - EMEP
Year: 2017
Resolution: 1x1 km

- ≤ -3 µg.m$^{-3}$
- -3 – -1.5 µg.m$^{-3}$
- -1.5 – 0 µg.m$^{-3}$
- 0 – 1.5 µg.m$^{-3}$
- 1.5 – 3 µg.m$^{-3}$
- > 3 µg.m$^{-3}$
- non EEA member or cooparating countries
- no available data

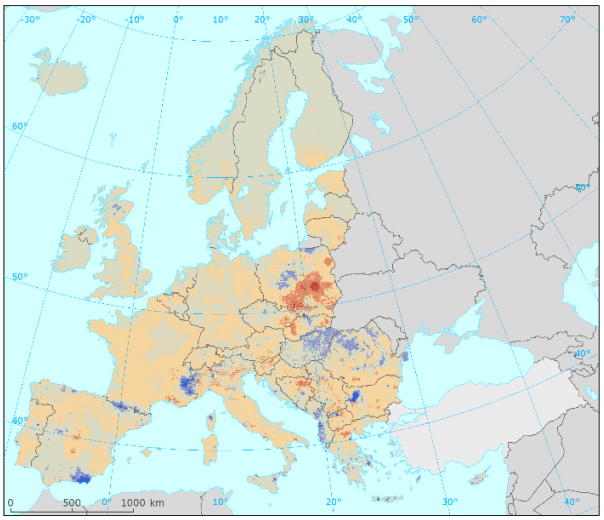


**Fine Particulate Matter ($PM_{2.5}$)**
**Annual Average**
**Difference Map**

Differ.: RIMM_CAMS-ENS-r - EMEP
Year: 2017
Resolution: 1x1 km

- ≤ -3 µg.m$^{-3}$
- -3 – -1.5 µg.m$^{-3}$
- -1.5 – 0 µg.m$^{-3}$
- 0 – 1.5 µg.m$^{-3}$
- 1.5 – 3 µg.m$^{-3}$
- > 3 µg.m$^{-3}$
- non EEA member or cooparating countries
- no available data

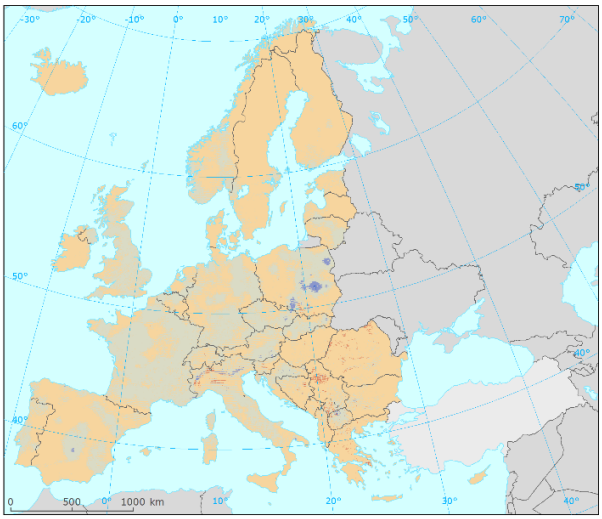


**Fine Particulate Matter ($PM_{2.5}$)**
**Annual Average**
**Difference Map**

Differ.: RIMM_CAMS-ENS-f - RIMM_CAMS-ENS-r
Year: 2017
Resolution: 1x1 km

- ≤ -3 µg.m$^{-3}$
- -3 – -1.5 µg.m$^{-3}$
- -1.5 – 0 µg.m$^{-3}$
- 0 – 1.5 µg.m$^{-3}$
- 1.5 – 3 µg.m$^{-3}$
- > 3 µg.m$^{-3}$
- non EEA member or cooparating countries
- no available data

*Map A.5 Map showing difference in concentrations between CAMS-ENS Forecast and EMEP (top), CAMS-ENS Interim Reanalysis and EMEP (middle) or CAMS-ENS Forecast and CAMS-ENS Interim Reanalysis (bottom) model outputs for the ozone indicator SOMO35, 2017*

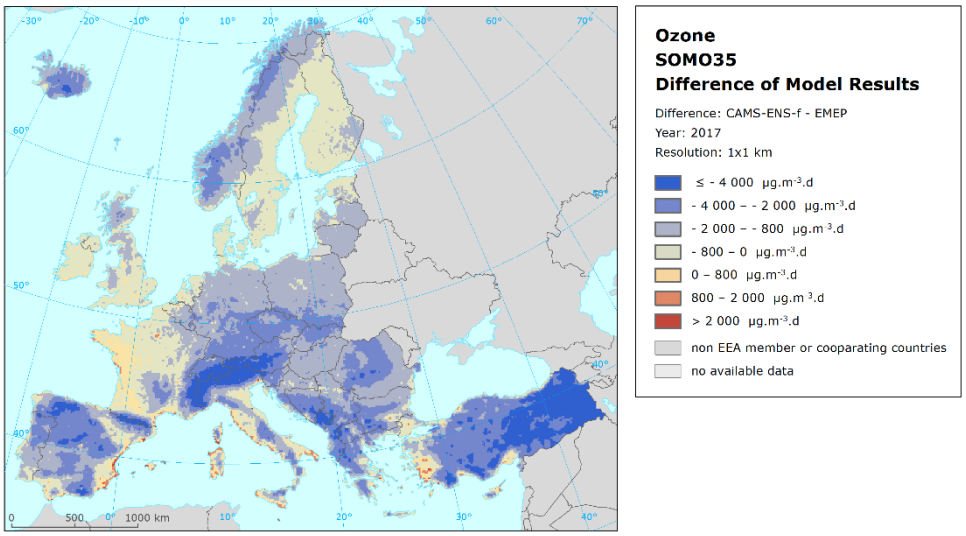


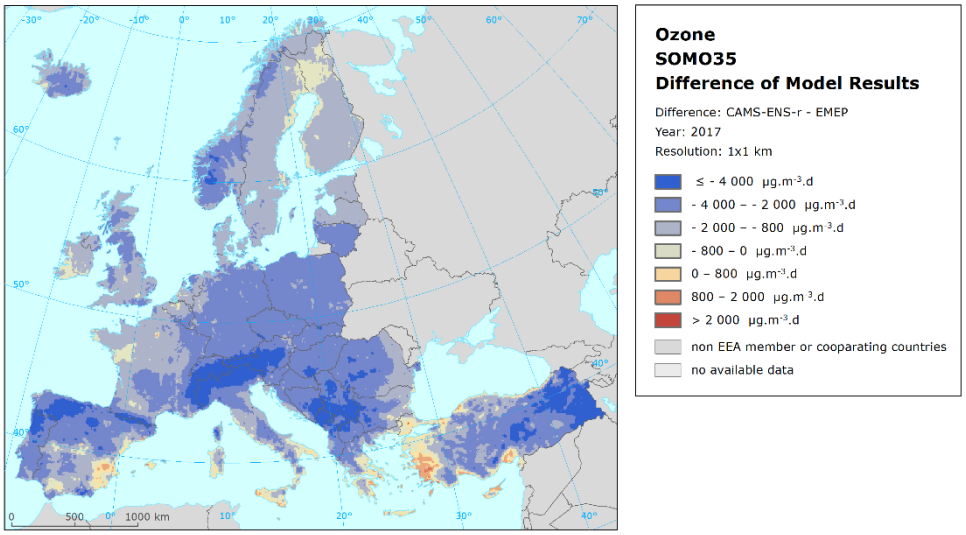


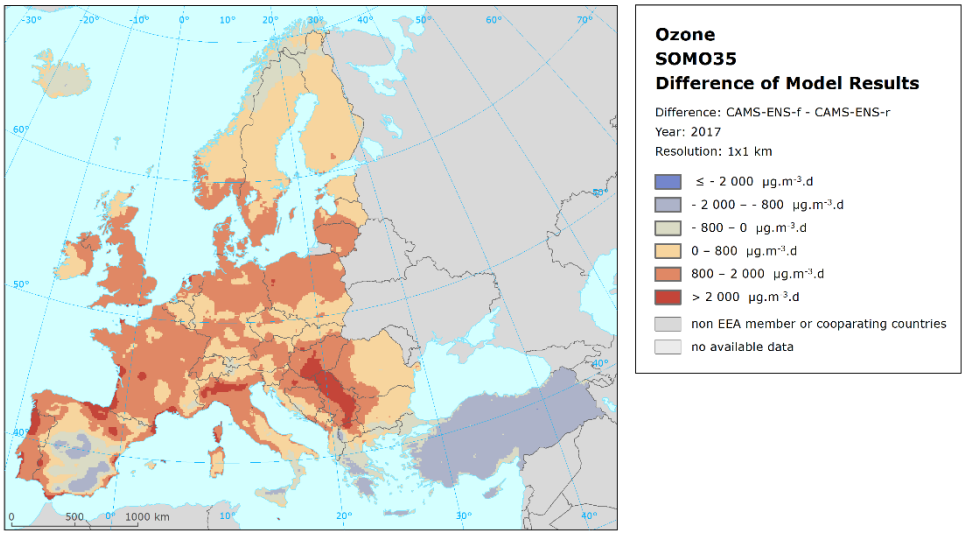

*Map A.6 Map showing difference in concentrations between RIMM using CAMS-ENS Forecast and RIMM using EMEP (top), RIMM using CAMS-ENS Interim Reanalysis and RIMM using EMEP (middle) or RIMM using CAMS-ENS Forecast and RIMM using CAMS-ENS Interim Reanalysis (bottom) model outputs for the ozone indicator SOMO35, 2017*

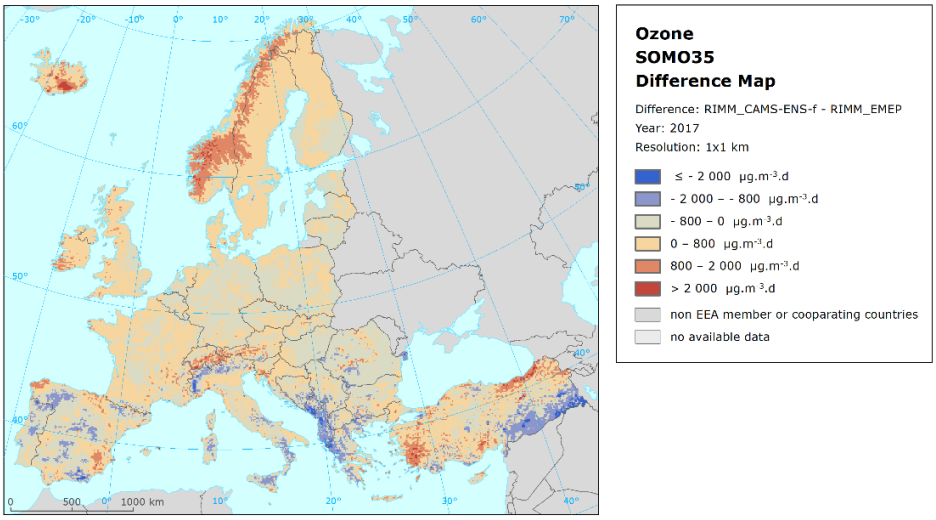


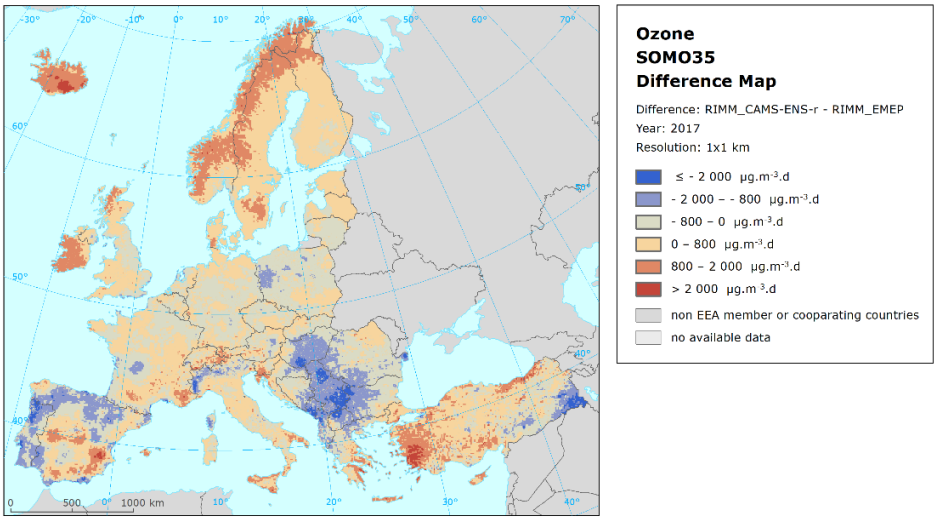


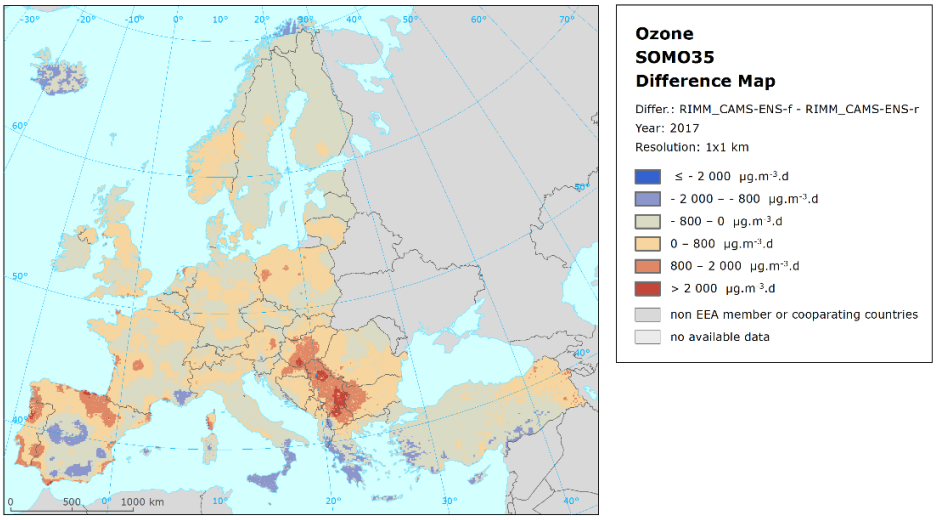

*Map A.7 Map showing difference in concentrations between CAMS-ENS Forecast and EMEP (top), CAMS-ENS Interim Reanalysis and EMEP (middle) or CAMS-ENS Forecast and CAMS-ENS Interim Reanalysis (bottom) model outputs for $NO_2$ annual average, 2017*

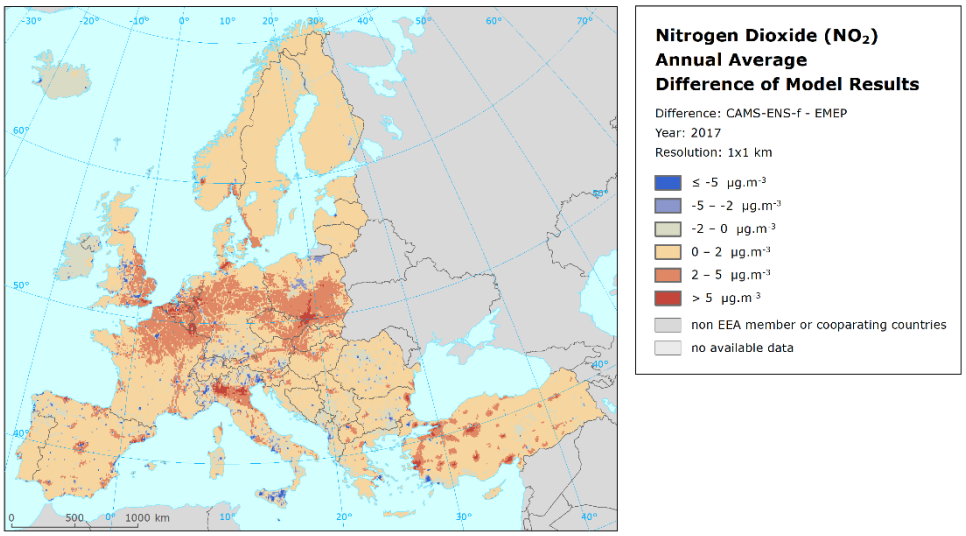


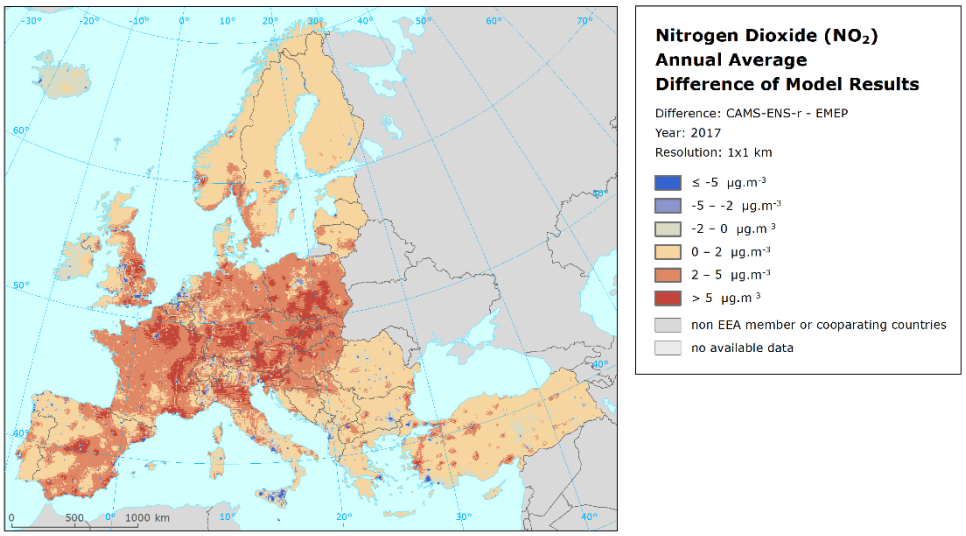


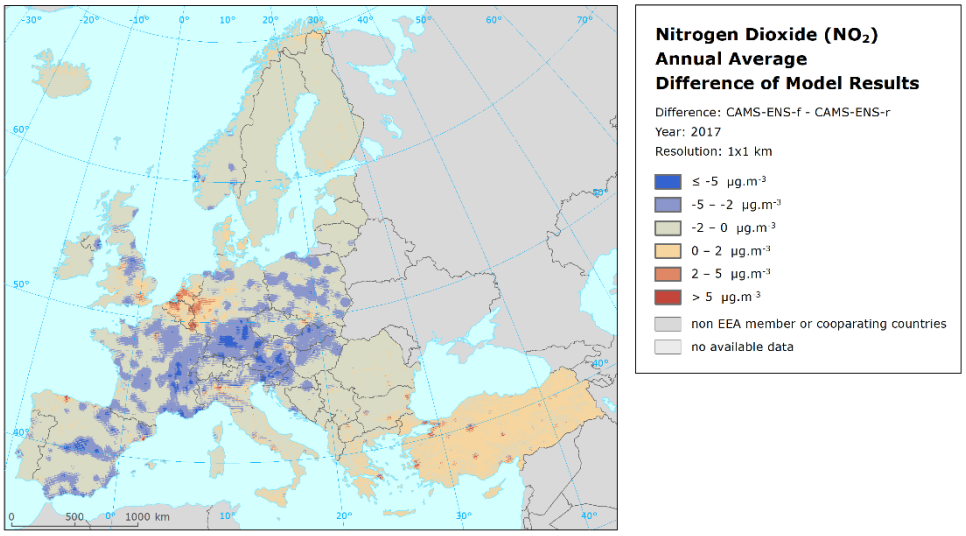

*Map A.8 Map showing difference in concentrations between RIMM using CAMS-ENS Forecast and RIMM using EMEP (top), RIMM using CAMS-ENS Interim Reanalysis and RIMM using EMEP (middle) or RIMM using CAMS-ENS Forecast and RIMM using CAMS-ENS Interim Reanalysis (bottom) model outputs for $NO_2$ annual average, 2017*

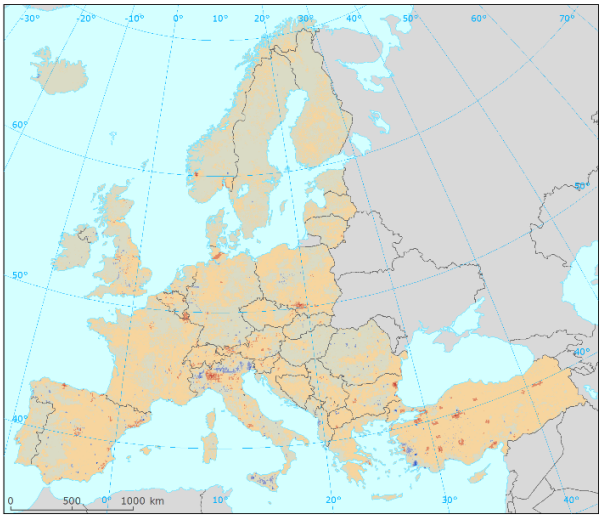


**Nitrogen Dioxide ($NO_2$)**
**Annual Average**
**Difference Map**

Difference: RIMM_CAMS-ENS-f - EMEP
Year: 2017
Resolution: 1x1 km

- ≤ -5 µg.m$^{-3}$
- -5 – -2 µg.m$^{-3}$
- -2 – 0 µg.m$^{-3}$
- 0 – 2 µg.m$^{-3}$
- 2 – 5 µg.m$^{-3}$
- > 5 µg.m$^{-3}$
- non EEA member or cooparating countries
- no available data

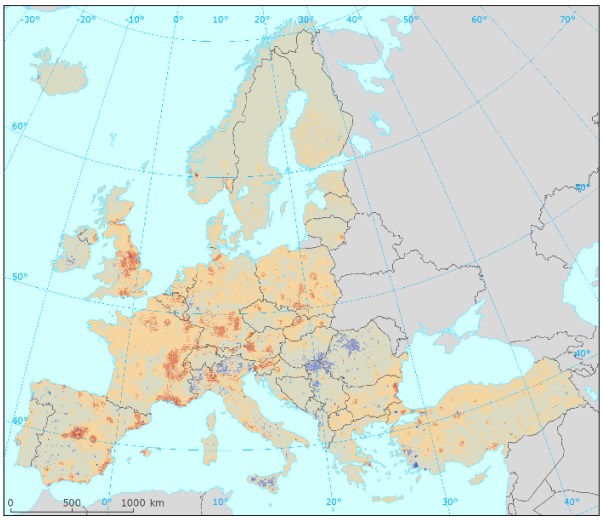


**Nitrogen Dioxide ($NO_2$)**
**Annual Average**
**Difference Map**

Difference: RIMM_CAMS-ENS-r - EMEP
Year: 2017
Resolution: 1x1 km

- ≤ -5 µg.m$^{-3}$
- -5 – -2 µg.m$^{-3}$
- -2 – 0 µg.m$^{-3}$
- 0 – 2 µg.m$^{-3}$
- 2 – 5 µg.m$^{-3}$
- > 5 µg.m$^{-3}$
- non EEA member or cooparating countries
- no available data

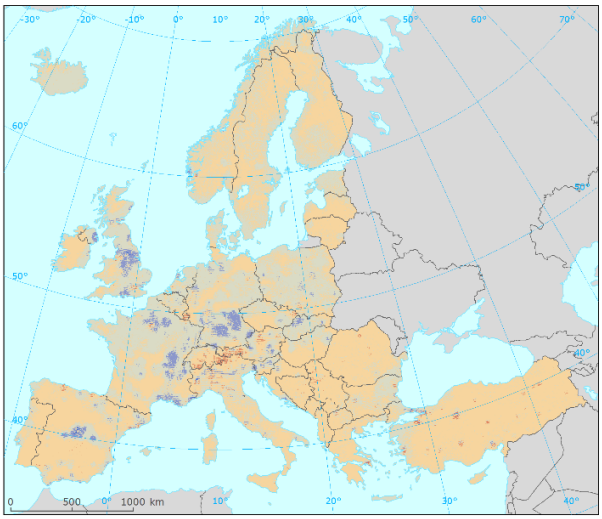


**Nitrogen Dioxide ($NO_2$)**
**Annual Average**
**Difference Map**

Differ..: RIMM_CAMS-ENS-f - RIMM_CAMS-ENS-r
Year: 2017
Resolution: 1x1 km

- ≤ -5 µg.m$^{-3}$
- -5 – -2 µg.m$^{-3}$
- -2 – 0 µg.m$^{-3}$
- 0 – 2 µg.m$^{-3}$
- 2 – 5 µg.m$^{-3}$
- > 5 µg.m$^{-3}$
- non EEA member or cooparating countries
- no available data

*Map A.9 Map showing difference in concentrations between RIMM (as routinely produced) and CAMS-ENS Interim Reanalysis model output for $PM_{10}$ annual average, 2017*

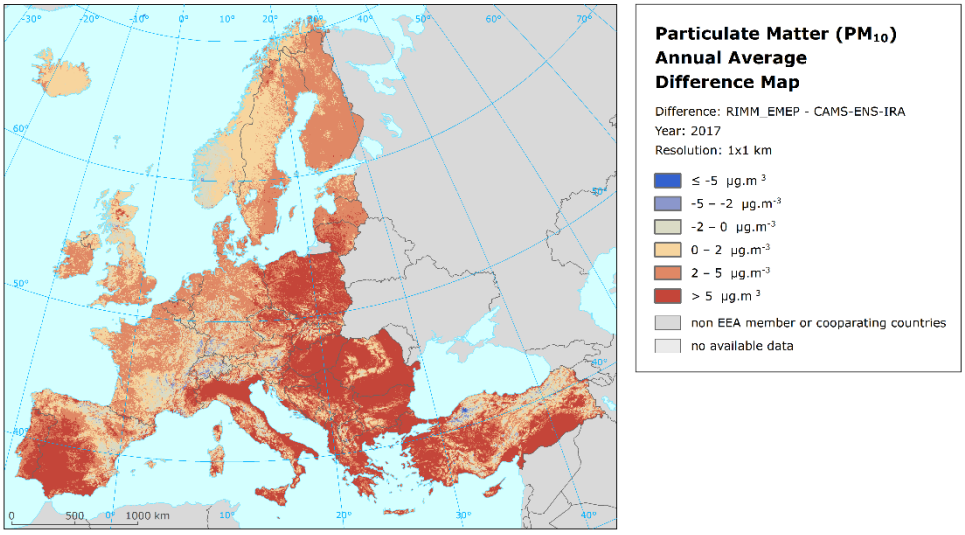


*Map A.10 Map showing difference in concentrations between RIMM (as routinely produced) and CAMS-ENS Interim Reanalysis model output for $PM_{2.5}$ annual average, 2017*

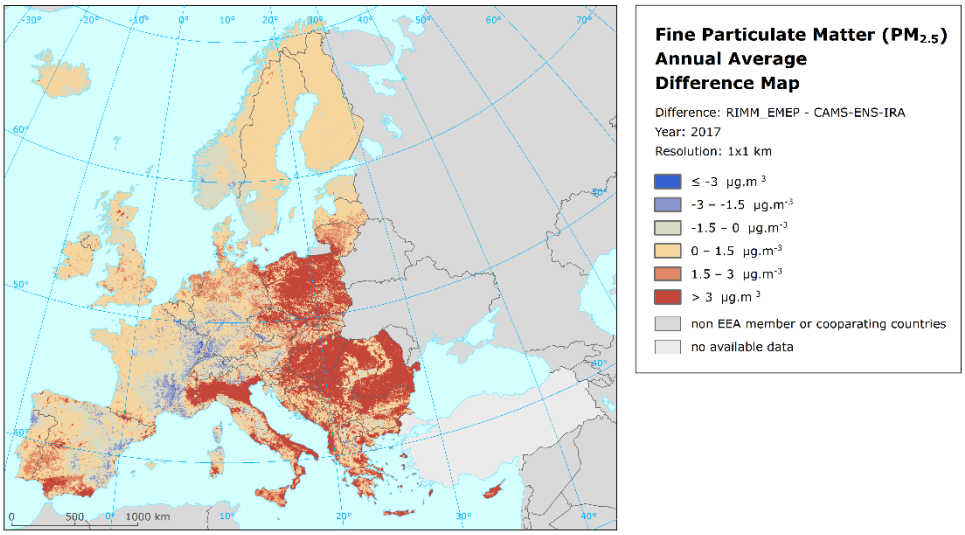

*Map A.11 Map showing difference in concentrations between RIMM (as routinely produced) and CAMS-ENS Interim Reanalysis model output for ozone indicator SOMO35, 2017*

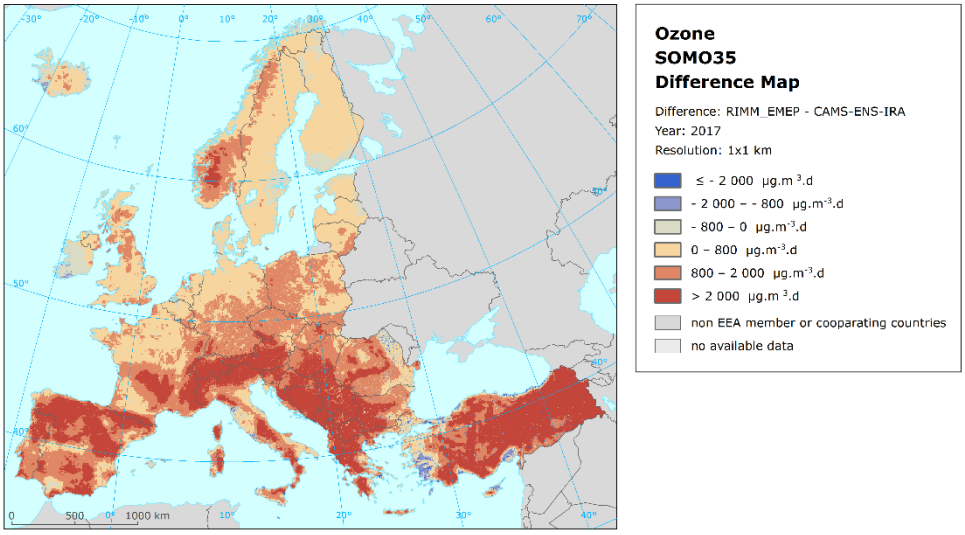


*Map A.12 Map showing difference in concentrations between RIMM (as routinely produced) and CAMS-ENS Interim Reanalysis model output for $NO_2$ annual average, 2017*

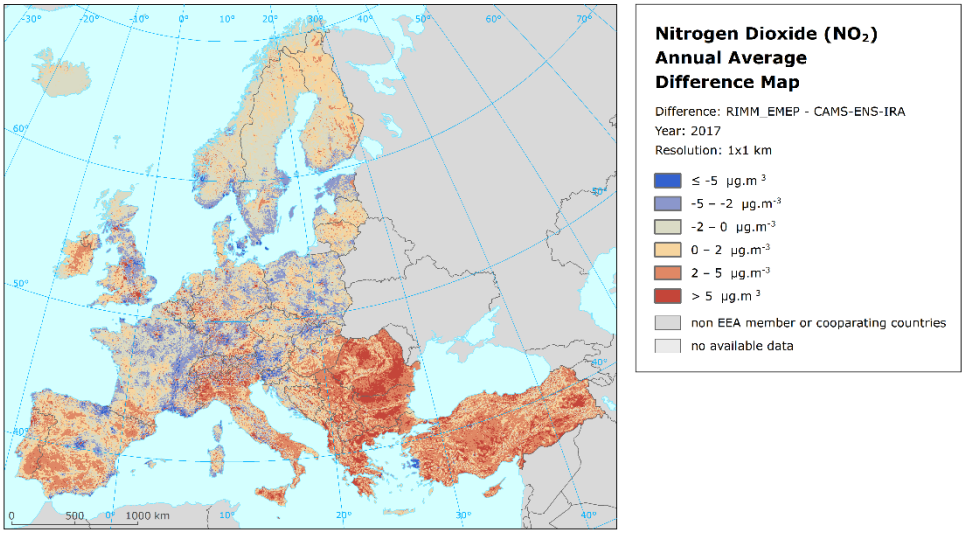

European Topic Centre on Air pollution,
transport, noise and industrial pollution
c/o NILU – Norwegian Institute for Air Research
P.O. Box 100, NO-2027 Kjeller, Norway
Tel.: +47 63 89 80 00
Email: etc.atni@nilu.no
Web : https://www.eionet.europa.eu/etcs/etc-atni

The European Topic Centre on Air pollution, transport, noise and industrial pollution (ETC/ATNI) is a consortium of European institutes under a framework partnership contract to the European Environment Agency.

European Environment Agency
European Topic Centre on Air pollution,
transport, noise and industrial pollution